

REPORT DOCUMENTATION PAGE

Form Approved
OMB No. 0704-0188

Public reporting burden for this collection of information is estimated to average 1 hour per response, including the time for reviewing instructions, searching existing data sources, gathering and maintaining the data needed, and completing and reviewing the collection of information. Send comments regarding this burden estimate or any other aspect of this collection of information, including suggestions for reducing this burden, to Washington Headquarters Services, Directorate for Information Operations and Reports, 1215 Jefferson Davis Highway, Suite 1204, Arlington, VA 22202-4302, and to the Office of Management and Budget, Paperwork Reduction Project (0704-0188), Washington, DC 20503.

1. AGENCY USE ONLY (Leave blank)		2. REPORT DATE		3. REPORT TYPE AND DATES COVERED	
4. TITLE AND SUBTITLE 175Hp CONTAROTATING HOMOPOLAR MOTOR DESIGN REPORT				5. FUNDING NUMBERS Program Element No. PEO 602121N Project No. RH21E41 ERH21E42 Work Unit Accession No. 1-8000-240	
6. AUTHOR(S) Michal J. Cannell, John L. Drake, Richard A. McConnell, William R. Martino					
7. PERFORMING ORGANIZATION NAME(S) AND ADDRESS(ES) Naval Surface Warfare Center, Carderock Division Code 811, Annapolis Lab 3A Leggette Circle Annapolis, Maryland 21402-5067				8. PERFORMING ORGANIZATION REPORT NUMBER CARDIVNSWC-TR-81-94/25	
9. SPONSORING / MONITORING AGENCY NAME(S) AND ADDRESS(ES) Office of Naval Research, ONR 4524 Ballston Center Tower #1 800 N. Quincy Street Arlington, VA 22217-5660				10. SPONSORING / MONITORING AGENCY REPORT NUMBER	
11. SUPPLEMENTARY NOTES					
12a. DISTRIBUTION / AVAILABILITY STATEMENT				12b. DISTRIBUTION CODE	
13. ABSTRACT (Maximum 200 words) A normally conducting contrarotating homopolar motor has been designed and constructed. The reaction torque, in the outer rotor, from the inner rotor is utilized to produce true contrarotation. The machine utilizes liquid cooled conductors, high performance liquid metal current collectors, and ferrous conductors in the active region. The basic machine output is 175 hp at $\pm 1,200$ rpm with an input of 4 volts and 35,000 amps.					
14. SUBJECT TERMS				15. NUMBER OF PAGES	
				16. PRICE CODE	
17. SECURITY CLASSIFICATION OF REPORT	18. SECURITY CLASSIFICATION OF THIS PAGE	19. SECURITY CLASSIFICATION OF ABSTRACT	20. LIMITATION OF ABSTRACT		

**Carderock Division
Naval Surface Warfare Center**

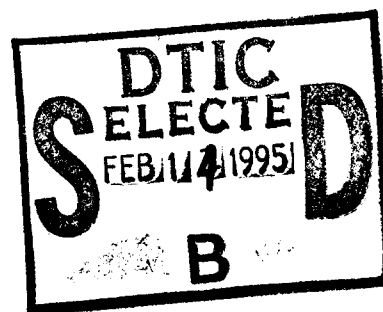
Bethesda, Maryland 20084-5000

CARDIVNSWC-TR-81-94/25 June 1994

Machinery Research & Development Directorate
Research and Development Report

**175 Hp CONTAROTATING HOMOPOLAR
MOTOR DESIGN REPORT**

by
Michael J. Cannell
John L. Drake
Richard A. McConnell
William R. Martino



Approved for public release; distribution is unlimited.

19950206 078

MAJOR CARDIVNSWC TECHNICAL COMPONENTS

- CODE 10 LOGISTICS & MACHINERY SYSTEMS/PROGRAM DIRECTORATE
- 20 SHIP SYSTEMS/PROGRAM DIRECTORATE
- 50 HYDROMECHANICS DIRECTORATE
- 60 SURVIVABILITY, STRUCTURES & MATERIALS DIRECTORATE
- 70 SIGNATURES DIRECTORATE
- 80 MACHINERY RESEARCH & DEVELOPMENT DIRECTORATE
- 90 MACHINERY IN-SERVICE ENGINEERING DIRECTORATE

CARDIVNSWC ISSUES THREE TYPES OF REPORTS:

1. **CARDIVNSWC reports, a formal series**, contain information of permanent technical value. They carry a consecutive numerical identification regardless of their classification or the originating department.
2. **Departmental reports, a semiformal series**, contain information of a preliminary, temporary, or proprietary nature or of limited interest or significance. They carry a departmental alphanumeric identification.
3. **Technical memoranda, an informal series**, contain technical documentation of limited use and interest. They are primarily working papers intended for internal use. They carry an identifying number which indicates their type and the numerical code of the originating department. Any distribution outside CARDIVNSWC must be approved by the head of the originating department on a case-by-case basis.

CONTENTS

	PAGE
ABSTRACT	1
ADMINISTRATIVE INFORMATION	1
ACKNOWLEDGMENTS	1
INTRODUCTION	1
BASIC PRINCIPLES	2
DESIGN APPROACH.....	5
MAJOR DESIGN DECISIONS AND RATIONALE	6
MACHINE TYPE	6
Disk	6
Drum	6
MACHINE SIZE.....	6
ASSEMBLY METHOD	7
EXCITATION	7
GENERAL MACHINE DESCRIPTION	8
OVERALL MACHINE LAYOUT	8
MAGNETIC CIRCUIT.....	8
ELECTRICAL CIRCUIT	9
BEARINGS AND COVER GAS SEALS	11
SERVICE MODULE	11
SLIP RINGS	11
DETAILED MACHINE DESIGN.....	12
MAGNETIC CIRCUIT.....	12
Ferrous Conductors	12
Flux-Load Current Interactions	12
Shielding	13
Finite Element Models	13
FIELD COILS.....	19
Conductor	19
Insulation.....	19
Lead Configuration	19
ELECTRICAL CIRCUIT	20
Inner Rotor	20
Outer Rotor	21
Terminals	21
CURRENT COLLECTORS	21
COOLING SYSTEM DESIGN AND ANALYSIS	21
Inner Rotor	21
Selecting cooling hole diameter and number of parallel paths	22
Outer Rotor	22
Terminals	29
Field coils.....	29
Fluids.....	29

Geometry	29
STRUCTURAL DESIGN	36
BEARINGS AND GAS SEALS	37
Bearings	37
Drive end	37
Service end	37
Seal Assembly	37
Gas seal	37
Exclusion seal	38
SERVICE MODULE	38
SLIP RINGS	38
COOLANT SEALS	38
ROTARY UNION	38
INSTRUMENTATION	38
Sensors	38
Telemetry	39
COVER GAS SYSTEM	39
ASSEMBLY PROCEDURES	39
PREDICTED MACHINE PERFORMANCE	39
CONCLUSIONS	40
REFERENCES	42

TABLES

Table 1. BH Curves for 1010 Steel With Air Voids	17
Table 2. Predicted Motor Performance at 35,000 amperes	40
Table 3. Predicted Motor Performance at 100,000 amperes	41

FIGURES

Fig. 1. Single Turn Disk Homopolar Motor	3
Fig. 2. Single Turn Drum Homopolar Motor	3
Fig. 3. Single Turn Contrarotating Drum Homopolar Motor	5
Fig. 4. Electrical Circuit Showing Current Path	10
Fig. 5. Finite Element Model Dimensions	15
Fig. 6. Permeability Regions Used in Finite Element Model	16
Fig. 7. Magnetic Circuit With Superimposed Flux Plot	18
Fig. 8. ΔT Vs. Diameter, $N=1$, 40 psi	24
Fig. 9. ΔT Vs. Diameter, $N=1$, 80 psi	24
Fig. 10. ΔT Vs. Diameter, $N=2$, 40 psi	25
Fig. 11. ΔT Vs. Diameter, $N=2$, 80 psi	25
Fig. 12. ΔT Vs. Diameter, $N=4$, 40 psi	26
Fig. 13. ΔT Vs. Diameter, $N=4$, 80 psi	26
Fig. 14. Inner Rotor Film Drop Vs. Diameter (32 Bars)	27

Fig. 15. Inner Rotor Film Drop ΔT Vs. Flow. Rate	28
Fig. 16. Outer Rotor Film Drop ΔT Vs. Flow Rate	28
Fig. 17. Fluid ΔT Vs. Hole Dia. for Coolanol 20 and 40 at 20 psi	31
Fig. 18. Fluid ΔT Vs. Hole Dia. for Coolanol 20 and 40 at 60 psi	31
Fig. 19. Fluid ΔT Vs. Coolant Hole Area at 20 psi	32
Fig. 20. Fluid ΔT Vs. Coolant Hole Area at 60 psi	32
Fig. 21. Fluid ΔT Vs. Coolant Hole Diameter	33
Fig. 22. Film Drop ΔT Vs. Diameter at 20, 40, 60, and 80 psi	34
Fig. 23. Fluid ΔT Vs. Flow Rate	34
Fig. 24. Fluid ΔT Vs. Pressure	35
Fig. 25. Flow Rate Vs. Pressure	35

APPENDIX A

INNER ROTOR THERMAL DESIGN

APPENDIX B

OUTER ROTOR THERMAL DESIGN

APPENDIX C

FIELD COIL THERMAL DESIGN

APPENDIX D

DETAILS OF STRUCTURAL ANALYSIS

APPENDIX E

MOTOR DETAIL DRAWINGS

APPENDIX F

SERVICE MODULE DETAIL DRAWINGS

Accession For	
NTIS GRA&I	<input checked="" type="checkbox"/>
DTIC TAB	<input type="checkbox"/>
Unannounced	<input type="checkbox"/>
Justification	
By	
Distribution	
Availability Codes	
Dist	Avail and/or Special
A-1	

ABSTRACT

A normally conducting contrarotating homopolar motor has been designed and constructed. The reaction torque, in the outer rotor, from the inner rotor is utilized to produce true contrarotation. The machine utilizes liquid cooled conductors, high performance liquid metal current collectors, and ferrous conductors in the active region. The basic machine output is 175 hp at $\pm 1,200$ rpm with an input of 4 volts and 35,000 amps.

ADMINISTRATIVE INFORMATION

The motor design effort described herein was initiated under the Independent Research and Independent Exploratory Development Program at this center under Work Unit 1-2711-100 and subsequently supported by the Office of Naval Research under Program Element 62121N Projects RH21E41 and RH21E42. This project milestone report is submitted in partial fulfillment of Milestone 1 Task 1 of the Advanced Electrical Systems Project (RH21E41) of the Surface Ship Technology Program (SC1A/PE0602121N). The work described herein was sponsored by ONR 334 and was performed by personnel of the Carderock Division, Naval Surface Warfare Center (CDNSWC 811), Annapolis, Maryland.

ACKNOWLEDGMENTS

The authors wish to acknowledge the valuable assistance of the following individuals: Mr. Charles Bielitz, Mr. Lawrence Foster, Mr. Thomas Hane, Mr. Dwight Lavinder, Mr. Peter McGraw, Mr. Kenneth Sabel, Mr. John Stevens, Mr. Harold Surosky, Mr. Jerry Webster, Mr. Ditmar Weiss, and Mr. Kevin Wilson

INTRODUCTION

As a result of numerous ship impact studies relating technology to performance and other attributes, contrarotating propulsion trains have been identified as viable candidates for future surface combatants¹. In addition, the homopolar DC. motor has been identified as an attractive long term electric drive option for both surface ships² and submarines³. Since the homopolar motor concept is well adapted to contrarotation we have an opportunity to provide the advantages of both advanced electric drive and contrarotation at the same time. In order to establish the feasibility of this approach, a development program to demonstrate direct drive contrarotation on a small scale was undertaken.

This report documents the basic design, design decisions, and philosophy that have gone into the development and detailed design of this 175 hp model contrarotating homopolar motor. This motor is being constructed as a demonstration both of contrarotation and of normally conducting homopolar motor technology. In addition, a variety of design and analysis techniques have been developed which will be applicable to other machines, both single and contrarotating, and with normal or superconductive excitation.

BASIC PRINCIPLES

This motor operates on the same basic principles as a single-rotating homopolar motor⁴. Torque is produced by the direct interaction of current in a conductor with a separately produced magnetic induction. The two basic types of homopolar motors are the disc machine, Fig. 1, and the drum machine, Fig. 2. In a disc machine, conducting discs, with radial current, are placed in an axial magnetic induction. The drum machine consists of conducting drums, with axial current, in a radial magnetic induction. Both machine types are fitted with current collectors to provide electrical contact between the rotating discs or drums and the stationary current return path that completes the electrical circuit and allows connection to the power source. This return path most commonly takes the same general form as the rotor current path. A disc machine has stationary discs that make up the return path while a drum machine is fitted with stationary drums that make up the return path.

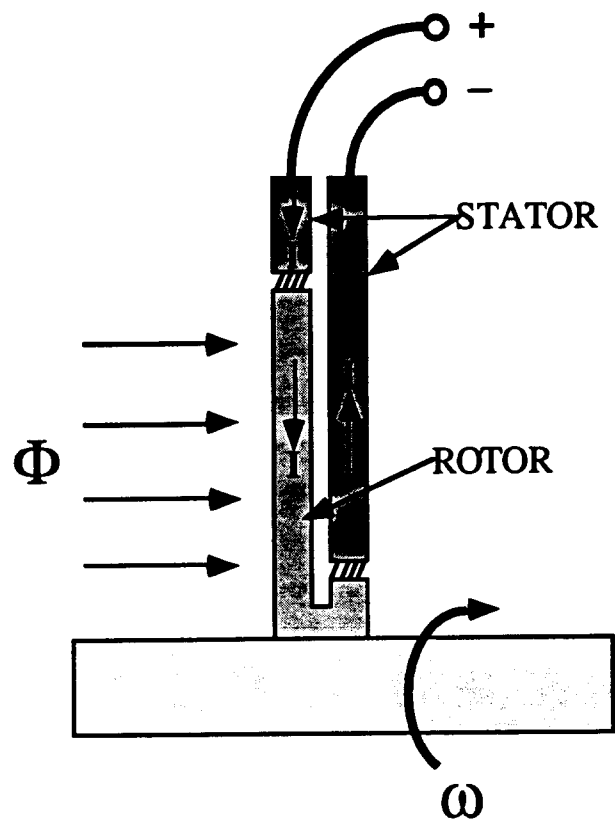


Fig. 1. Single Turn Disk Homopolar Motor

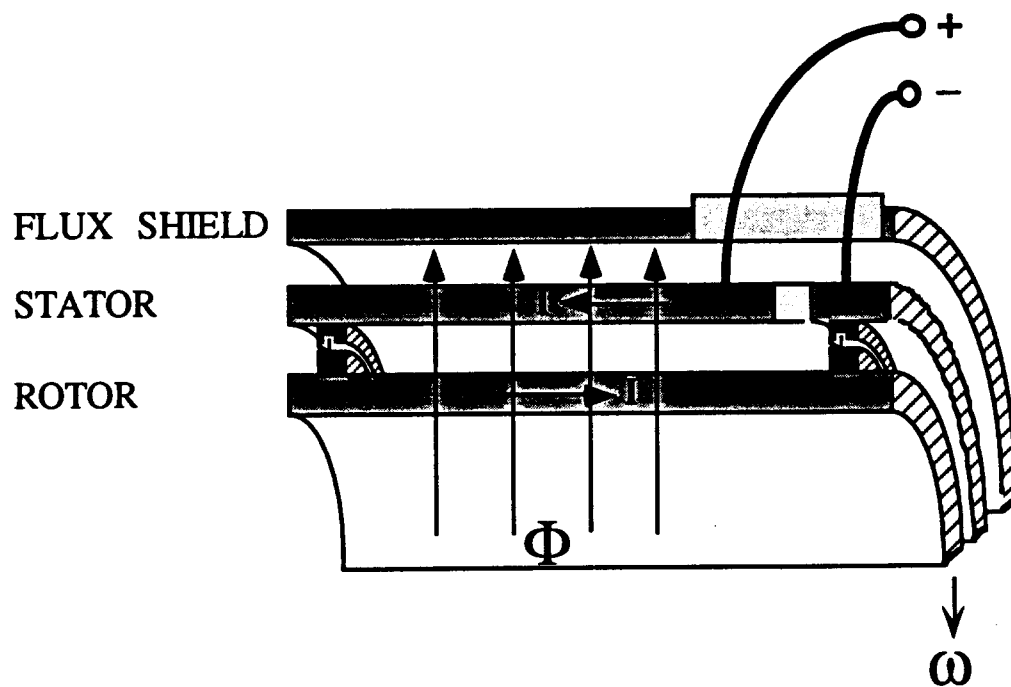


Fig. 2. Single Turn Drum Homopolar Motor

In both types of machines the current and magnetic induction interact, by means of a vector cross product, to produce a force that is at right angles to both the current and magnetic induction vectors. Due to the symmetry of both the magnetic induction and the current carrying elements of the machine, the summation of these forces results in a torque on the rotor elements and an equal but opposite reaction torque on the stator elements that make up the stationary current return path.

In a single-rotating motor, the reaction torque produced in the stationary elements can produce no power. In the case of a contrarotating motor, Fig. 3, the normally stationary current return path, now called the outer rotor, is allowed to rotate and thus can also produce power. The rotor, now called the inner rotor, continues to produce the same torque and power as before. Due to the fact that outer rotor torque is the reaction torque from the inner rotor, the torque on the two rotors must be equal in magnitude but opposite in direction. If the applied loads are equal, then the rotors will rotate at the same speed, but in opposite directions, and will both produce the same power, effectively doubling the output power of the motor. Of course this increased output power is not available for free. The electrical input power is also doubled. Since the differential speed between the inner and outer rotors is now twice as high, the motor will produce twice the back EMF, effectively doubling the terminal voltage of the machine. Two additional current collectors, called terminal collectors, are required to make electrical contact with the outer rotor. The outer rotor must additionally be fitted with bearings, seals, rotating instrumentation hookups, etc., to accommodate rotation. A stationary housing surrounds the outer rotor providing a mounting point for the bearing housings and also functions as a flux shield.

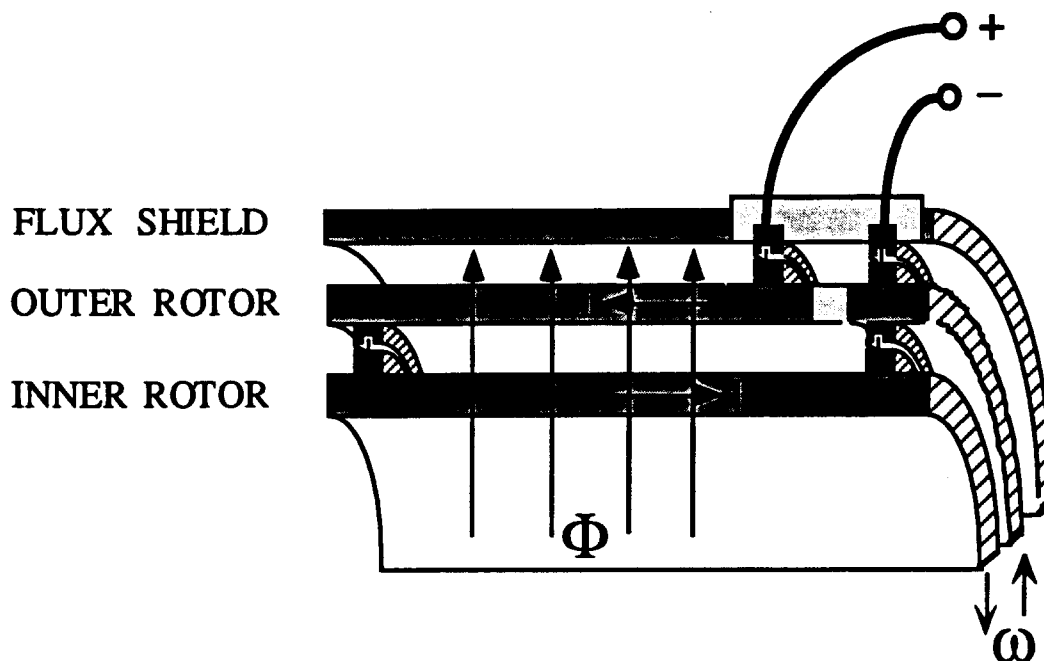


Fig. 3. Single Turn Contrarotating Drum Homopolar Motor

DESIGN APPROACH

This motor is intended to be a basic proof of principle and demonstration machine. It is not intended to demonstrate full scale machine parameters, such as power density or rotational speed, as this would compromise the design of a small motor, resulting in excessive risk and increased cost. The basic approach was to design a machine that was large enough to allow meaningful evaluation of motor design and operation yet small enough to be constructed in-house. In keeping with the basic intent of the machine, we also tried to keep the motor simple to operate even if it meant giving up some power density. One area that was not compromised, however, is the thermal design. The machine could have been considerably simplified if it was not fully cooled, since most of the current carrying conductors are rotating and thus require seals and a complex manifold arrangement for coolant. However an un-cooled motor would have been difficult to evaluate since steady state operation would be impossible to achieve. An un-cooled design also would have been too large a deviation from a full scale machine design approach, reducing the usefulness of this model in demonstrating and evaluating the required technologies.

MAJOR DESIGN DECISIONS AND RATIONALE

MACHINE TYPE

The homopolar concept was chosen for this design because of its many recognized advantages as a direct drive propulsion motor^{2,3} and its adaptability to direct contrarotation. The relatively straightforward magnetic and armature circuits simplify the outer rotor. This allows for the design of a true contrarotating motor where the outer rotor is driven by inner rotor reaction torque.

Disk

Disk type homopolar machines have been built but they are more difficult to cool. They also present some unique problems for liquid metal current collectors which must operate at two different radii. As a result of the geometry, liquid metal transfer between collectors has been a problem requiring elaborate recirculation systems which have always been problematic.

Drum

The drum type homopolar has been the most successful design to date for several reasons. The liquid metal current collectors are all at one radius and liquid metal migration can easily be controlled. A subset of the drum type machine is the bar type. In this arrangement, the drum set is replaced by bars evenly spaced around the rotor. This construction is particularly good from a cooling standpoint. Each bar can be provided with one or more cooling holes connected to coolant manifolds at each end of the rotor. Electrical interconnection is also facilitated with the bar arrangement. Since the bars are run the entire length of the rotor, for ease of cooling, any collector disk can be connected to the appropriate bar. In a motor with normally conducting excitation the bar construction has the added advantage of lower reluctance in the active region. This is accomplished either by placing copper bars in slots cut in a ferrous rotor or by using ferrous conductors in the active region. For these reasons bar type construction was chosen for the model contrarotating motor.

MACHINE SIZE

Since this is a demonstration machine and not a scale model, the size and power are somewhat arbitrary. Therefore the size was based on more practical considerations rather than on some particular set of parameters derived from a scale down. Based on prior experience with the DTRC 400 hp motor⁴ we felt that a machine of approximately the same overall physical dimensions would be desirable. This machine was large

enough to allow meaningful evaluation but not so large as to be difficult to construct in-house. Rough calculations indicated that a machine with a magnetic circuit that produced between 0.1 and 0.2 Webers of flux in the active region would be in the desired size range. A more detailed magnetic design was done for both the 0.1 and 0.2 Weber cases. The 0.1 Weber design yielded a machine of the desired physical size and with reasonable electrical parameters. The 0.1 Weber design was therefore selected for continuation to detailed design.

ASSEMBLY METHOD

There are two basic assembly options for single-rotating homopolar machines.

The first consists of splitting the stator clam-shell fashion. This allows the complete rotor to be placed into the lower stator. Split line seals are applied to the lower stator half. The upper stator half is then placed over the lower stator-rotor combination and secured to the lower stator half. This assembly is then placed in the flux shield and fitted with the bearings and seals.

The second method is the axial stackup. With this assembly method the stator need not be split. The machine is generally assembled with the shaft oriented vertically. The rotor and stator components are alternately placed onto the assembly, generally around the shaft. This assembly can then be placed in the flux shield, returned to the horizontal, and fitted with bearings and seals.

A non split assembly method was chosen for this contrarotating motor for several reasons. In a contrarotating motor, what would normally be the stator in a single rotating motor is now the outer rotor. Thus, it must handle rotational forces as well as reaction torque. There was concern that this combination of forces might result in geometric distortion of the outer rotor. A full scale machine would have much lower centrifugal loading since it would operate at relatively lower speeds. In addition, for a one turn machine, this design offers construction simplicity, although assembly difficulty is increased somewhat. The assembly / disassembly procedure will be somewhat time consuming and require care and precision. Vertical assembly fixtures will be required to aid the process.

EXCITATION

The choices for excitation of a homopolar motor are superconductive field coils or conventional air or liquid cooled coils. Since this is a demonstration machine we felt that the simplicity of operation provided by a conventional liquid cooled field was more important than the higher power density a superconductive design could provide. A

machine based on a conventional field will still address many technologies that are common to both types of contrarotating homopolars, i.e. current collectors, basic design and analysis, construction and assembly techniques. In addition, this design addressed the unique aspects of non-superconductive designs, i.e. ferrous flux path, rotating field coils, and the use of ferrous conductors in the active regions.

GENERAL MACHINE DESCRIPTION

OVERALL MACHINE LAYOUT

All detail drawings are included in appendix E. An assembly section of the complete motor is shown on drawing A27-19992-4. Assembly sections of the inner rotor, outer rotor, and housing are shown on drawings A27-19992-7, A27-19992-8, and A27-19992-64 respectively. Section views at various axial positions are shown on A27-19992-2, A27-19992-3, A27-19992-5, and A27-19992-6. A27-19992-1 is a detailed parts and drawing list showing the detail drawing for each piece. All piece numbers refer to one or more of these drawings and are consistent among these drawings. Drawings of the rough forgings are not included.

This machine is a single turn, normal conducting, contrarotating homopolar motor. The motor will produce 175 hp at ± 1200 r/min. with a nominal input of 4 volts and 35,000 amperes. Contrarotation is accomplished by fitting the normally stationary current return path (stator) with bearings, seals, and an additional pair of current collectors which allow it to rotate opposite to the inner rotor. Magnetic flux is generated by a pair of liquid cooled coils, in a quadrupole configuration, that rotate with the inner rotor. The motor has a complete ferrous path for the magnetic flux. Included in the ferrous path are iron conductors in the active regions of both inner and outer rotors. Current transfer between inner and outer rotors and between the outer rotor and terminals is accomplished with close clearance liquid metal current collectors. Both rotors are fitted with rolling element bearings and high performance cover gas seals. All electrically active elements are directly cooled by forced flow liquid coolant.

MAGNETIC CIRCUIT

The magnetic circuit is made up of the two field coils, piece 2, the iron bar sets of the inner and outer rotors, pieces 8 and 16, and the various other ferrous members that shape and direct the magnetic flux through the active regions of the inner and outer rotors. Because of the limited ampere turns available from a conventional coil, ferrous material must be provided around the complete flux path to lower its reluctance, thereby increasing the flux generated by a given number of ampere turns in the field coils. The

iron bars in the active regions of both the inner and outer rotor are a unique aspect of this design. A more conventional approach in a non superconductive homopolar machine is to place conducting bars in slots cut in a solid ferrous rotor. The axial current is then carried by the conducting bars and the radial flux is carried by the iron between the slots.

ELECTRICAL CIRCUIT

The electrical circuit includes all those components required to transport the axial current through the active regions of both the inner and outer rotors. It is comprised of the two single rotating terminal current collectors, pieces 15, 18, 26, and 27, two contrarotating current collectors, pieces 9, 12, 14, and 19, a set of 32 inner rotor bars, piece 8, a set of 36 outer rotor bars, piece 16. Both the inner and outer rotor bar sets are brazed to continuous copper rings, pieces 10 and 11, at both ends. This braze joint provides the electrical connection to the iron bars as well as connecting the bars electrically in parallel. All of these components are connected electrically in series. It is the interaction of the axial current with the radial magnetic field in the active region that produces the torque on the inner rotor and the reaction torque on the outer rotor. The basic electrical circuit with the current path is shown in Fig. 4.

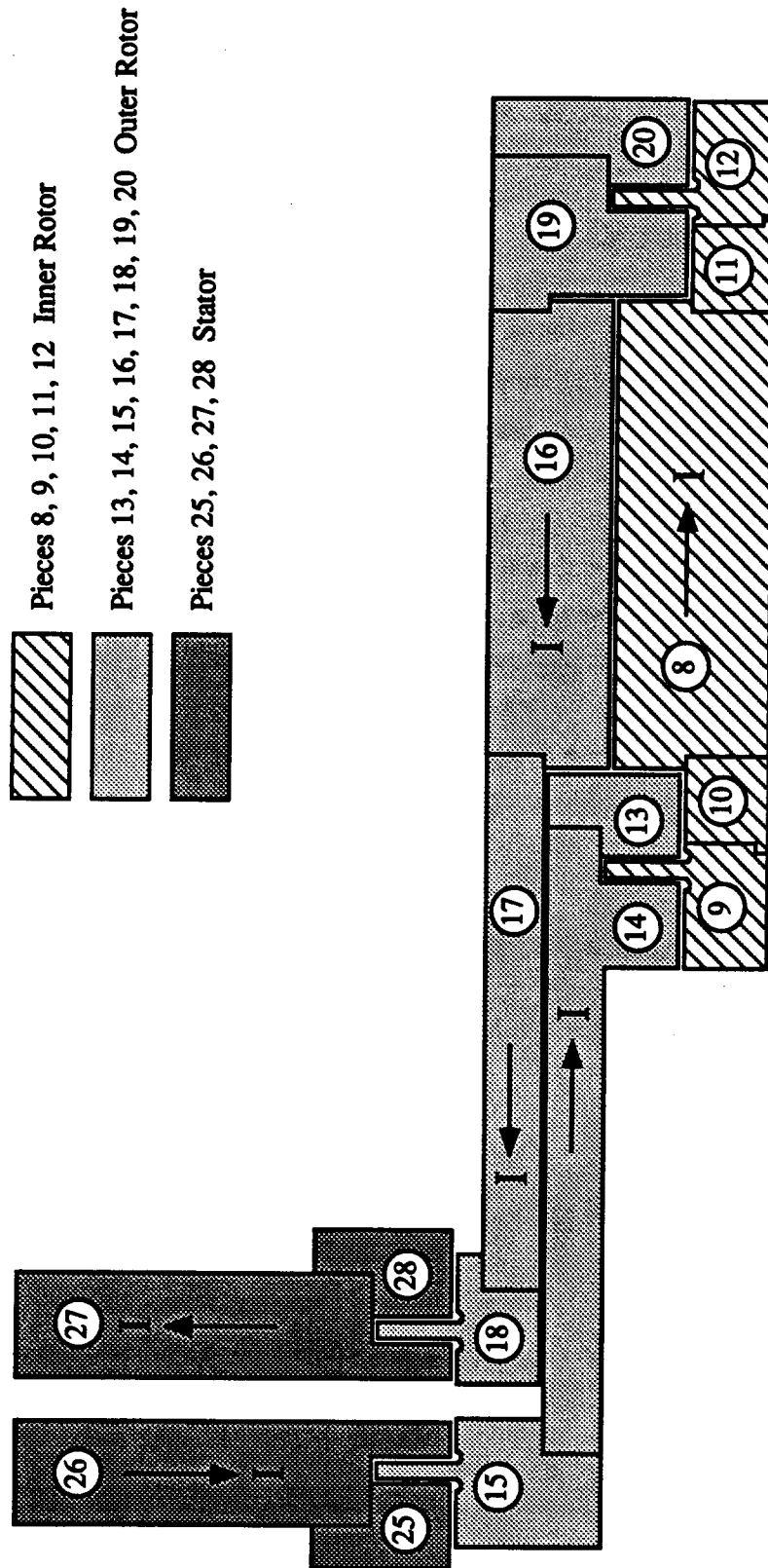


Fig. 4. Electrical Circuit Showing Current Path

COOLING SYSTEM

The motor design features liquid cooling in both the inner and outer rotors, including the bars in the active regions, the current collectors, and the field coils. Baseline design requirements stipulated an armature current of 35,000 amperes at full load, with an overload requirement of 100,000 amperes. In accordance with the decision to design the motor to the overload conditions wherever practicable, the thermal analysis was performed at the 100,000 ampere operating condition.

BEARINGS AND COVER GAS SEALS

The inner rotor is supported by rolling element bearings, pieces 46 and 50, which are mounted internal to the outer rotor stub shafts, pieces 33 and 35. These bearings operate in a contrarotating mode with the outer and inner races rotating in opposite directions. The outer rotor is in turn supported by bearings, pieces 45 and 49, mounted in carriers, pieces 24 and 40, which are mounted in the stationary housings, pieces 39 and 41. These bearings are operated in a single rotating mode with a stationary outer race.

Mechanical face seals with carbon faces running on Al_2O_3 coated runners are required at both ends of the machine to seal the high purity cover gas in the motor. Contrarotating seals, pieces 44 and 48, are fitted between the inner rotor and the outer rotor stub shafts. Single rotating seals, pieces 43 and 47, are also fitted between the outer rotor stub shafts and the bearing housings. Self lubricating lip seals, pieces 103, 104, and 105, are located between the cover gas seals and the bearings to insure that no bearing lubricant contaminates the dry gas seals

SERVICE MODULE

To reduce the risk that a failure in any of the ancillary systems (e.g. cooling system, instrumentation, etc.) could cause damage to or require disassembly of the motor itself, a removable service module contains all required field coil slip rings, instrumentation connections, and cooling fluid seals and unions. The module is a totally separate assembly bolted to the shafts and the bearing housing. Detailed drawings of the service module are included in appendix F.

SLIP RINGS

A slip ring assembly, to provide excitation current to the rotating field coils, is located on the service end of the machine. It is of conventional design using copper slip rings and metal graphite brushes.

DETAILED MACHINE DESIGN

MAGNETIC CIRCUIT

Normally the required electrical characteristics of the motor, along with the desired number of turns, determines the required flux. In this case, the desired overall physical size of the motor dictated the desired flux. With a requirement for 0.1 Webers total flux we could proceed with the magnetic design. Since this is a single turn machine, a quadrupole configuration was chosen, as it provides a symmetric geometry. Each half of the magnetic circuit needed to produce 0.05 Webers of flux. Using the required flux and a flux density of 1.8 Tesla, a magnetic circuit that provided a constant cross sectional area was designed. The required ampere turns in the coil was calculated using the total path length in iron and in air. This rough design was modeled in two dimensions with finite element software. Based on the finite element results, the coil size and iron geometry were adjusted to provide a relatively constant field in the iron while preventing saturation in the highest field areas. Details of the finite element modeling are covered in a later section of this report

Ferrous Conductors

In this machine, iron bars are used to carry the radial magnetic flux as well as the axial load current in both the inner and outer rotor active regions. The advantage of this approach is that the entire volume of the active region is available for both flux and current transport, since the conductors are ferrous. In a slotted design, the functions of current and flux transport are separate with approximately one half of the active region volume available for each function. Because of this combination of functions, the active region of the iron bar design is smaller, thereby reducing the overall machine size. The higher resistivity of iron is mostly compensated for by the increased cross sectional area available for conductor and by the fact that the active region is approximately one half the length of the active region in a slotted design.

Flux-Load Current Interactions

There are interactions between the load current and radial magnetic induction that must be analyzed and accounted for in this design. The axial load current in the bars generates a circumferential as well as an internal magnetic field intensity that effectively reduces the permeability of the iron bars. This occurs because the magnetic field intensity in the material is the vector sum of the radial field intensity from the coils and the internal and circumferential field intensities generated by the load current. The bars are separated from each other by G-10 (glass-epoxy laminate) insulators. These provide

a non ferrous break which reduces the circumferential field produced by the load current. This combination of fields proved to be difficult to model in two dimensions. Due to the geometry of the active region and direction of the fields, unique boundary conditions are required in the finite element model. The modeling was finally done using an in-house developed finite element program, that could utilize the required boundary conditions, interactively with a commercial finite element package. This approach allowed us to accurately model the field interactions in the iron bars. This is described in detail in Ref. 5

Shielding

In a normally conducting design such as this, the shielding serves several functions. First is the minimization of the external stray field. The second is providing a low reluctance path for the main working flux. The low reluctance path is required because of the limited number of ampere turns available from normally conducting field coils. Providing a large enough coil to drive the flux through a large air gap would have significant negative impacts on both machine size and efficiency. The flux shield also serves as the motor's outer housing.

Finite Element Models

Finite element models were used to determine the overall iron dimensions and to verify the final magnetic design. PE2D, a two dimensional nonlinear finite element package from Vector Fields was used for the final analysis. A three dimensional finite element package was available in-house, but the added time and expense of deriving three dimensional models were beyond the scope of this project. The basic iron dimensions were determined by running many models and iterating the dimensions so that the iron would be equally loaded throughout the magnetic circuit. Once the overall dimensions were determined, a more detailed final model was derived to verify that 0.1 Weber of flux would cross the active region of the bars. The dimensions used in the final magnetic model are shown in Fig. 5.

Although the geometry of the motor is basically axisymmetric, there are some localized three dimensional effects such as the flux-load current interaction in the iron bars and voids in the iron due to construction necessities such as screw holes and service holes. Since the finite element package was only two dimensional, these three dimensional effects were accounted for by modifying the iron BH curves at the places where these irregularities occurred. Modifying the BH curves to account for the flux-load interaction was a complex process and is described in detail in Ref. 5. The BH curves for

the voids in the iron were more simply derived by estimating the percentage of void in the iron material for specific regions and then modifying the BH curve for solid 1010 steel for those regions. The formula for deriving a BH point for iron is given by:

$$B' = (\mu s + \mu_0(1 - s)) H \quad (1)$$

were

B = B point for solid 1010 steel

H = H point for solid 1010 steel

B' = Modified B point with void in material

s = Iron fraction of material

$\mu_0 = 1.2566 \times 10^{-6}$ (B = Tesla, H = At / m)

$\mu_0 = 1.0$ (B = Gauss, H = Oersted)

Noting that $\mu = B / H$ equation (Eq.1) can be rewritten as

$$B' = (B s + H (1 - s) \mu_0) \quad (2)$$

Six regions were identified as having a lower permeability due to voids in the steel, and are shown in Fig. 6.

They are:

- 1: (Mate 4, 96%) The area of the inner rotor core just inside the field coil which has slots for the field coil leads.
- 2: (Mate 8, 95%) The screw holes above the outer rotor bars and inside the inner rotor bars that attach the rotor bars to the steel rotor cylinders.
- 3: (Mate 7, 75%) The area around the screw heads of 2.
- 4: (Mate 10, 65.4%) The area above the screw heads in the outer rotor cylinder.
- 5: (Mate 6, 55%) The outer rotor flux return ring which has cutouts for the copper of the outer rotor to carry the load current to the outer rotor collectors
- 6: (Mate 9, 27.3%) The area below the screw heads in the inner rotor cylinder.

The BH curves used for these regions are tabulated in table 1, and a flux plot from the model solution is shown in Fig. 7. The three dimensional effects did not reduce the total flux as much as was expected. The total reduction was only about 5% from the runs assuming solid steel. The final finite element solution predicted a total flux of 0.104 Weber.

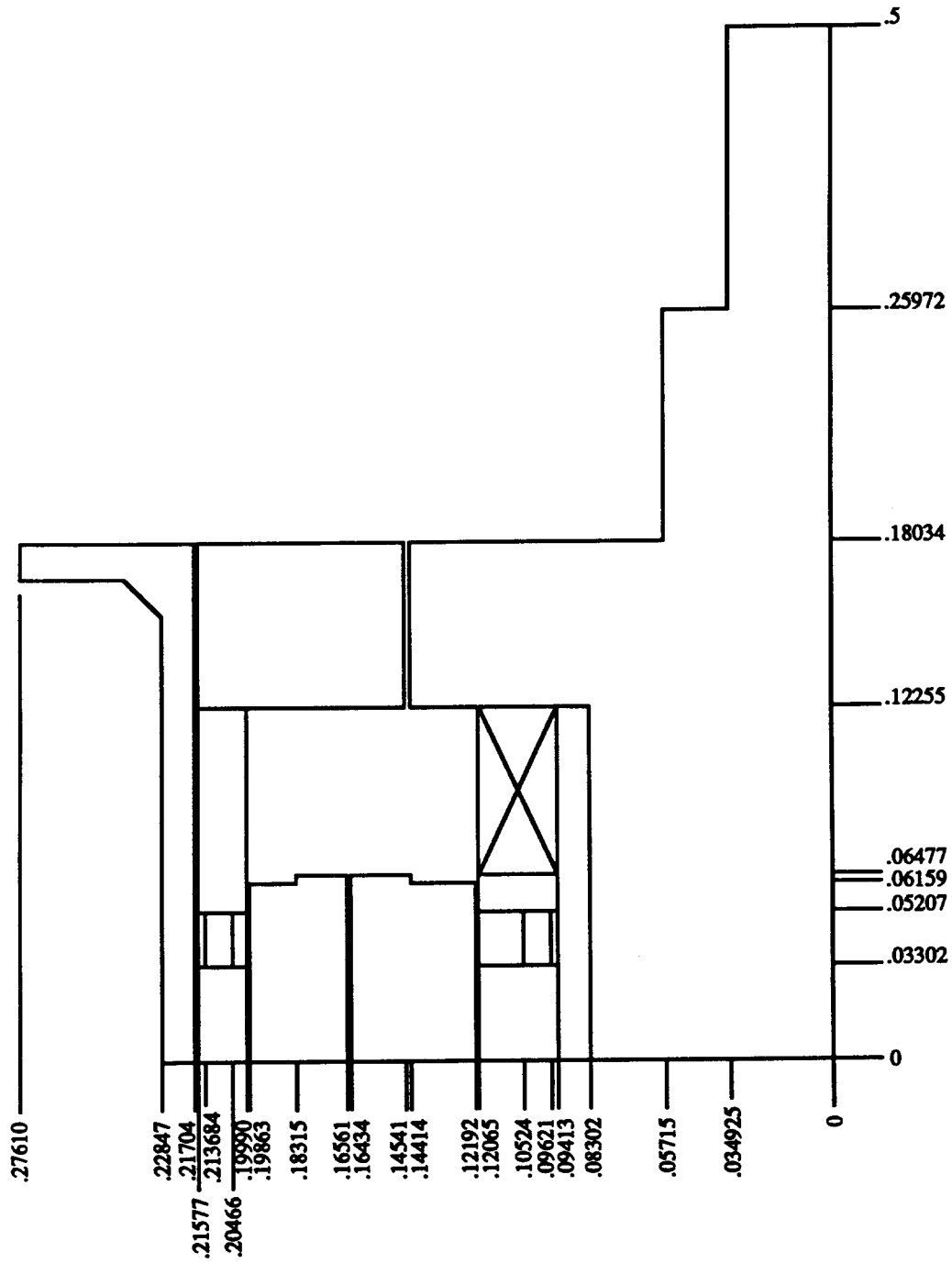


Fig. 5. Finite Element Model Dimensions

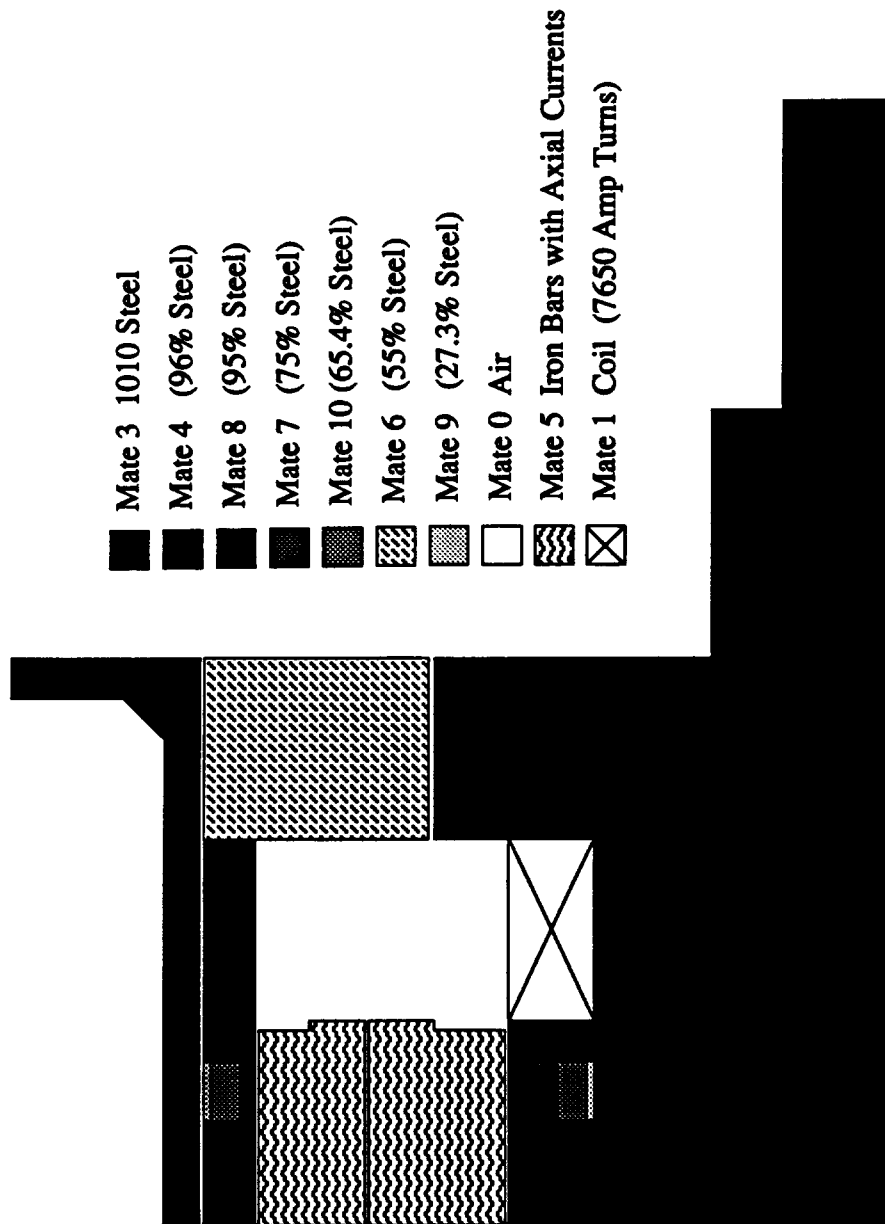


Fig. 6. Permeability Regions

Table 1. BH Curves for 1010 Steel With Air Voids

Field in Oersteds	Magnetic induction in Gauss						
	(100% is all Iron and no Air)						
	MATE=3	MATE=4	MATE=8	MATE=7	MATE=10	MATE=6	MATE=9
	100%	96%	95%	75%	65.4%	55%	27.3%
0.00	0	0	0	0	0	0	0
2.24	8944	8587	8497	6709	5850	4920	2443
3.70	12000	11520	11400	9001	7849	6602	3279
6.30	14000	13440	13300	10502	9158	7703	3827
10.01	15000	14400	14251	11253	9813	8255	4102
22.56	16000	15361	15201	12006	10472	8810	4384
35.97	16500	15841	15677	12384	10803	9091	4531
55.08	17000	16322	16153	12764	11137	9375	4681
75.95	17500	16803	16629	13144	11471	9659	4833
102.06	18000	17284	17105	13526	11807	9946	4988
133.01	18500	17765	17582	13908	12145	10235	5147
171.00	19000	18247	18059	14293	12485	10527	5311
216.45	19500	18729	18536	14679	12828	10822	5481
266.00	20000	19211	19013	15067	13172	11120	5653
336.20	20500	19693	19492	15459	13523	11426	5841
424.20	21000	20177	19971	15856	13881	11741	6041
480.25	21250	20419	20212	16058	14064	11904	6150
550.40	21500	20662	20453	16263	14251	12073	6270
659.02	21750	20906	20695	16477	14453	12259	6417
829.40	22000	21153	20941	16707	14675	12473	6609
1250.00	22500	21650	21438	17188	15148	12938	7051
1774.50	23069	22217	22004	17745	15701	13486	7588
2666.20	23996	23143	22930	18664	16616	14398	8489
5341.20	26706	25851	25638	21365	19314	17092	11174
10690.00	32070	31215	31001	26725	24673	22449	16527
26741.00	48134	47278	47064	42786	40732	38507	32581
42790.00	64186	63330	63116	58837	56783	54558	48631

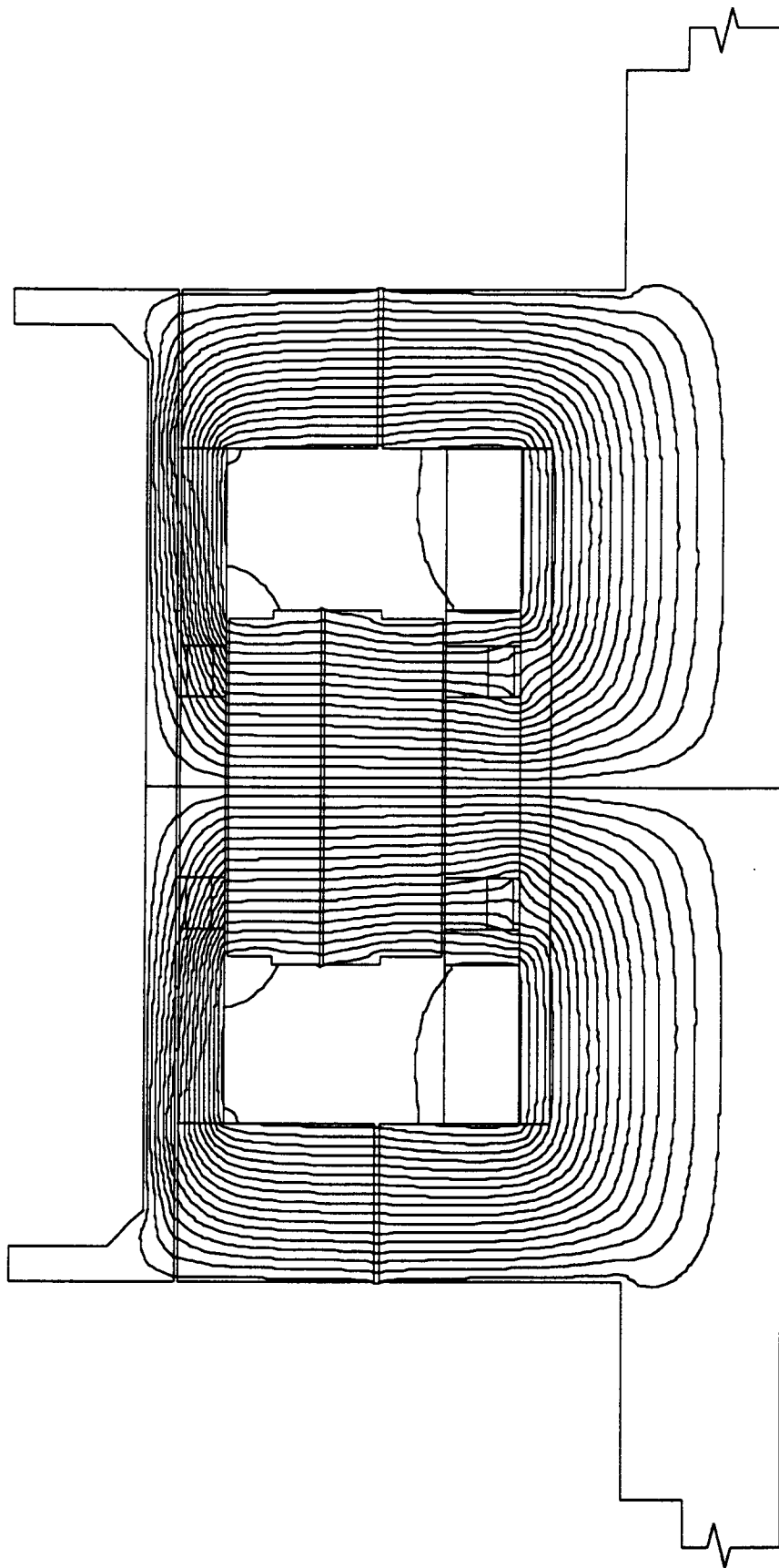


Fig. 7. Magnetic Circuit with Superimposed Flux Plot

FIELD COILS

Each coil consists of 34.5 turns of hollow copper conductor wound in the form of a solenoid, producing 7650 ampere turns. The total effective magnetic flux produced is 0.104 Webers. The coils have a calculated DC resistance of $0.0267\ \Omega$ and a calculated free air inductance of 253 μH . At the operating current of 222 amps, each coil will have a terminal voltage of 5.93 volts and dissipate 1.3 kW. Coolant flows through the hollow conductors to remove the generated heat. The coils are connected electrically in series to minimize the current carried by the slip rings. The cooling circuits are in parallel to minimize the required coolant supply pressure. The coils were manufactured by Mohler Technologies Inc. of Boonville, Indiana. The detail design of the coils can be found on drawing A27-19992-13 in appendix E.

Conductor

The conductor used for the coils is square copper, OFHC 102 alloy, 0.218 in. on a side. It has a round hole 0.174 in. in diameter for coolant flow and is custom extruded. Due to the small size of the coils and limited number of turns, one continuous length of conductor could be used for each coil, thereby eliminating joints within the coils.

Insulation

The individual conductors are wrapped with half lap turns of .007 in mica paper/glass tape impregnated with B-staged epoxy resin. The final conductor insulation thickness is .014 in. on a side. The coil ID, OD, and both ends have ground wall insulation consisting of cross ply glass and B-staged epoxy resin per MIL-P-25421, Rev B. After winding, the conductor and ground wall insulation is oven cured. During curing, the B-staged epoxies flow together forming a solid composite. Both the conductor insulation and the ground wall insulation are class F with a test voltage rating of 1,500 volts.

Lead Configuration

Two coil leads, consisting of extended conductor, are provided 180° apart. Both leads are bent inward so that they are at the same radius and can clear the bore of the other coil. An adapter is soft soldered to the ends of the leads. This adapter provides a round surface for the terminal clamps to attach to as well as a barbed end for the coolant hose connections. The terminal clamps are bolted to, but insulated from, the inner rotor. This provides mechanical support for the coil leads.

ELECTRICAL CIRCUIT

With a known flux, the electrical parameters of the machine can be determined. The terminal voltage of single turn homopolar motor is given by:

$$V = \frac{\Phi N}{60} \quad (3)$$

Where Φ is the flux cut by the rotor per revolution and N is the differential rotor speed in revs/min. For this motor the flux is 0.104 webers; therefore the terminal voltage is:

$$V = \frac{0.104N}{60} \quad (4)$$

At the nominal design speed of $\pm 1,200$ RPM this results in a open circuit terminal voltage of 4.16 volts.

Inner Rotor

The electrical circuit of the inner rotor consists of 32 iron bars, piece 8, two copper transition rings, pieces 10 and 11, and two current collector rings, pieces 9 and 12. The iron bars conduct the current through the active region of the machine. The bars, which are trapezoidal in cross section, are fastened to the inner rotor cylinder, piece 3. The bars are separated from each other by G-10 (glass-epoxy laminate) insulators. In a multi-turn motor these would provide the electrical isolation between circuits. They also provide a non-ferrous break as previously described. The outer surface of the inner rotor cylinder is plasma sprayed with a 0.015 in thick coating consisting of a mixture of aluminum oxide and titanium dioxide (Al_2O_3 and TiO_2) for electrical isolation. Bolts with insulated shanks and insulating washers, pieces 60 and 63, are used to secure the bars to the inner rotor cylinder. The copper inner rotor transition rings are brazed to the ends of the bar assembly. These rings have pockets machined in the inner face to accommodate the cooling tube U-bends, piece 57 and have tapped holes on the outer faces to which the current collector disk bolt. The mating faces of the transition ring and the collector disk are gold plated to minimize contact resistance. The cross sectional area of the bars is 50.8 square inches. This results in a current density of 688 amps/square inch at 35,000 amps and 1967 amps/square inch at 100,000 amps.

Outer Rotor

The electrical circuit of the outer rotor consists of 36 iron bars, piece 16, two copper current collector channels, pieces 14 and 19, the copper outer rotor outer drum, piece 17, and two terminal collector disks, pieces 15 and 18. The bar assembly has a copper current collector, piece 19, brazed on one end and the outer rotor outer drum, piece 17, brazed to the other end. This assembly is insulated with glass-epoxy on its OD and is bolted to the ID of the outer rotor cylinder, piece 22, with insulated bolts and washers, pieces 59 and 63. The service end terminal collector disk, piece 15, is bolted to the end of the outer rotor service end collector, piece 14, and the drive end terminal collector disk is bolted to the end of the outer rotor outer drum, piece 17. The mating faces are gold plated as on the inner rotor.

Terminals

Two terminal collectors, pieces 26 and 27 are fitted between the motor housing, piece 37, and the service end, end plate housing, piece 39. The collectors are insulated from each other and from the housing with bonded on G-10 (Glass-epoxy laminate). Each collector has 4 input terminal ears, that protrude through the terminal housing, piece 38, that are the motor's input terminals.

CURRENT COLLECTORS

The collectors used in this machine are close clearance liquid metal braid type collectors. These collectors have only been used in single rotating applications at CDNSWC in the past. There are some fluid flow and stability questions concerning operation of these collectors in a contrarotating mode that were addressed as part of this project. The collector development is being approached both theoretically and by test rig evaluations of candidate current collectors. The results of these evaluations will be used to select the final current collector configuration for both the single and contrarotating collectors in this design. Details of these studies can be found in Ref. 6

COOLING SYSTEM DESIGN AND ANALYSIS

Inner Rotor

The inner rotor bar set is the critical portion of the inner rotor from a thermal perspective. Appendix A documents the detailed thermal analysis performed on the inner rotor bars.

Selecting cooling hole diameter and number of parallel paths

The criterion for selecting the diameter for the cooling hole was to choose the minimum cooling hole size that would adequately cool the bars while preserving the maximum iron cross section to carry the current. This also minimizes the power loss in the armature circuit. Figs. 8–13 display how the film drop and fluid changes in temperature are affected by varying the diameter of the cooling passage. The figures show the results for 40 and 80 psi pressures as well as different numbers of parallel paths. Increasing the diameter decreases the fluid temperature change at a higher rate than the film drop temperature, because the film drop varies linearly with diameter (surface area) and the change in fluid temperature varies with the square of the diameter (cooling hole cross sectional area).

The graphs also shows how the temperature changes are affected by the number of parallel paths in the system. For one parallel path, the coolant must make a series run through all the bars before returning to the heat exchanger. By increasing the number of cooling paths, the change in fluid temperature (less heat to be removed per cooling loop) declines more than the film drop (less heat to be removed per cooling loop but surface area is also decreased). Fig. 14 shows how the film drop temperature varies with diameter and pressure.

Based on the above information, a diameter of .25" with 2 parallel paths was chosen to cool the rotor bars. This diameter size provided a good flow rate, used minimum iron bar area, and had the proper U bend radius for construction purposes. Fig. 15 displays the film drop temperature verses pressure and flow for 2 parallel paths and .25" diameter. The film drop is the driving parameter in determining rotor bar temperature.

Outer Rotor

The outer rotor bar cooling analysis is very similar to the inner rotor bar analysis. The only relevant difference is that the outer rotor has 36 bars each of a smaller cross section resulting in a greater cooling passage length. This results in increased pressure drop as well as increased surface area. However, the heat generation in the outer rotor is the same as the inner rotor since the total current, area, and active length for both rotors are the same. Appendix B shows the differences between the inner and outer rotor calculations.

Fig. 16 shows the film drop of the outer bars for various flow rates at 2 parallel passes and a diameter of .25". The film drop for the outer rotor is a few degrees lower than for the inner rotor under the same conditions. Although the pressure drop is higher

due to the greater number of bars, the surface area also increases, and it has a larger effect on the film drop than does the pressure drop. The change in bulk fluid temperature increases for the outer rotor compared the inner rotor results, but it is still small in magnitude when compared to the film drop.

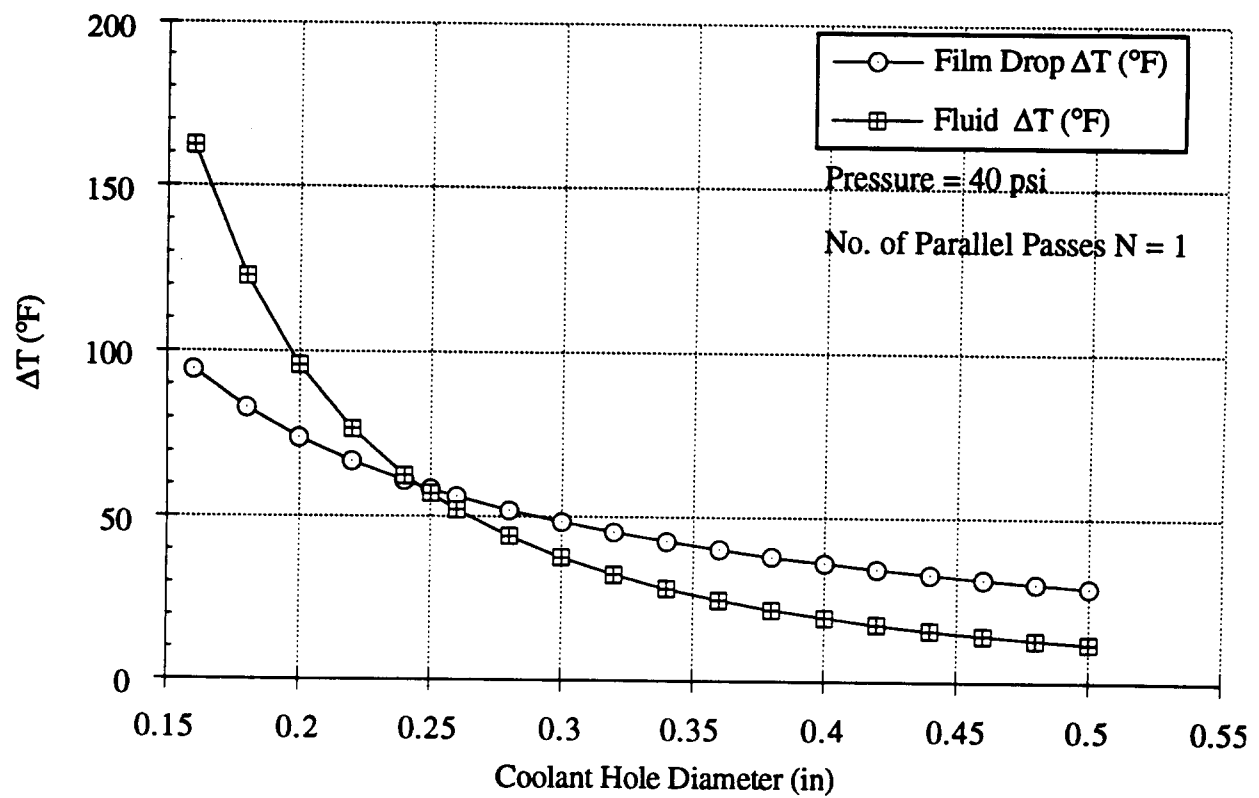


Fig. 8. ΔT Vs. Diameter, N= 1, 40 psi

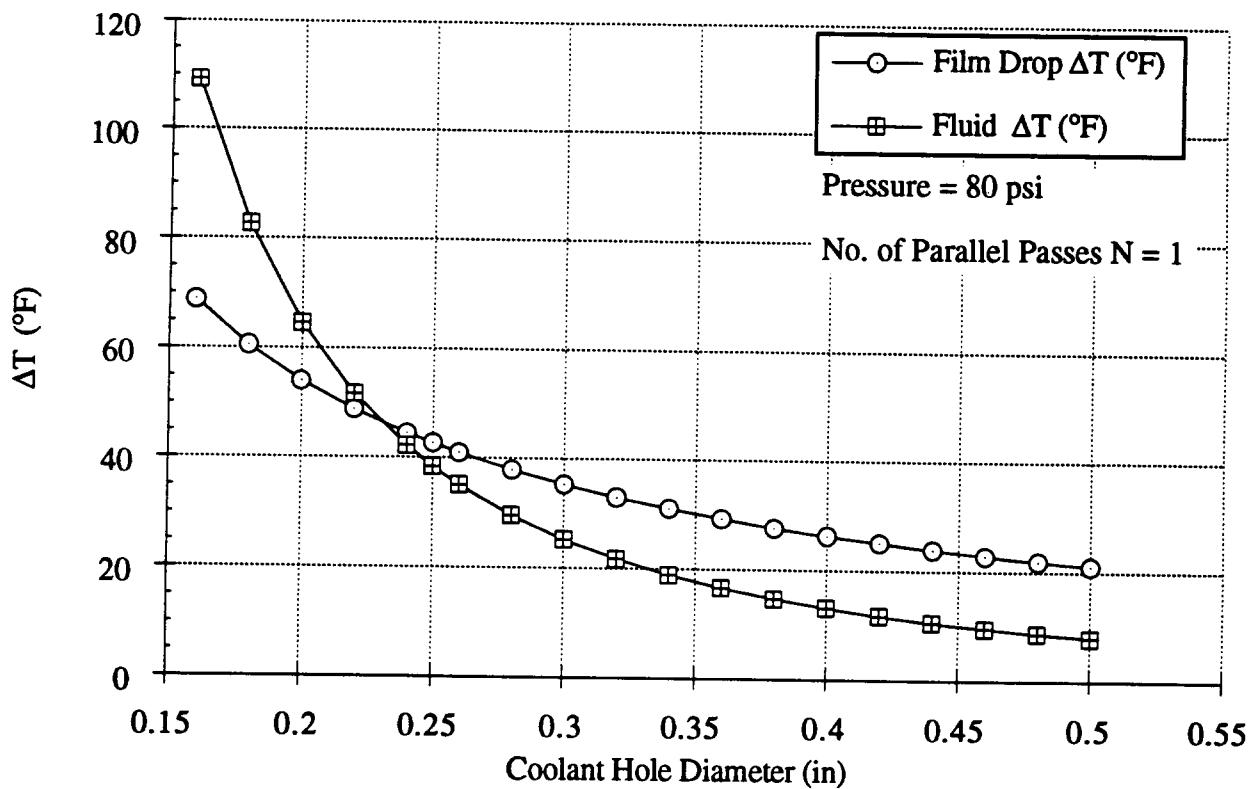


Fig. 9. ΔT Vs. Diameter, N= 1, 80 psi

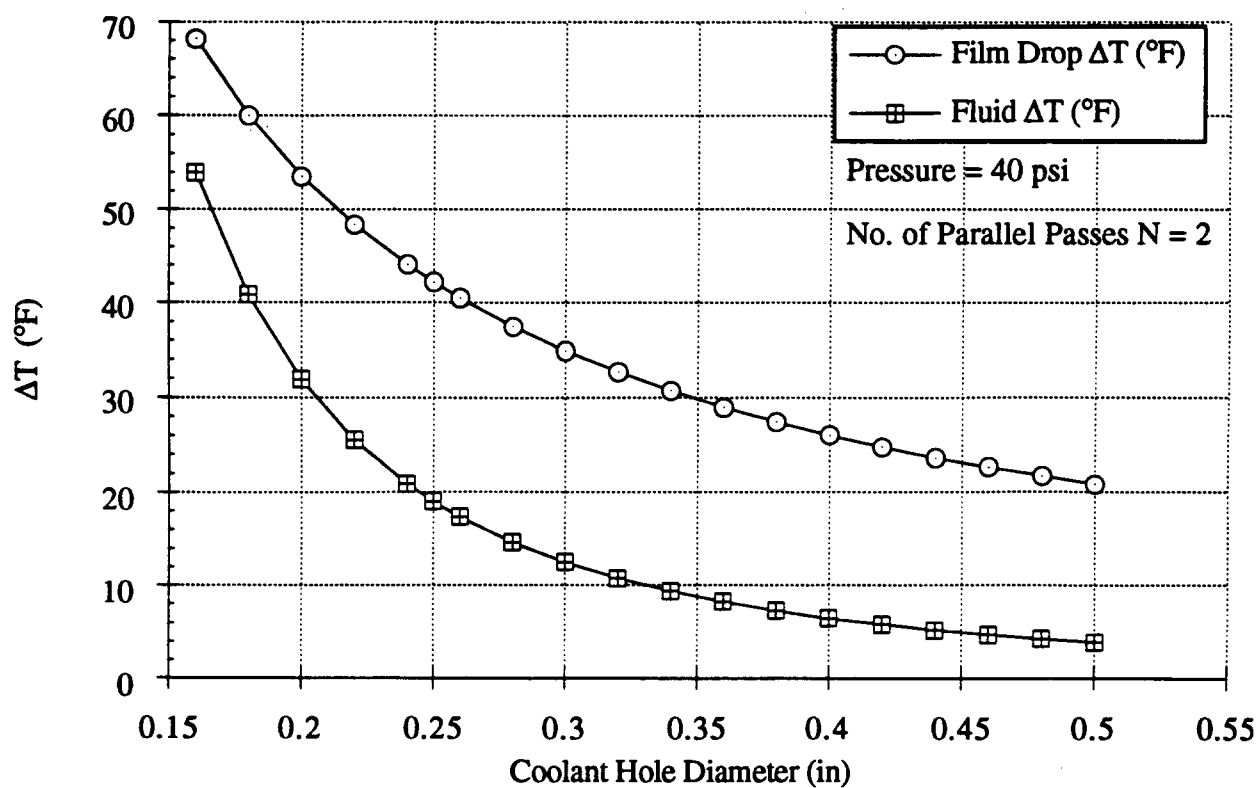


Fig. 10. ΔT Vs. Diameter, N= 2, 40 psi

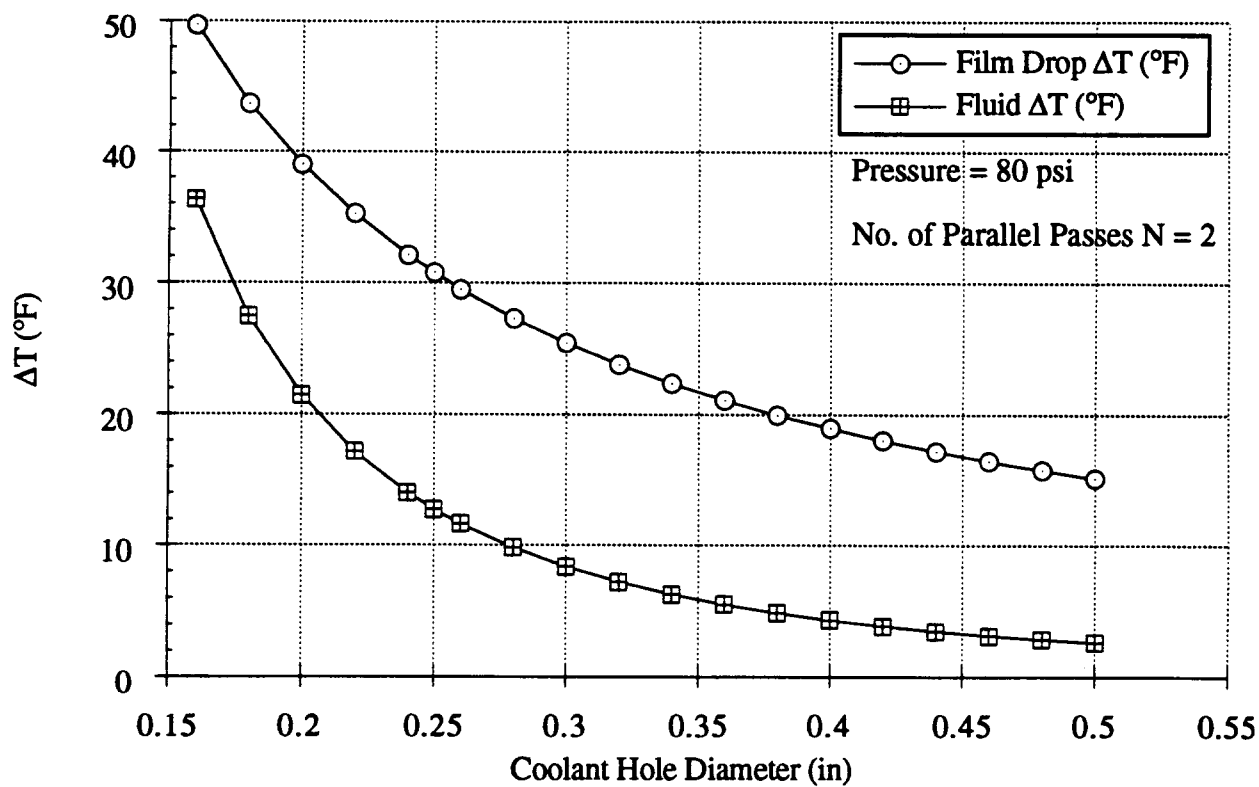


Fig. 11. ΔT Vs. Diameter, N= 2, 80 psi

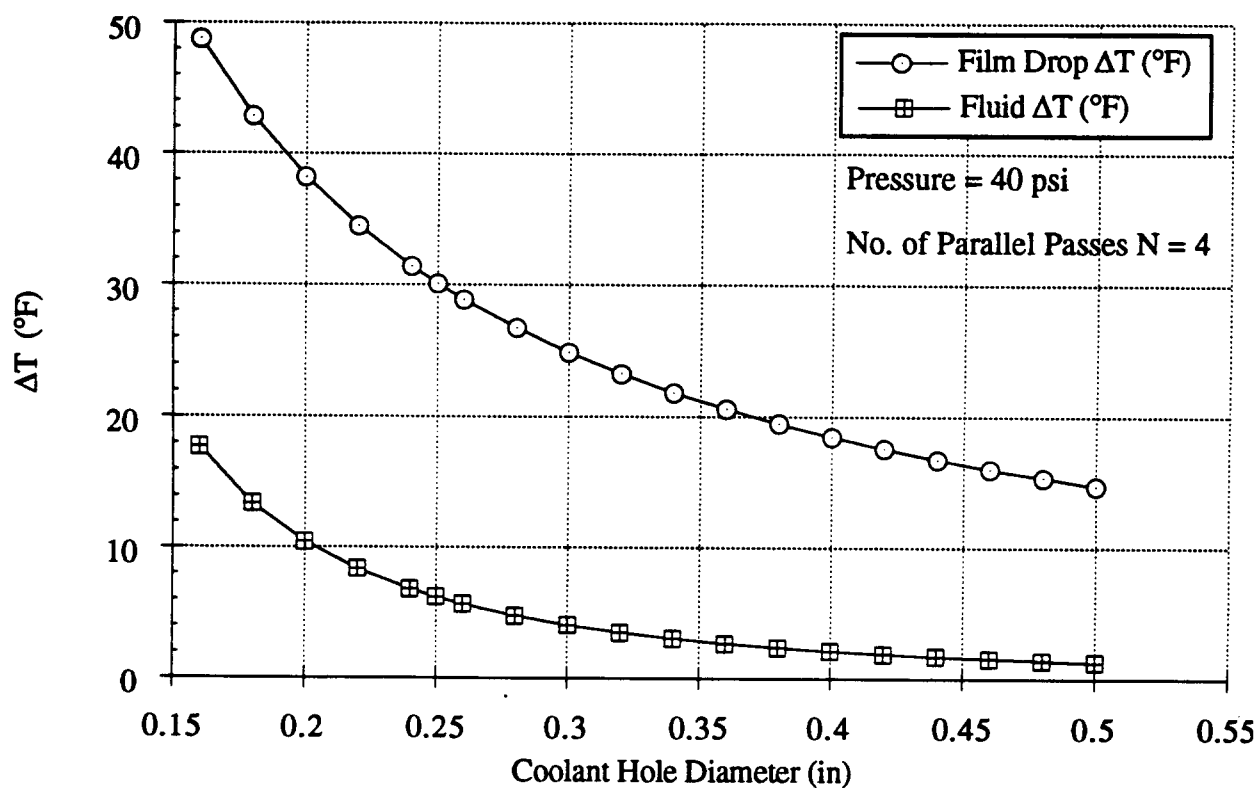


Fig. 12. ΔT Vs. Diameter, $N = 4$, 40 psi

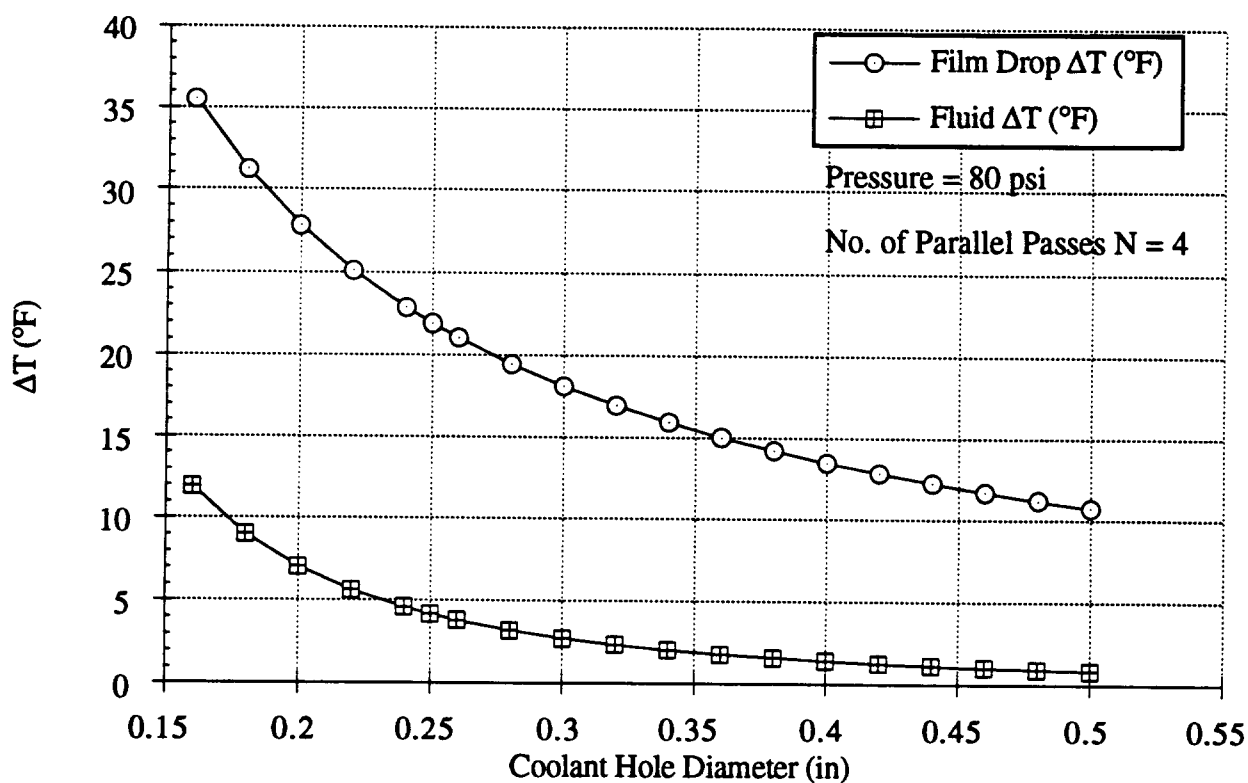


Fig. 13. ΔT Vs. Diameter, $N = 4$, 80 psi

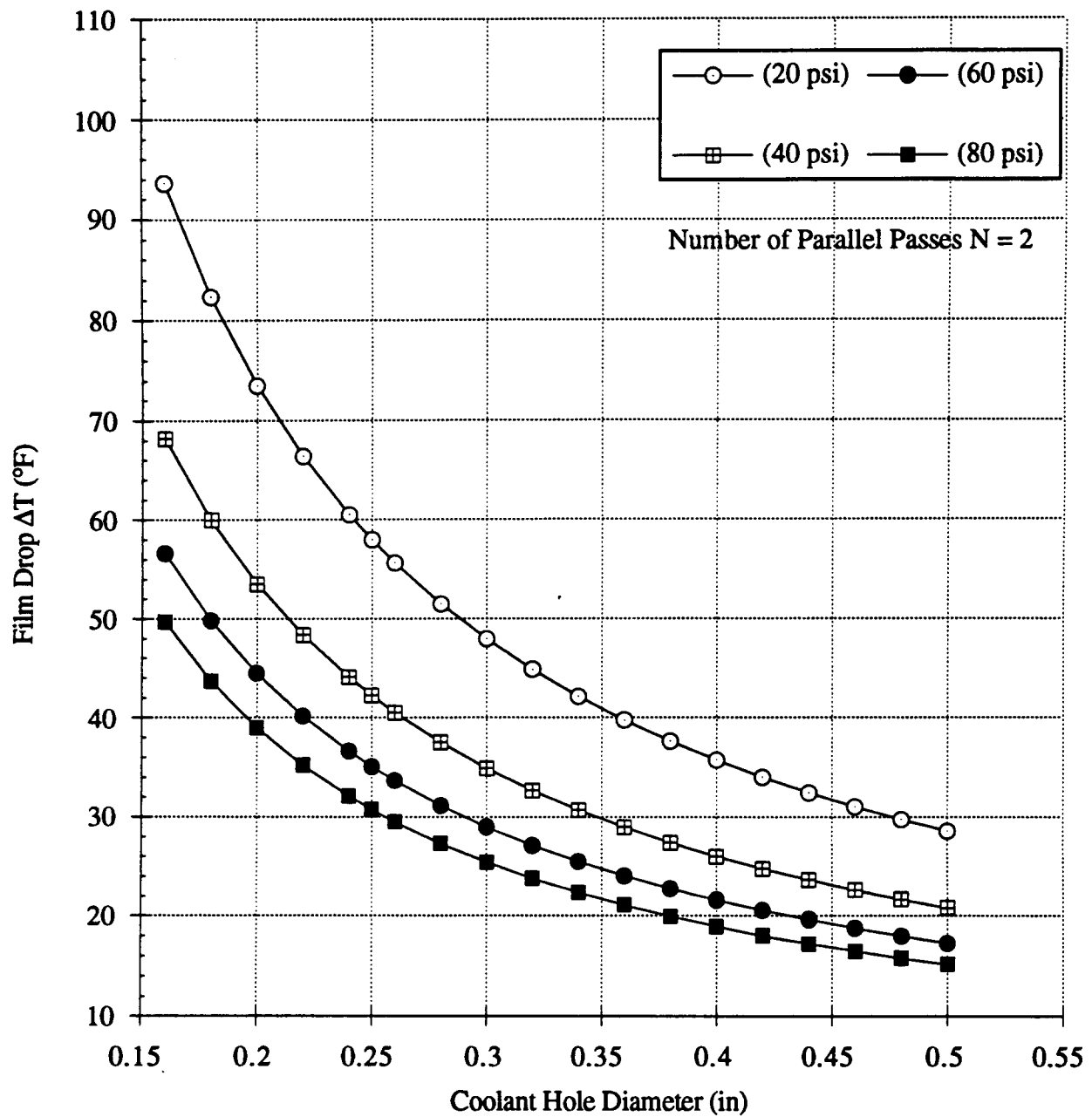


Fig. 14. Inner Rotor Film Drop Vs. Diameter (32 Bars)

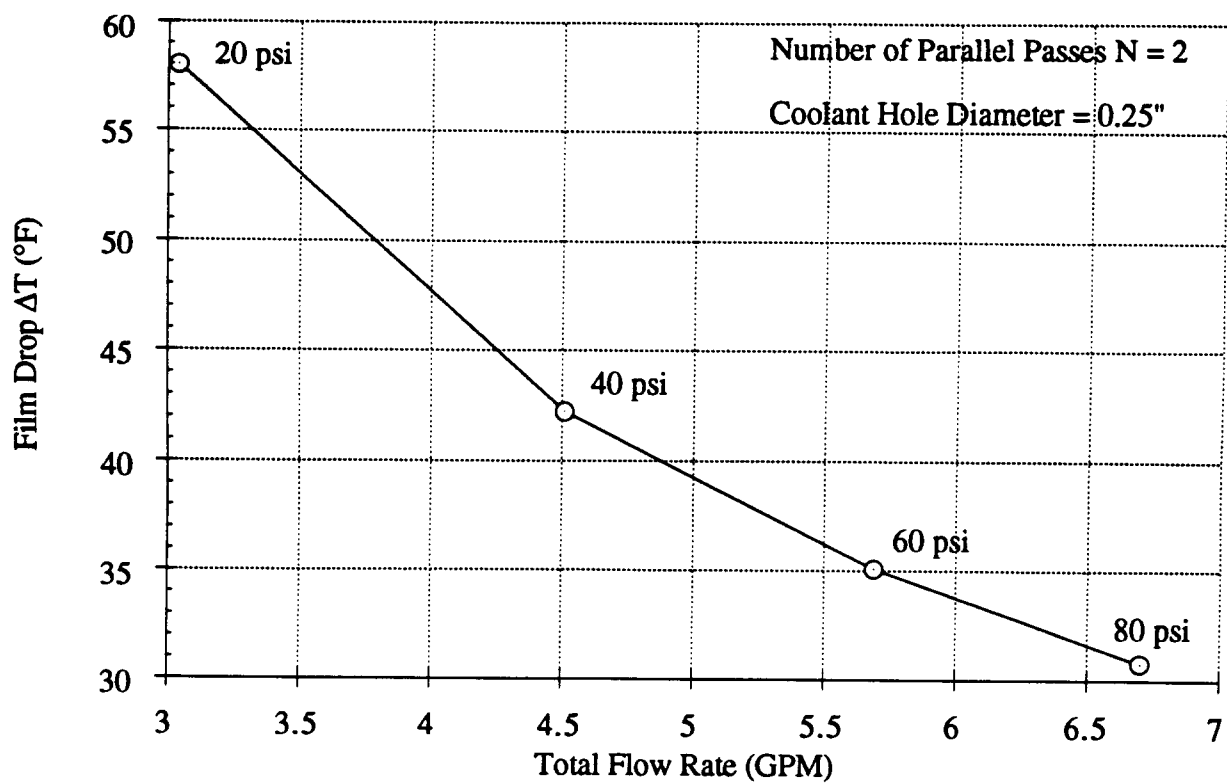


Fig. 15. Inner Rotor Film Drop ΔT Vs. Flow Rate

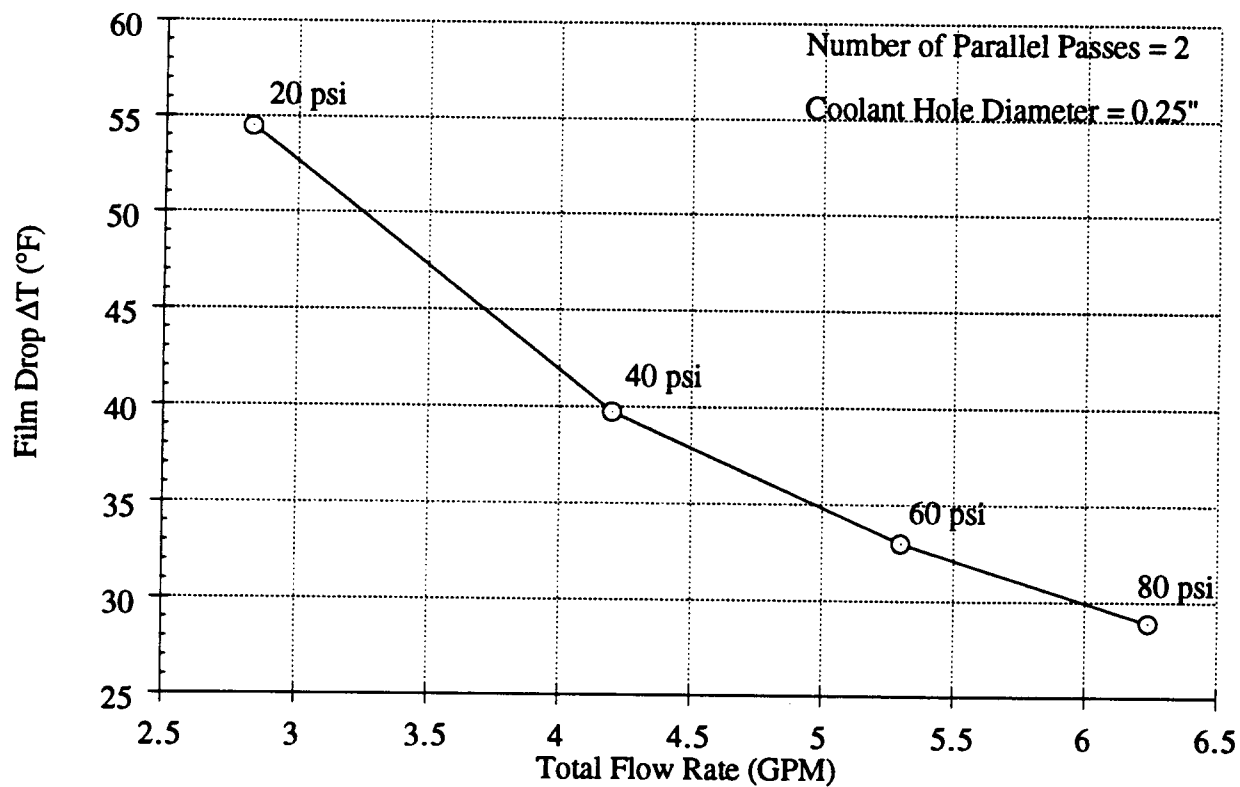


Fig. 16. Outer Rotor Film Drop ΔT Vs. Flow Rate

Terminals

Each of the terminal collector rings are cooled by four soldered-in 5/16 in copper tubes. Since these are completely outside the cover gas region of the motor, water will be used as the coolant. The tubing provides 70 in² of surface area per ring which, when water cooled, should be more than adequate for the anticipated heat load. No detailed thermal analysis of the terminal cooling was performed.

Field coils

Appendix C documents the thermal analysis procedure used in designing the field coils.

Equations 1a through 7b of Appendix C were analyzed to determine which combination of parameters resulted in the lowest change in temperature for the cooling fluid. The change in fluid temperature was the driving parameter in determining the cooling hole size and flow rates.

Fluids

Figs. 17 and 18 show the differences in thermal performance (ΔT_{fl}) between Coolanol™ 20 and Coolanol™ 40 heat transfer fluids at 20 and 60 psi of pressure. Since the Coolanol™ 20 produces approximately 25 °F less temperature change of the fluid than the Coolanol™ 40 (due to its lower viscosity), it is the fluid chosen to cool the coils.

Geometry

Both the square and round cooling holes were evaluated over a range of cross sectional areas for 20 and 60 psi pressures as shown in Figs. 19 and 20. For a fixed current, the electrical losses are dependent on the cross sectional area of conductor, but the cooling capacity is dependent on the flow rate, which in turn is dependent on the hole area. When the area of the hole is small compared to the area of the conductor, incremental increases of the hole dimension yield a large percentage increase in flow area and a small percentage decrease in conductor area. As hole dimension becomes significant compared to the overall dimensions of the conductor, incremental increases of the hole dimension result in small percentage increases in the coolant flow area but large percentage decreases in the conductor area. Since the round hole offers better thermal performance due to the higher flow rate (9.4%) it provides for the same cross sectional area and pressure drop, the round hole was chosen for the geometric shape of the cooling hole. The optimum diameter for the round hole (based on lowest temperature change of

the fluid) is found to be $d = 0.185$ " as shown in Fig. 21. For reasons of wall thickness and availability of tubing a hole size of 0.174" was chosen. The difference in performance is not significant as can be seen in Fig. 21. The analysis also revealed that the optimum diameter is only a function of geometric parameters, and is not dependent on fluid properties or the magnitude of the heat load. A diameter smaller than optimum results in a higher temperature rise due to the low flow rate for a given pressure drop. Conversely, a larger than optimum hole will produce a higher temperature rise of the fluid since the reduction in copper area increases the I^2R losses more rapidly than the increase in coolant flow rate can compensate for.

The change in fluid temperature (ΔT_{fl}) is dependent on the hole area, while the film drop (ΔT_{fd}) is dependent on the surface area of the cooling hole. Fig. 22 shows the film drop temperature difference (round hole) versus diameter for various pressures. For a diameter of $d = .174$ " the largest film drop is 8.5 °F at 20 psi (lowest pressure considered). Since the film drop is small in magnitude compared to ΔT_{fl} there is no need to be concerned about this parameter.

Based on equations 8 through 12 of Appendix C Figs. 23–25 show the relationship between pressure and flow rate and how they affect the change in temperature of the fluid.

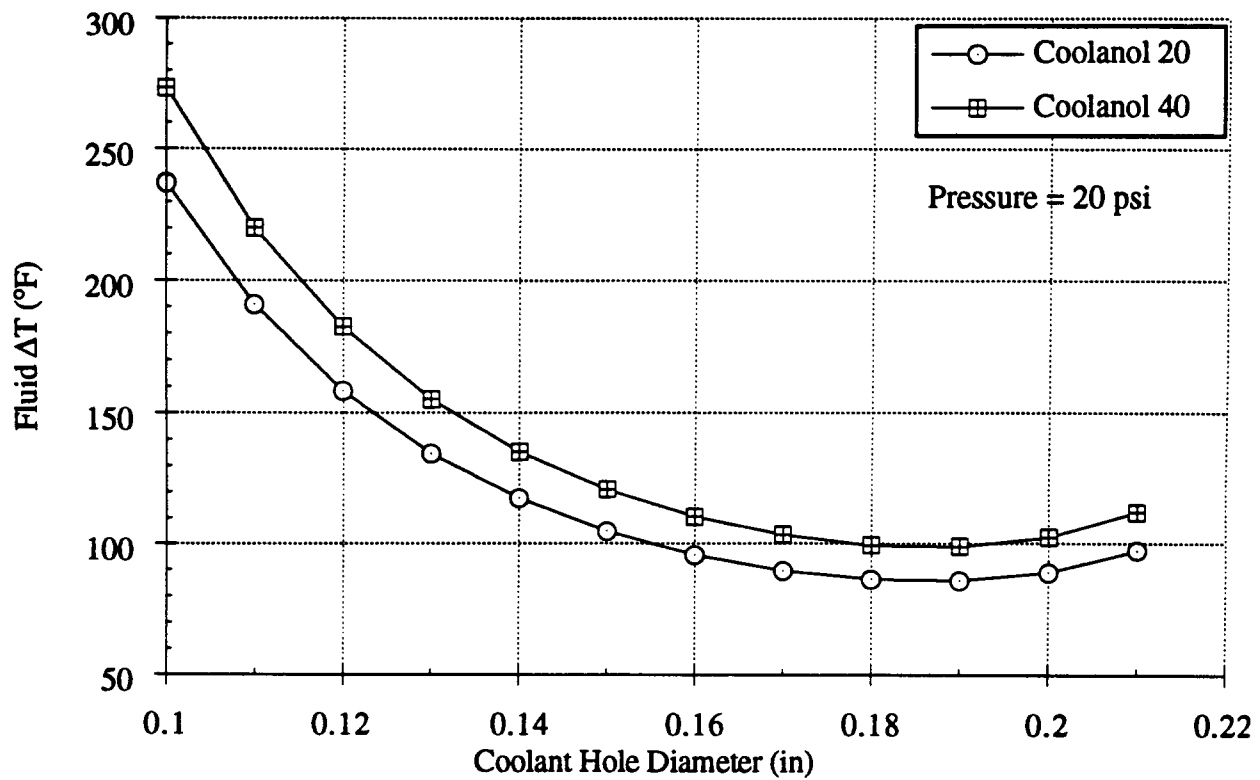


Fig. 17. Fluid ΔT Vs. Hole Dia. for Coolanol 20 and 40 at 20 psi

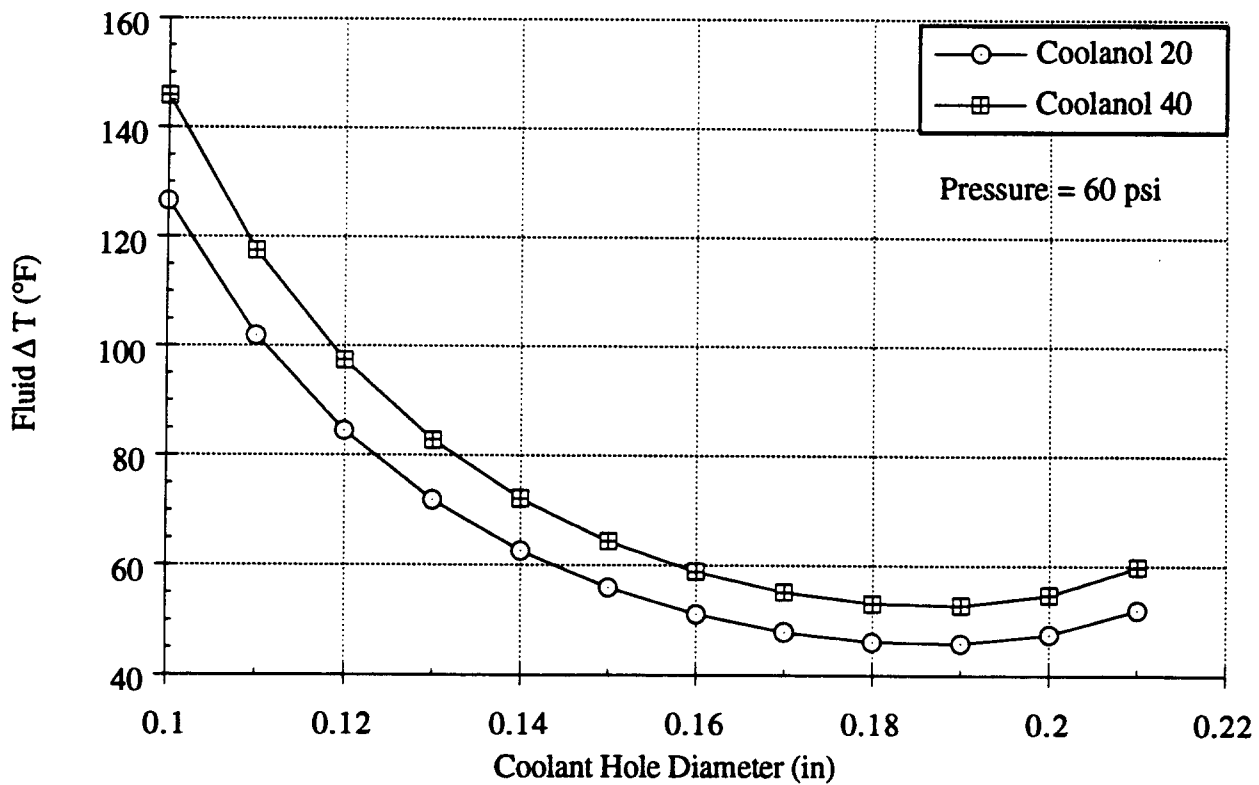


Fig. 18. Fluid ΔT Vs. Hole Dia. for Coolanol 20 and 40 at 60 psi

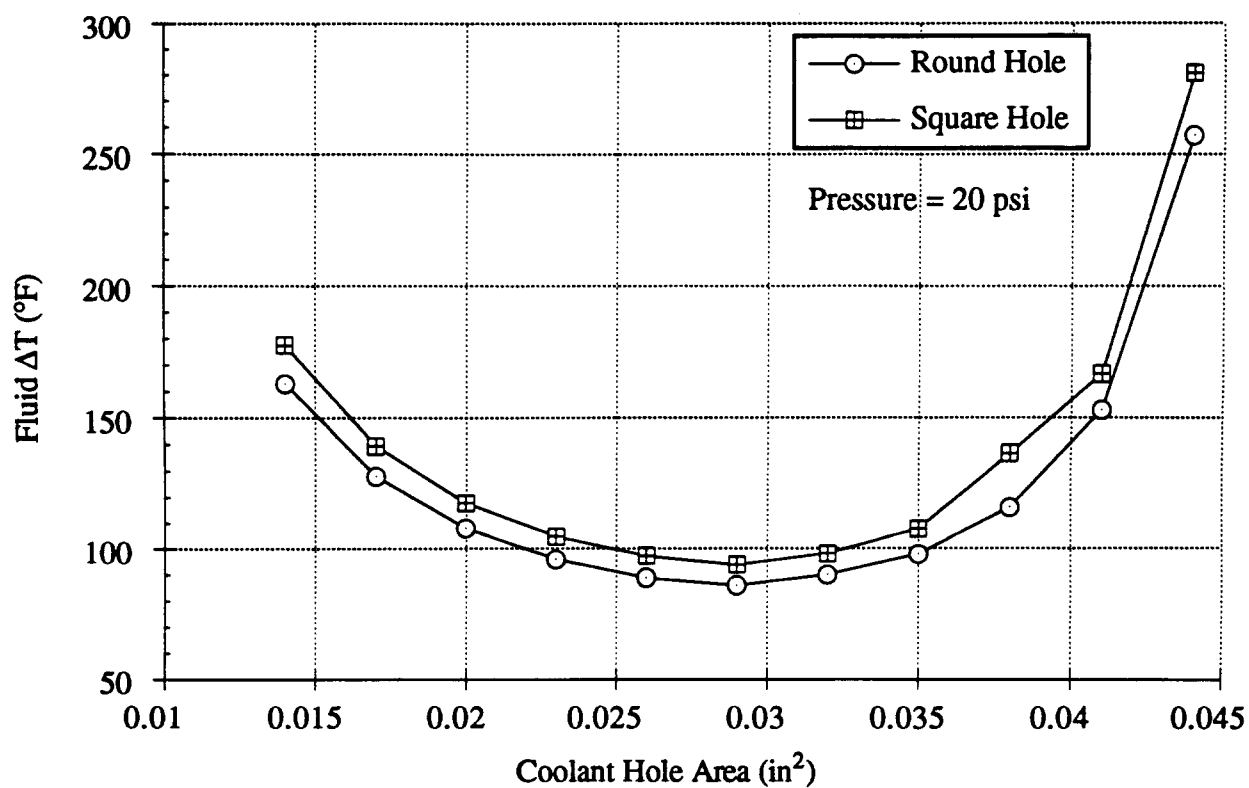


Fig. 19. Fluid ΔT Vs. Coolant Hole Area at 20 psi

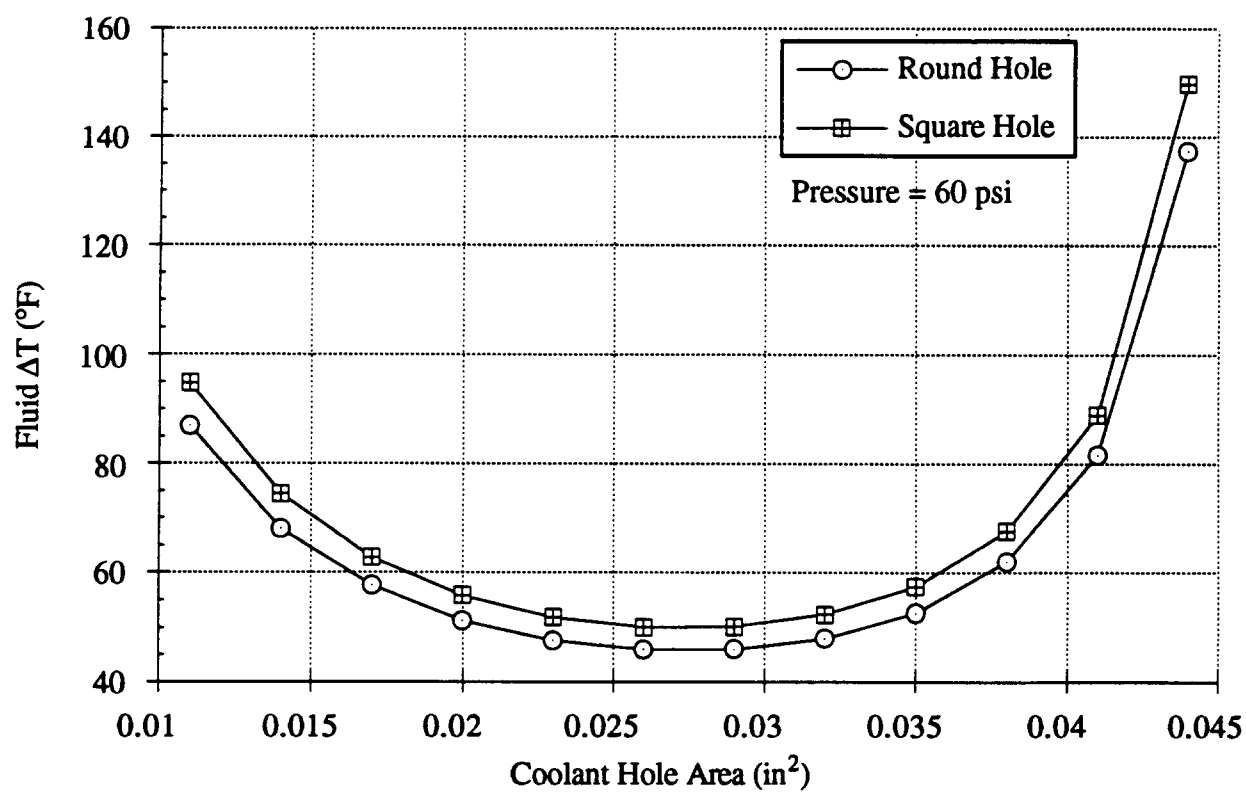


Fig. 20. Fluid ΔT Vs. Coolant Hole Area at 60 psi

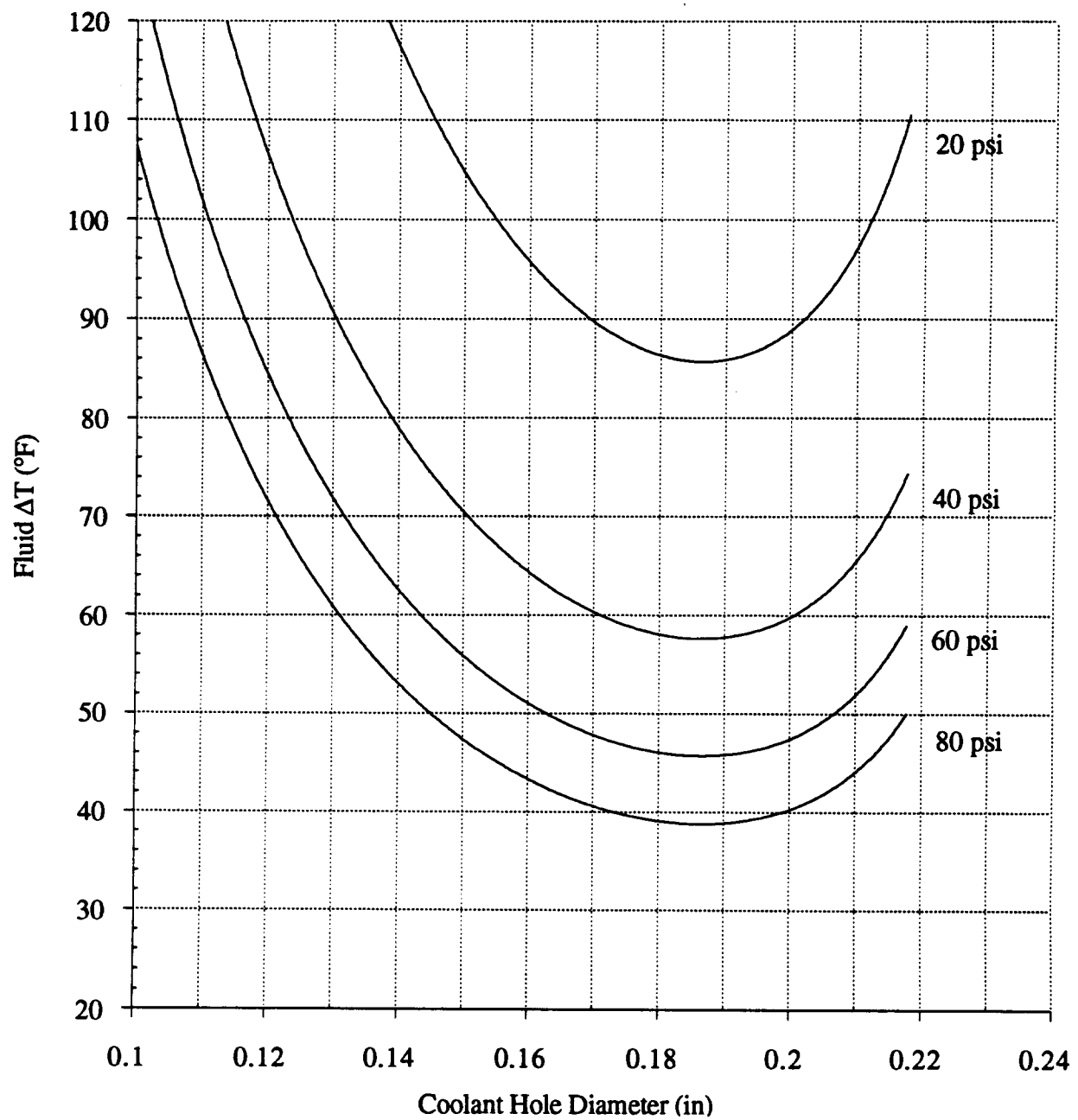


Fig. 21. Fluid ΔT Vs. Coolant Hole Diameter

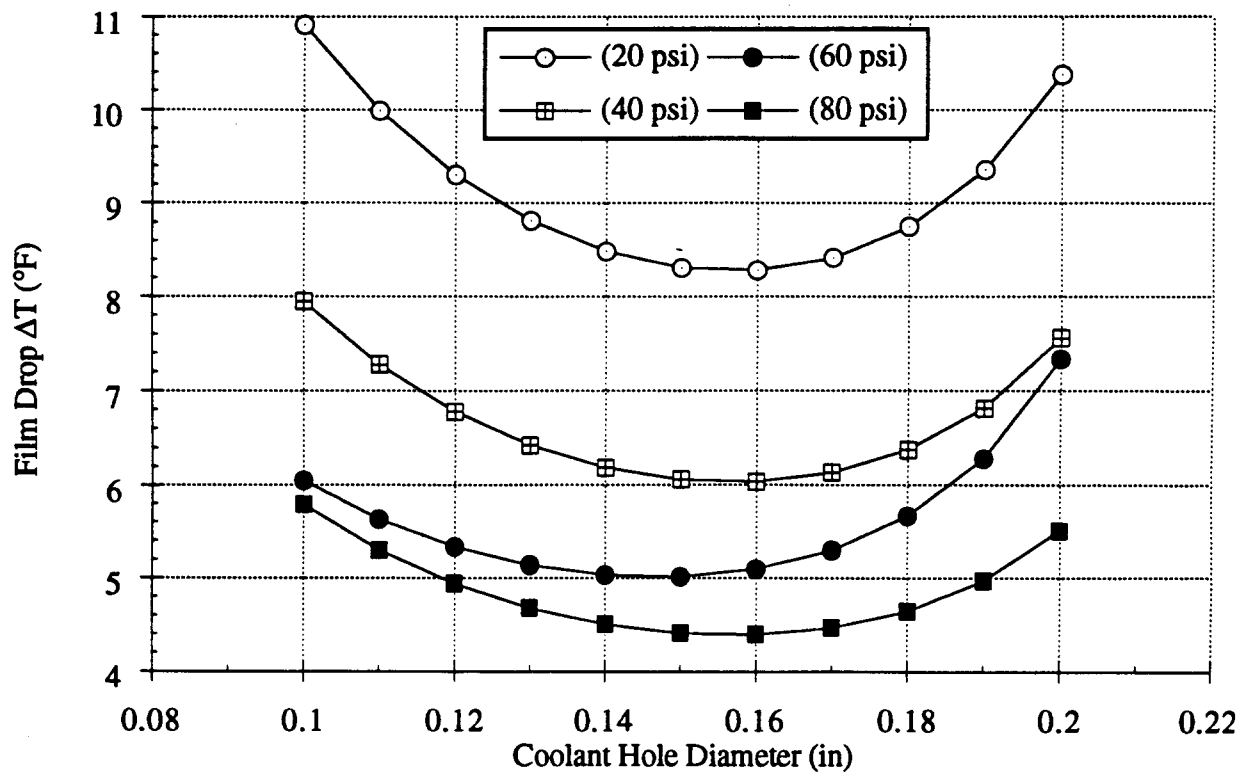


Fig. 22. Film Drop ΔT Vs. Diameter at 20, 40, 60, and 80 psi

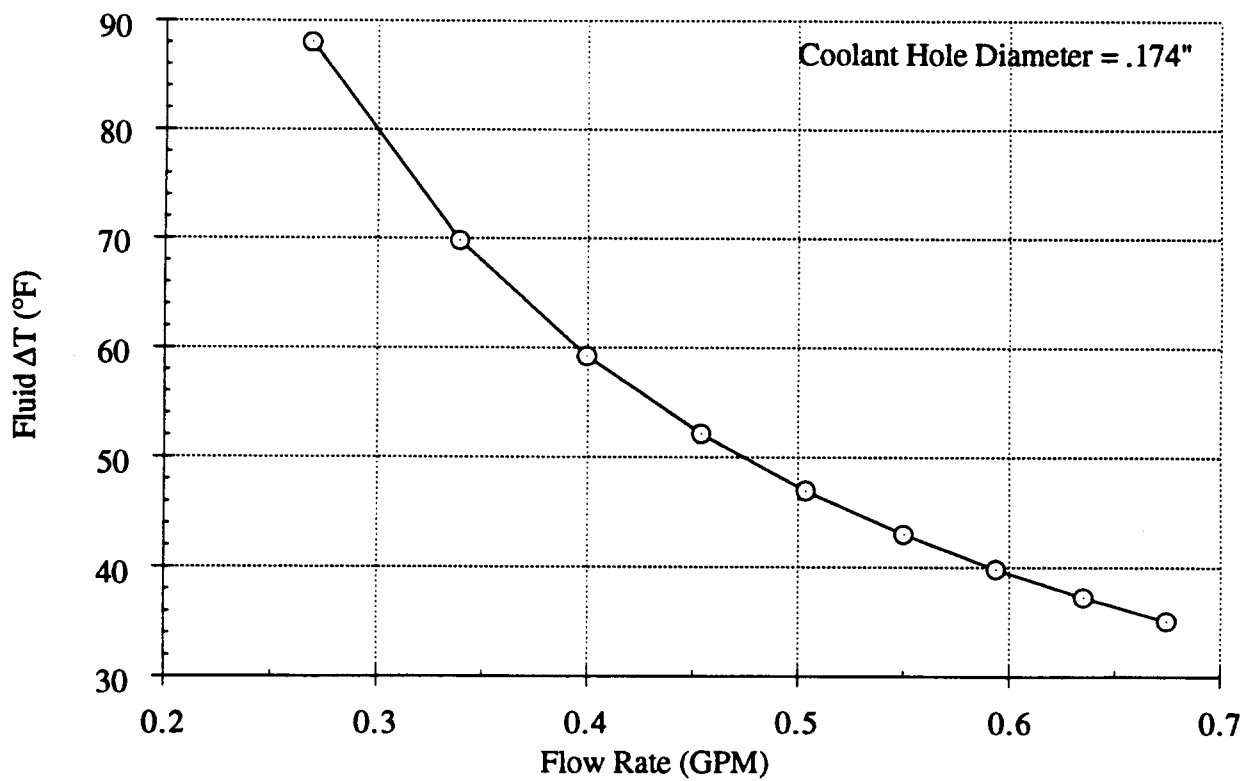


Fig. 23. Fluid ΔT Vs. Flow Rate

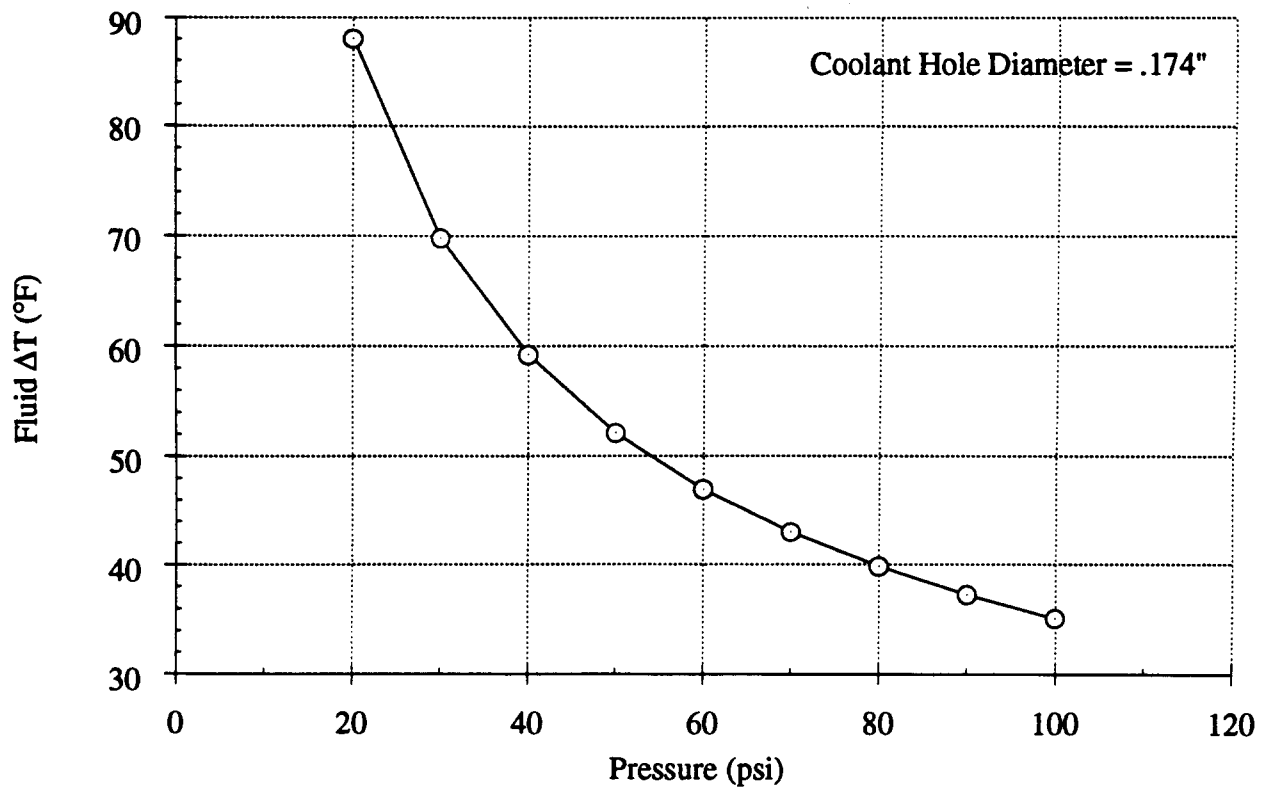


Fig. 24. Fluid ΔT Vs. Pressure

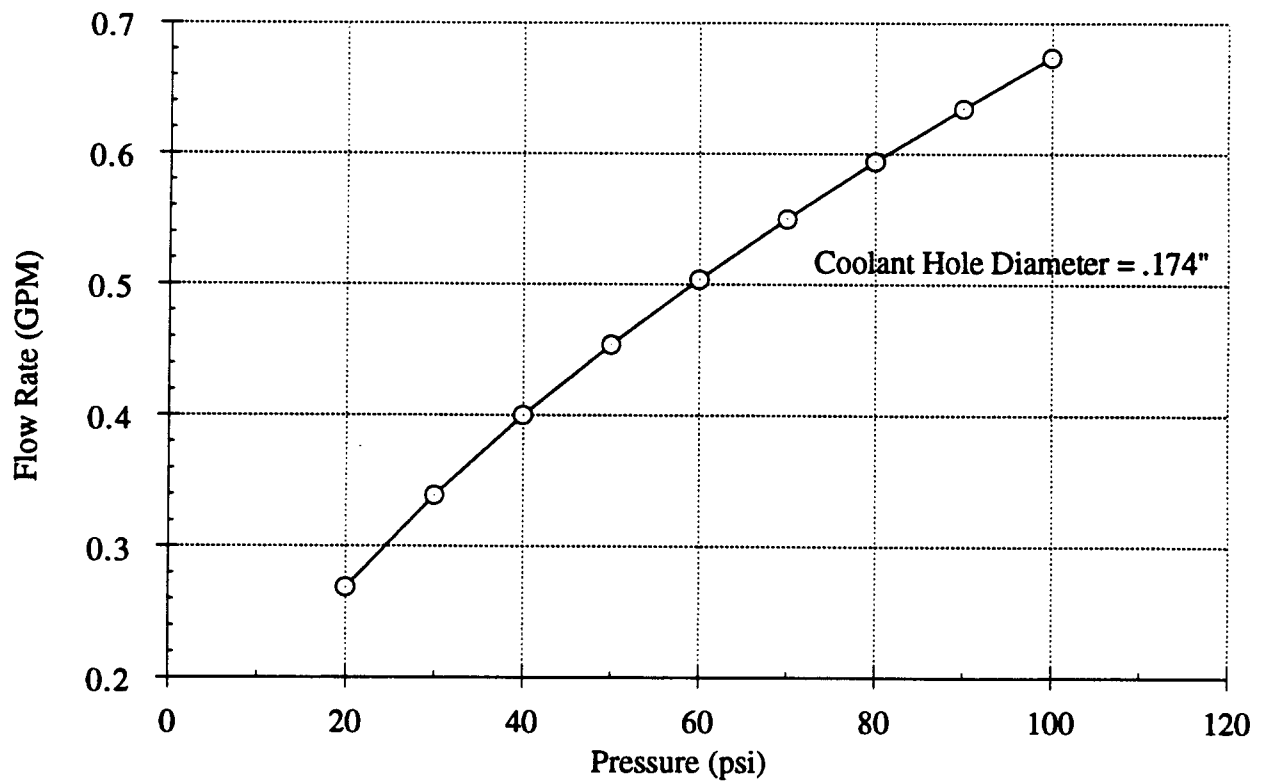


Fig. 25. Flow Rate Vs. Pressure

STRUCTURAL DESIGN

Stress and deflection analyses were performed on the rotating elements of the motor. This included: (1) manual calculations using traditional "textbook" methods to provide an adequate design starting point and (2) a finite element analysis during the detail design stage when the final geometry was more firmly established. The following summarizes the assumptions and results of the first analysis while appendix D presents the results of the second analysis which determined the final detail design.

While the motor has a nominal rating of 175 hp at ± 1200 rpm (87.5 hp per shaft), the overload rating of 600 hp was used (300 hp per shaft) for the analysis. As the method for loading the motor was unknown at the time of the analysis, a Browning "Poly-V" multi-rib V-belt drive was selected as a worst case (largest overhung load) method for transfer of power to the load device. Combining sheave weight and belt tension forces, an overhung load of 400 lb with an assumed moment arm of 24 inches was used for the analysis. Rotor weights were conservatively estimated based on the weight of solid copper resulting in inner and outer rotor weights of 526 lb and 739 lb, respectively. The analysis was conducted using the smallest diameter portion (2.953 inch O.D.) of the inner shaft as the structural member. All analyses were performed using 304 stainless steel shafting with a yield strength of 35,000 psi and a fully modified endurance limit of 18,100 psi.

The stress analysis was performed using three methods. The first method was for static loading conditions and resulted in a maximum shear stress of 3650 psi and a factor of safety of 4.8. The second method was for reversed bending and steady torsion and resulted in an alternating stress of 3790 psi and a factor of safety of 4.8. The third method was the Soderberg approach, which is very conservative and appears to be the basis for the Navy propulsion shafting design data sheet. The Soderberg approach resulted in a required minimum shaft diameter of 1.91 inches and a factor of safety of 3.6. Applying a stress concentration factor of 1.5 for the shaft step reduced the three factors of safety to 3.2, 3.2, and 2.4, respectively.

The deflection analysis predicted radial deflections of 0.0021 and 0.0026 inches for the inner rotor service end and drive end, respectively. Using the ratio of inner to outer rotor loads and moments of inertia, an outer rotor maximum deflection of less than 0.0006 inches is predicted. Thus, an inner rotor to outer rotor maximum net deflection of approx. 0.002 inches is anticipated. The predicted outer rotor to motor casing maximum net deflection is 0.0006 inches.

These initial stress and deflection analyses utilize conservative assumptions in regards to loading and structural stiffness. The outer shaft is much stronger than the inner shaft and the center portion of the inner and outer rotor are much stronger than the necked down shaft sections. Therefore, general stresses are not considered to be a problem. Similarly, while maximum net radial deflections of 0.002 inches were calculated, the actual deflection will probably be less than 0.001 inches.

BEARINGS AND GAS SEALS

Bearings

Due to the necessity of placing bearings between the inner and outer rotors and the desire to keep the machine as compact as possible, bearings of the smallest cross section that had an adequate load rating were selected. To prevent eddy currents through the bearings, the surface of the shafts are coated with a plasma deposited ceramic under the inner race of the bearings.

Drive end

The bearings selected for the drive end are deep groove ball bearings which are grease prelubricated and shielded, pieces 49 and 50. These bearings provide both axial and radial support and location for the rotors. The pairs of bearings will be shimmed to minimize play.

Service end

For the service end, double row, cylindrical roller bearings were chosen to provide radial support as well as to accommodate axial thermal growth, and are of JIS Class 4 precision, grease prelubricated and shielded, pieces 45 and 46.

Seal Assembly

Gas seal

Due to the reactive nature of NaK a dry, oxygen free cover gas must be maintained in the machine at a pressure several PSI above atmosphere. This necessitates the use of high performance gas seals on both shafts, pieces 43, 44, 47, and 48. Mechanical face seals provide both the required performance and low leakage rate. A carbon face running on a Al_2O_3 coating on the shoulder has worked well in similar applications in the past and will be utilized here. The Al_2O_3 coating provides an insulating break to prevent eddy currents through the seals. Most carbons depend on

atmospheric moisture to form a lubricating film. Since these seals operate in a very dry environment a special grade of carbon (Pure Carbon P5N) is used to prevent rapid wear.

Exclusion seal

To prevent contamination of the face seals with bearing lubricant, exclusion seals, pieces 103, 104, and 105, are located between the face seals and the bearings. These seals are of a simple lip design. They utilize a self lubricating plastic sealing element, in a metal housing, running on hardened steel sleeves, pieces 71, 72, 77, and 79, on the shafts.

SERVICE MODULE

SLIP RINGS

A slip ring assembly, to supply current to the field coils, is attached to the service module. This is of conventional design consisting of copper slip rings and silver graphite brushes. The copper terminal rods of the inner rotor extend through the slip ring assembly so that connections to the slip rings can be made. The slip ring assembly is a commercial unit produced by Fabricast Inc., So. El Monte, CA 91733

COOLANT SEALS

The service module contains a combination of mechanical face seals and lip seals to provide coolant flow paths to and from the inner and outer rotor. The face seals provide both the required performance and low leakage rate. A carbon face running on a Al_2O_3 coating on the shoulder is utilized. The lip seals utilize a self lubricating plastic sealing element, in a metal housing, running on a hardened steel sleeve on the shaft. The lip seals are used in the less critical locations in the service module where some leakage can be tolerated.

ROTARY UNION

A rotary union is fitted on the end of the service module, outboard of the slip ring assembly, to supply coolant to the machine.

INSTRUMENTATION

Sensors

Thermocouples are fitted to measure the temperature of coolant, inner and outer rotor bars, inner and outer rotor bearings, and current collectors.

Telemetry

Provisions were made in the design to allow both inner and outer rotor to be fitted with telemetry systems in the future. They will consist of a multiplexing unit and a transmitter on each rotor which will transmit the thermocouple data to a fixed receiver.

COVER GAS SYSTEM

The space between the inner and outer rotor and between the outer rotor and housing is supplied with high purity nitrogen cover gas to prevent reaction of the sodium-potassium used in the current collectors with oxygen or water vapor. A pre-purified grade of nitrogen is generally supplied from K cylinders and is regulated to several psig. The cover gas is supplied to both ends of the motor to minimize flow through the motor which would increase the reaction with the liquid metal.

ASSEMBLY PROCEDURES

Assembly will begin with the inner rotor which will be fitted with the bar set and the field coils. Coolant connections will be made with flexible hose to the passages in the shaft. Coil electrical connections will be made with split clamps and rigid copper rods interconnecting with the terminal rods in the shaft. The outer rotor bar set is semi-permanently mounted internal to the outer rotor cylinder. Both inner and outer rotor current collector rings and disks will be bolted in place sequentially as the outer rotor assembly is built up around the inner rotor. The flux return rings will then be bolted in place. Bearings and seals will be installed in the outer rotor stub shafts which will then be bolted to the outer rotor assembly. Bearings and seals will be fitted in the outer rotor bearing carriers which will then be installed over the outer rotor shafts. These bearings and seals need not be disturbed to accomplish the level of disassembly required for cleaning or other minor maintenance. The assembly will be inserted in the housing and the various terminal collector components installed. The coolant connections for the outer rotor components will be made with flexible hose to the passages in the stub shafts. Installation of the two outer rotor bearing housings completes the basic machine assembly.

PREDICTED MACHINE PERFORMANCE

Output power calculations for a homopolar motor are rather straight forward. The open circuit terminal voltage is only a function of machine flux and rotor speed. The internally generated torque is a function of motor flux and load current. The actual

terminal voltage and output torque, however, are affected by the motor's internal losses. These losses can be divided into three basic categories.

Resistive voltage drops in the internal conductors, joints, and current collectors add to the generated back EMF thereby increasing the terminal voltage of the motor. The increase in terminal voltage is linear with load current. The power loss due to the motor's internal resistance is proportional to the square of the load current. Both are primarily independent of motor speed and flux.

Frictional drag subtracts from the actual internally generated torque and reduces the output torque produced by the machine. Frictional drag from the rolling element bearings and seals is relatively constant and does not change with motor speed or load. Windage drag is a function of motor speed and geometry and is completely independent of load.

The losses in the liquid metal current collectors consist of resistive, frictional, fluid shear, eddy current, and magneto hydrodynamic type losses. These losses are a complicated function of collector speed, load current, geometry, magnetic field, and the fluid properties of the liquid metal.

Tables 3 and 4 detail the predicted performance of the motor at 35,000 and 100,000 amperes load current respectively.

Table 2. Predicted Motor Performance at 35,000 amperes

Output power (both shafts)	185 hp
Shaft speed	$\pm 1,200$ RPM
Torque (per shaft)	405 lb-ft
Effective magnetic flux	.104 Webers
Back EMF (at $\pm 1,200$ RPM)	4.16 volts
Terminal voltage (at 35,000 amps)	4.28 volts
Input current	35,000 amps
Estimated efficiency	92%

Table 3. Predicted Motor Performance at 100,000 amperes

Output power (both shafts)	545 hp
Shaft speed	$\pm 1,200$ RPM
Torque (per shaft)	1,192 lb-ft
Effective magnetic flux	.104 Webers
Back EMF (at $\pm 1,200$ RPM)	4.16 volts
Terminal voltage (at 100,000 amps)	4.50 volts
Input current	100,000 amps
Estimated efficiency	90%

CONCLUSIONS

From a basic point of view a contrarotating homopolar motor is simply one in which the stator is allowed to rotate and produce power. From the outset we realized that this would be a difficult design challenge. It turned out to be much more difficult than we anticipated. Providing the required magnetic flux, adequate cross-section for the current, sufficient coolant flow, and providing the structure required to transmit the torque did not turn out to be the most difficult part of the design. The real complexity turned out to be the multitude of details. All the rotating members must be supplied with coolant. This required a number of connections, passages, seals, and temperature sensors for both the inner and outer rotor. Both rotors must be fitted with bearings and seals. The sizes of suitable, available bearings had a significant impact on shaft sizes. A great deal of effort also went into the assembly / disassembly procedures since this machine does not have a split outer rotor or outer housing. Although simple in concept, the contrarotating homopolar design is not simple to execute. Although it took considerable time in the design phase, we were able to come up with a design that provided for the many unique requirements of this motor. At this time, motor construction is complete and assembly is underway. Based on our experience in construction and assembly of this motor the basic design appears viable and, with some changes, suitable for larger motors. In fact, a larger motor presents fewer difficulties because it removes the volume constraints of a small motor.

References

1. Levedahl, W. J., Shank, S. R., O'Reagan, W. P., "DD21A- A Capable, Affordable, Modular 21 st Century Destroyer, "CARDIVNSWC-TR-93/013 (Dec. 1993)
2. Doyle, T. J., Levedahl, W. J., and Adams, L. G., "Superconductive Machinery for Naval Applications," NSRDC Report 7-645 (Jan. 1972)
3. "Advanced Submarine Electric Drive (ASED) Phase 1 Concept Study" Final Report, April 1990 by Westinghouse Electric Corporation Marine Division. Prepared for Defense Advanced Research Project Agency under Newport News Shipbuilding Purchase Order Number P2277T-0-Y2
4. Doyle, T. J. and Cannell, M. J., "Development of the Shaped Field Superconductive Motor," NSRDC Report # 4178 (Jan. 1974)
5. Cannell M. J. and McConnell R. A. "Flux-Load Current Interactions in Iron Conductors," CDNSWC PAS-92-27 (Jun. 1992)
6. Fernandez, A., Really, P., Whetstone R., Sondergaard, N. "Studies of Liquid Metal Contrarotating Current Collectors," CDNSWC-PAS-92-11 (Jun. 1992)
7. Fox, R., W., and McDonald, A., T., "Introduction to Fluid Mechanics," NY., (1985).
8. Incropera, F., P. and Dewitt, D., P., "Fundamentals of Heat and Mass Transfer," NY., (1985).
9. "Coolanol", (Dielectric Heat Transfer Fluids for Electronic Equipment), Monsanto, St. Louis, Mo., (1987).
10. Miller, D.S., "Internal Flow Systems," p-205-222, Cranfield, Bedford, UK, (1990).
11. Shigley, J., "Design for Fatigue Strength," in: Mechanical Engineering Design, Ch. 7, pp. 270-342, McGraw-Hill Co., New York (1983)

APPENDIX A

APPENDIX A

INNER ROTOR THERMAL DESIGN

The inner rotor bar set is the critical portion of the inner rotor from a thermal perspective. This section documents the thermal analysis performed on the inner rotor bars. The thermal analysis is presented in three sections that include design constraints, assumptions, and the results.

DESIGN CONSTRAINTS

The geometry of the inner rotor's bars was determined by magnetic, electrical, and space considerations. The length of the bar was driven mainly by magnetics. Height of the bar was driven by space in the machine. Width and number of bars were determined by electrical, cooling, and insulation characteristics. There are 32 bars on the inner rotor that each have a length of 5 inches, and liquid coolant is passed axially through the center of each iron bar.

ASSUMPTIONS

Based on the thermal analysis accomplished on the machine's field coils, the thermal analysis performed on the rotor will also use a round cooling hole, assume constant properties over the machine's temperature range, and use Coolanol™ 20 as the cooling fluid. Coolanol™ 20 displays good thermal characteristics, has low electrical conductivity, and does not react with liquid metal (NaK). Since this motor rotates at low speeds and has a small rotor radius, it was assumed that the centrifugal forces acting on the cooling fluid would have no significant effect on its performance.

RESULTS

The results consist of 5 sections of calculations consisting of evaluating geometry, heat generation of the bars, head loss and flow rates, convection coefficient, and film drop and fluid change in temperature. The overall objective was to determine the differences between the input and output temperatures of the fluid (ΔT_f) and the differences between the average temperatures of the copper and fluid (ΔT_{fd} - film drop), verses the required flow rate and pressure drop.

LIST OF ABBREVIATIONS

A_{cool} = total cooling area - (in²)

A_s = surface area of cooling hole ft²

C_p = specific heat Btu/lbm -°F
 d = dimension of the cooling hole (in)
 f = friction factor across the coils inner surface (dimensionless number)
 g_c = gravitational constant 32.2 lbm ft/lbf sec²
 h = convection coefficient Btu/hr-ft-°F
 k = thermal conductivity Btu/hr.- ft -°F
 L = length of the conductor ft
 L_e = equivalent length ft
 m = mass flow rate lbm/min
 N = number of parallel paths
 Nu = Nusset number (dimensionless number)
 q = flow rate gpm
 Q = heat generation Btu/min
 P = wetted perimeter in
 P_r = Prandtl number (dimensionless number)
 r = resistivity of copper ohm-in
 Re = Reynolds number (dimensionless number)
 s = height and width of conductor - in
 α thermal diffusivity ft²/hr
 ΔP = pressure drop (psi)
 ΔT_{fd} = film drop (($\Delta T_{fd} = T_s - T_m$)
 ΔT_{fl} = temperature change of fluid °F ($\Delta T_{fl} = T_{\text{output}} - T_{\text{input}}$ of fluid)
 T_s = surface temperature of the conducting metal
 T_m = mean temperature of the fluid at a cross section in the flow
 ρ = density lbm/ ft³
 μ = dynamic viscosity lbm/ft-sec

TABLE A-1. Fluid Properties of Coolanol™ 20 at 100°F

Properties	Units	Coolanol™ 20
density	lbm/ ft ³	55.2
dynamic viscosity	lbm/ft-sec	.0011886
specific heat	Btu/lbm -°F	.47
thermal conductivity	Btu/hr.- ft -°F	.067

ROUND HOLE GEOMETRY

Inner rotor - 32 bars

d = dimension of the cooling hole (in)

L = actual length of the bars in a parallel path - $5/12' * 32/N = 13.33/N$ (ft)
(bar length = 5 inches)

$32/N$ = number of bars / parallel path

$32/N - 1$ = number of U - bends / per parallel path

Equivalent length of head loss to that of a straight pipe for U - bends

L_e (180° U - bends) = $50d/12$

Equivalent length of head loss to that of a straight pipe - total

L_e (U - bends + bars) = $32/N(5/12) + 50d/12(32/N - 1)$

Cross sectional area of the cooling hole

A_{cool} = cooling cross sectional area - $\pi d^2/4(144)$ (1)

= $.00545d^2$ ft² (1.1)

Surface area of the cooling hole (length times perimeter)

$A_s = \pi dL/12N = \pi d/12 (32 (5/12))/N$

= $3.49d/N$ (ft²) (1.2)

HEAD LOSS AND FLOW RATES

Flow was assumed to be fully turbulent, smooth tubing, and incompressible fluid.

f = friction factor across the coils inner surface

(a) $Re = \rho Vd/\mu$

Re = Ratio of the inertia and viscous forces (Reynolds number)

(b) $f = .32/Re^{.25} = .32\mu^{.25}/(V^{.25} d^{.25} \rho^{.25})$ for $Re < 10^5$ - Blasius correlation

ΔP = pressure drop

(c) $\Delta P = f (L_e/d) (\rho V^2/2g_c)$ (straight pipe assumption)

substituting (b) into (c)

$\Delta P = .16L_e V^{1.75} \mu^{.25} \rho^{.75} / (d^{1.25} g_c)$ (psi) (2)

substituting for the fluid's properties into (2)

$\Delta P = .00287L_e V^{1.75} / d^{1.25}$ (psi) (2.1)

therefore the velocity is

$V = (349\Delta P d^{1.25} / L_e)^{.57143}$ (ft/s) (2.2)

where:

L_e = ft , V = ft/sec , d = in , ρ = lbm/ft³ , ΔP = psi , μ = .0011886 ft²/sec ,

$g_c = 32.2$ lbm ft/lbf sec²

(d) $m = \rho VA$ mass flow rate

$$m = 1084d^2V \text{ lbm/hr} \quad (3)$$

$$\text{flow rate} = q = VA$$

Flow rate per parallel path on the inner rotor section

$$q = 2.45d^2V \text{ (gpm/parallel path)} \quad (4)$$

Total flow rate over the inner rotor

$$Nq = \text{total gpm}$$

CONVECTION COEFFICIENT

Nusselt number, and colburn equation

$$(a) \quad Nu = .0223 Re^{.8} Pr^{.333} - \text{colburn equation where assumptions} \\ (.7 < Pr < 160, L/D > 10)$$

$$(b) \quad Pr = \nu/\alpha \text{ (Prandtl number)}$$

Pr = Ratio of momentum and thermal diffusivities

$$(c) \quad \alpha = K/\rho C_p \text{ (thermal diffusivity (Re} > 2300))$$

$$(d) \quad h = NuK/d \text{ (convection coefficient)}$$

substituting (a), (b), and (c) into (d)

$$h = .0223 \rho^{.8} V^{.8} C_p^{.333} K^{.667} / (\mu^{.467} d^{.2}) \quad (5)$$

substituting for the fluid's properties into (5)

$$h = 42.57 V^{.8} / d^{.2} \text{ (Btu/hr.- ft}^2 \text{ -}^\circ\text{F)} \quad (5.1)$$

where:

$$V = \text{ft/sec}, d = \text{in}, \rho = \text{lbm/ft}^3, \mu = .0011886 \text{ ft}^2/\text{sec}, C_p = \text{Btu/lbm -}^\circ\text{F},$$

$$K = \text{Btu/hr.- ft -}^\circ\text{F}, h = \text{Btu/hr.- ft}^2 \text{ -}^\circ\text{F}$$

FILM DROP AND FLUID CHANGE IN TEMPERATURE

Film drop:

$$Q = hA_s \Delta T_{fd} \text{ } (\Delta T_{fd} = T_s - T_m) \text{ (mean difference between the mean temperature} \\ \text{of the fluid and the iron bar)}$$

$$(a) \quad \Delta T_{fd} = Q/A_s N h$$

substituting (5.1) & (1.2) & $Q = 17,802 \text{ Btu/hr}$ into (a)

$$\Delta T_{fd} = 119.8/V^{.8} d^{.8} \text{ } (^\circ\text{F)} \quad (6)$$

where:

$$h = \text{Btu/hr.- ft}^2 \text{ -}^\circ\text{F}, d = \text{in}, Q = \text{Btu/min}, \Delta T_{fd} = ^\circ\text{F}$$

Fluid change in temperature:

$$Q = m C_p \Delta T_{fl} \text{ } (\Delta T_{fl} = T_{\text{output}} - T_{\text{input}} \text{ of fluid)}$$

$$(b) \quad \Delta T_{fl} = Q/(m C_p)$$

substituting (3) & $C_p = .47 \text{ Btu/lbm} \cdot ^\circ\text{F}$ & $Q = 17,802 \text{ Btu/hr}$ into (b)

$$\Delta T_{fl} = 34.94/Nd^2V \quad (^\circ\text{F}) \quad (7)$$

where:

$V = \text{ft/sec}$, $C_p = \text{Btu/lbm} \cdot ^\circ\text{F}$, $d = \text{in}$, $Q = \text{Btu/min}$, $\Delta T_{fl} = ^\circ\text{F}$

The above equations were analyzed for determining the cooling hole diameter, number of parallel cooling paths, and pressures needed to adequately cool the rotor bars. Unlike the field coil analysis (selecting optimum parameters), the objective here was to chose the minimum parameters required to adequately cool the bars. A minimum number of parallel paths is desirable in order to reduce the mechanical difficulty of rotating seals and balancing the system.

APPENDIX B

APPENDIX B

OUTER ROTOR THERMAL DESIGN

The only changes in the calculations from the inner rotor are noted below:

ROUND HOLE GEOMETRY

Outer rotor - 36 bars

d = dimension of the cooling hole (in)

L = actual length of the bars in a parallel path - $5/12' * 36/N = 15/N$ (ft)

$36/N$ = number of bars / parallel path

$36/N - 1$ = number of U - bends / per parallel path

Equivalent length of head loss to that of a straight pipe - total

L_e (U - bends + bars) = $36/N(5/12) + 50d/12(36/N - 1)$

Surface area of the cooling hole (length times perimeter)

$A_s = \pi dL/12N = \pi d/12 (36 (5/12))/N$

$= 3.93d/N$ (ft²)

APPENDIX C

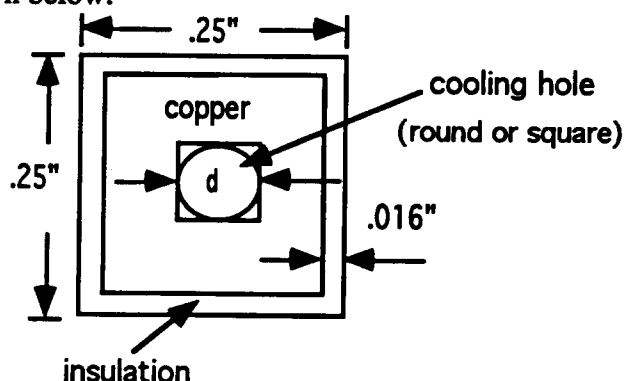
APPENDIX C

FIELD COIL THERMAL DESIGN

The objective of this section is to document the thermal analysis procedure used in designing the field coils. The procedure for the thermal analysis is broken up into four sections which include, design constraints, assumptions, design variables, and the results.

DESIGN CONSTRAINTS

The coil's geometry was dictated by magnetic, electrical, and space considerations. The only unknowns were the size and shape of the cooling hole needed to adequately remove the heat generated by the field current. A cross sectional view for a single turn of the coil is shown below:



There are 34.5 turns per coil, giving a total length of 80 ft of tubing per coil. The coils have inner and outer diameters of 7.42" and 9.6" respectively and are 2.275" long.

The coil produces 7650 ampere turns, with a winding cross sectional area of 2.25 in², thus yielding a overall current density of 3400 amps per square inch.

Removing the heat generated by the current will be accomplished by liquid cooling. The fluids considered were Coolanol™ 20 and Coolanol™ 40 (silicate ester), because they exhibit low electrical conductance and relatively good thermal characteristics (dielectric heat transfer fluid).

ASSUMPTIONS

During the thermal analysis, two assumptions were made in order to simplify the assessment. The first assumption established the fluid's properties and copper resistivity for the cooling system. It was assumed that the properties (which are temperature dependent) would not change enough to affect the final calculations. All the properties were taken at 100 °F (estimated average temp of the fluid), and remain constant through

the system. The second assumption relates to the pressure drop or head loss along the length of the coil. The head loss was assumed to be equivalent to a straight pipe analysis; that is, the coil's curvature was not taken into account.

DESIGN VARIABLES

In the thermal analysis of the field coils, there were two different variables that needed to be analyzed for the purpose of determining the best thermal performance. They were the geometry of the cooling hole (square or round) and the type of fluid (Coolanol™ 20 or 40). Each of the two fluids were analyzed, based on their thermal properties, to determine which fluid produced the better cooling characteristics. In the case of the geometry of the cooling hole, the square hole and the round hole were compared to each other to determine which one would produce the better flow rate for the same area.

RESULTS

The results consist of 6 sections of calculations that are comprised of evaluating the fluids' properties, geometry, heat generation of the coil, head loss and flow rates, convection coefficient, and film drop and fluid change in temperature. The overall objective was to determine the differences between the input and output temperatures of the fluid (ΔT_{fl}) and the differences between the average temperatures of the copper and fluid (ΔT_{fd} - film drop), versus the required flow rate and pressure drop. At the conclusion of the calculations, the above assumptions were compared to a more realistic approach to determine their validity.

LIST OF ABBREVIATIONS

A_{cool} = total cooling area - (in²)

A_{cu} = conductor cross section - (in²)

A_t = total cross sectional area - (in²)

A_s = surface area of cooling hole ft²

C_p = specific heat Btu/lbm - °F

d = dimension of the cooling hole (in)

D = average diameter of the coil (in)

$D_h = 4A_{cool}/P$ = hydraulic diameter

f = friction factor across the coils inner surface (dimensionless number)

g_c = gravitational constant 32.2 lbf ft/lbf sec²

h = convection coefficient Btu/hr-ft-°F

k = thermal conductivity Btu/hr.- ft - °F

J_c = current density over the copper amps/in²
 J_t = current density of the entire coil amps/in²
 L = length of the conductor ft
 m = mass flow rate lbm/min
 Nu = Nusset number (dimensionless number)
 q = flow rate gpm
 Q = heat generation Btu/min
 P = wetted perimeter in
 P_f = packing factor
 P_r = Prandtl number (dimensionless number)
 r = resistivity of copper ohm-in
 Re = Reynolds number (dimensionless number)
 s = height and width of conductor - in
 t = thickness of the insulation - in
 v_c = volume of conductor in³
 v_t = total volume of coil in³
 α = thermal diffusivity ft²/hr
 ΔP = pressure drop (psi)
 ΔT_{fd} = film drop (($\Delta T_{fd} = T_c - T_f$)
 ΔT_{fl} = temperature change of fluid °F($\Delta T_{fl} = T_{output} - T_{input}$ of fluid)
 ρ = density lbm/ ft³
 μ = dynamic viscosity lbm/ft-sec

TABLE C-1. Fluid Properties of Coolanol™ 20 and 40 at 100°F

Properties	Units	Coolanol™ 20	Coolanol™40
density	lbm/ ft ³	55.2	54.91
dynamic viscosity	lbm/ft-sec	.0011886	.00402
specific heat	Btu/lbm - °F	.47	.48
thermal conductivity	Btu/hr.- ft - °F	.067	.078

GEOMETRY

Round hole:

s = height and width of conductor - .25 (in)
 d = dimension of the cooling hole (in)

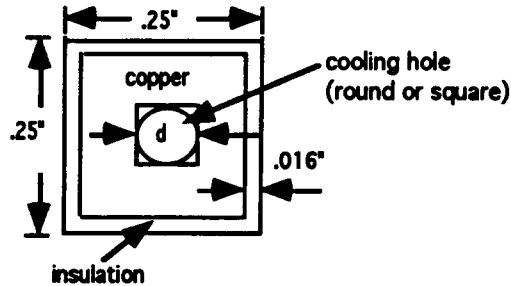
t = thickness of the insulation - .016 (in)

A_t = total cross sectional area - s^2 (in²) = .0625 (in²)

A_{cu} = conductor cross section - $(s-2t)^2 - \pi d^2/4$ (in²)

A_{cool} = total cooling area - $\pi d^2/4$

P_f = packing factor - $A_{cu}/A_t = [(s-2t)^2 - \pi d^2/4]/s^2 = .7604 - 12.56d^2$



Square hole:

A_t = total cross sectional area - s^2 (in²)

A_{cu} = conductor cross section - $(s-2t)^2 - d^2$ (in²)

A_{cool} = total cooling area - d^2

P_f = packing factor - $A_{cu}/A_t = [(s-2t)^2 - d^2]/s^2 = .7604 - 16d^2$

$D_h = 4A_{cool}/P$ = hydraulic diameter used for correlating turbulent pipe flow for use with non circular geometry's. For a square $D_h = 4d^2/4d = d$ (P = wetted perimeter).

v_c = volume of conductor (in³) = $A_{cu} L = A_t P_f L$

L = length of the conductor

HEAT GENERATION

(a) $Q = J_c^2 r v_c$ (Watts) (heat generation across the conductor)

(b) $J_c = J_t/P_f$ current density over the conductor

J_t = current density of the entire coil

(c) $v_t = A_t L$ total volume of coil

(d) $v_c = v_t P_f$ volume of conductor

substituting (c) into (d):

(e) $v_c = A_t L P_f$

substituting (b) and (e) into (a):

$$Q = (J_t/P_f)^2 r (A_t L P_f) = J_t^2 r A_t L / P_f$$

converting to English units:

(f) $Q = 6826 J_t^2 r s^4 L / [(s-2t)^2 - \pi d^2/4]$ Btu/min (round hole)

$r = 7.87e-7$ ohm-in (resistivity of copper at 100 °F)

substituting $J_t = 3400 \text{ amps/in}^2$, $s = .25"$, $t = .016"$, and $L = 80'$ into (f)

$$Q = 1.941/((.047524 - .785d^2) \text{ Btu/min (round hole)}) \quad (1a)$$

$$Q = 6826 J_t^2 r s^4 L / [(s-2t)^2 - d^2] \text{ Btu/min (square hole)}$$

$$Q = 1.941/((.047524 - d^2) \text{ Btu/min (square hole)}) \quad (1b)$$

where:

$$L = \text{ft} , s = \text{in} , t = \text{in} , Q = \text{Btu/min} , d = \text{in} , r = \text{ohm-in} , J = \text{Amp/in}^2$$

HEAD LOSS AND FLOW RATES

Flow was assumed to be fully turbulent, smooth tubing, and incompressible fluid.

f = friction factor across the coils inner surface

$$(a) \quad R_e = \rho V d / \mu$$

R_e = Ratio of the inertia and viscous forces (Reynolds number)

$$(b) \quad f = .32/R_e^{.25} = .32\mu^{.25}/(V^{.25} d^{.25} \rho^{.25}) \text{ (RH \& SH) for } R_e < 10^5 \text{ - Blasius correlation}$$

ΔP = pressure drop

$$(c) \quad \Delta P = f (L/d) (\rho V^2 / 2g_c) \text{ (Horizontal pipe assumption)}$$

substituting (b) into (c)

$$\Delta P = 1.9856 V^{1.75} \mu^{.25} \rho^{.75} / (d^{1.25} g_c) \text{ (psi) (RH \& SH)} \quad (2)$$

where:

$$L = \text{ft} , V = \text{ft/sec} , d = \text{in} , \rho = \text{lbm/ft}^3 , \Delta P = \text{psi} , \mu = .0011886 \text{ ft}^2 / \text{sec} ,$$

$$g_c = 32.2 \text{ lbm ft/lbf sec}^2$$

$$(d) \quad m = \rho V A \text{ mass flow rate}$$

$$m = .326 \rho d^2 V \text{ lbm/min (round hole)} \quad (3a)$$

$$m = .415 d^2 V \text{ lbm/min (square hole)} \quad (3b)$$

$$\text{flow rate} = q = V A$$

$$q = 2.45 d^2 V \text{ (round hole) (gpm)} \quad (4a)$$

$$q = 3.12 d^2 V \text{ (square hole) (gpm)} \quad (4b)$$

Convection coefficient

Nusset number, and colburn equation

$$(a) \quad Nu = .0223 Re^{.8} Pr^{.333} \text{ - colburn equation where assumptions } (.7 < Pr < 160, L/D > 10)$$

$$(b) \quad P_r = \nu / \alpha \text{ (Prandtl number)}$$

P_r = Ratio of momentum and thermal diffusivities

$$(c) \quad \alpha = K / \rho C_p \text{ (thermal diffusivity (Re > 2300))}$$

$$(d) \quad h = Nu K / d \text{ (convection coefficient)}$$

substituting (a), (b), and (c) into (d)

$$h = .0223\rho^{.8}V^{.8}C_p^{.333}K^{.667}/(\mu^{.467}d^{-2}) \text{ (RH \& SH)} \quad (5)$$

where:

$$V = \text{ft/sec}, d = \text{in}, \rho = \text{lbm/ft}^3, \mu = .0011886 \text{ ft}^2/\text{sec}, C_p = \text{Btu/lbm} \cdot ^\circ\text{F},$$

$$K = \text{Btu/hr.} \cdot \text{ft} \cdot ^\circ\text{F}, h = \text{Btu/hr.} \cdot \text{ft}^2 \cdot ^\circ\text{F}$$

FILM DROP AND FLUID CHANGE IN TEMPERATURE

Film drop:

(a) $Q = hA_s\Delta T_{fd}$ ($\Delta T_{fd} = T_s - T_m$) (temperature difference between the fluid and the copper)

(b) $A_s = \pi dL$ (surface area of hole) (round hole)

substituting (b) into (a)

$$\Delta T_{fd} = 2.865Q/(hd) \text{ (round hole)} \quad (6a)$$

(c) $A_s = 4dL$ (surface area of hole) (square hole)

substituting (c) into (a)

$$\Delta T_{fd} = 2.25Q/(hd) \text{ (square hole)} \quad (6b)$$

where:

$$h = \text{Btu/hr.} \cdot \text{ft}^2 \cdot ^\circ\text{F}, d = \text{in}, Q = \text{Btu/min}, \Delta T_{fd} = ^\circ\text{F}$$

Fluid change in temperature:

(a) $Q = mC_p\Delta T_{fl}$ ($\Delta T_{fl} = T_{\text{output}} - T_{\text{input}}$ of fluid)

$$\Delta T_{fl} = Q/(\cdot 326\rho d^2VC_p) \text{ (round hole)} \quad (7a)$$

$$\Delta T_{fl} = Q/(\cdot 415\rho d^2VC_p) \text{ (square hole)} \quad (7b)$$

where:

$$V = \text{ft/sec}, C_p = \text{Btu/lbm} \cdot ^\circ\text{F}, d = \text{in}, Q = \text{Btu/min}, \Delta T_{fl} = ^\circ\text{F}$$

SOLUTION FOR THE FINAL SELECTED GEOMETRY

Geometry of the cooling hole (round), type of fluid (Coolanol™ 20), and the optimum diameter ($d = .174"$) have been established based on thermal performance and practical mechanical considerations. Also, it has been established that the fluid's change in temperature (ΔT_{fl}) is the dominating force in the thermal analysis, and the film drop has less of an impact. The above equations can be solved in terms of pressure and ΔT_{fl} , since the geometry, diameter, and fluid properties (100 °F) have been determined.

Geometric factors

$$A_{cu} = \text{conductor cross section} = (s-2t)^2 - \pi d^2/4 = .02376 \text{ (in}^2\text{)}$$

$$A_{cool} = \pi d^2/4 = .0238 \text{ (in}^2\text{)}$$

$$P_f = \text{packing factor} - A_{cu}/A_t = .7604 - 12.56d^2 = .3801$$

Heat generation

from equation (1a)

$$Q = 1.941/(\text{.047524} - .785d^2) \text{ Btu/min} \quad (8)$$

substituting $d = .174$ " into equation (1)

$$Q = 81.7 \text{ Btu/min}$$

Head loss and flow rates

from equation (2)

$$\Delta P = 1.9856 V^{1.75} \mu^{.25} \rho^{.75} / (d^{1.25} g_c) \text{ (psi)} \quad (9)$$

substituting $d = .174$ ", $\rho = 55.2 \text{ lbm/ft}^3$, $\mu = .0011886 \text{ lbm/ft-sec}$ into (2)

$$\Delta P = 2.09 V^{1.75} \text{ (psi)}$$

from equation (3a)

$$m = .326 \rho d^2 V \text{ lbm/min} \quad (10)$$

substituting $d = .174$ ", $\rho = 55.2 \text{ lbm/ft}^3$ into (3)

$$m = .545 V \text{ lbm/min}$$

from equation (4a)

$$Q = 2.45 d^2 V \text{ (gpm)}$$

substituting $d = .174$ " into (4a)

$$Q = .0742 V \text{ (gpm)} \quad (11)$$

Fluid change in temperature:

from equation (7a)

$$\Delta T_f = Q / (.326 \rho d^2 V C_p) \text{ (}^\circ\text{F)}$$

substituting $d = .174$ ", $\rho = 55.2 \text{ lbm/ft}^3$, $C_p = .47 \text{ Btu/lbm} \cdot ^\circ\text{F}$ into (7a)

$$\Delta T_f = 319.16 / V \text{ (}^\circ\text{F)} \quad (12)$$

The first of two assumptions that were applied in order to simplify the calculations, was that the fluid properties and copper resistivity (taken at 100 °F) would have a negligible affect on ΔT_f as the temperature changes through the coil. Fig. C-1. summarizes the change in temperature of the fluid (ΔT_f) varying over a range of average temperatures. Since the increased copper losses at higher temperatures (as a result of higher resistivity) are almost equally offset by lower coolant viscosity (and thus higher flow at a given pressure differential), ΔT_f is relatively insensitive to fluid temperature. The assumption is valid. The second assumption involved the pressure drop across the coil. The pressure drop was calculated to be a straight pipe unaffected by the coil's

curvature. Fig. C-2. displays how the change in temperature of the fluid is affected by the increased pressure drop due to the curvature of the coil. There is a 5 °F difference in the change in temperature of the fluid between the straight pipe assumption and the actual curved pipe conduction.

Pressure drop across a coil (including the curvature)

$$\Delta P = [.32/Re^{.25} + .048(d/D)^{-5}] (L/d) (\rho V^2/2g_c) \quad (\text{for } Re = 1.5 \times 10^4) \quad (13)$$

D = average diameter of the coil = 8.51"

substituting D = 8.51", d = .174", $\rho = 55.2 \text{ lbm/ft}^3$, $\mu = .0011886 \text{ lbm/ft-sec}$,

L = 80' into Eq. 5

$$\Delta P = [.3614V^{1.75} + .226V^2] \quad (14)$$

where:

L = ft , V = ft/sec , d = in , $\rho = \text{lbm/ft}^3$, $\Delta P = \text{psi}$, $\mu = .0011886 \text{ lbm/ft-sec}$, D = in
 $g_c = 32.2 \text{ lbm ft/lbf sec}^2$

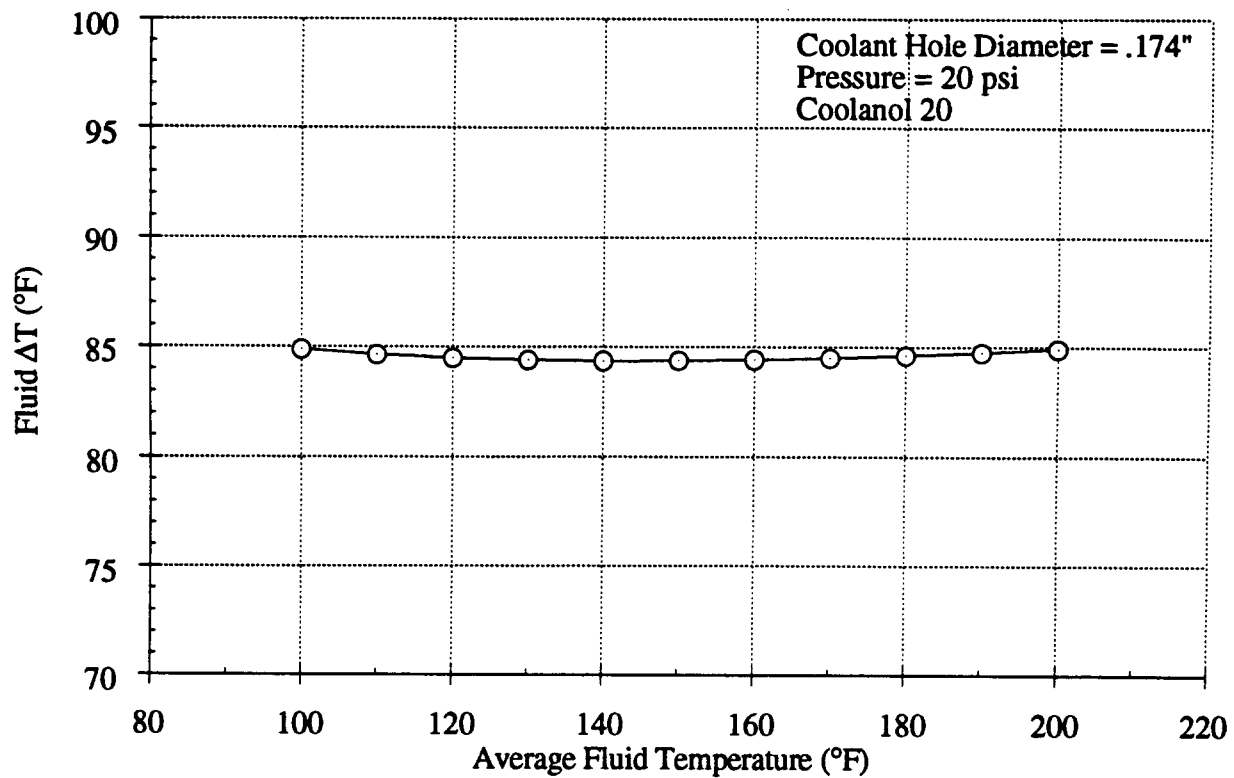


Fig. C-1. Fluid ΔT Vs. Average Fluid Temperature

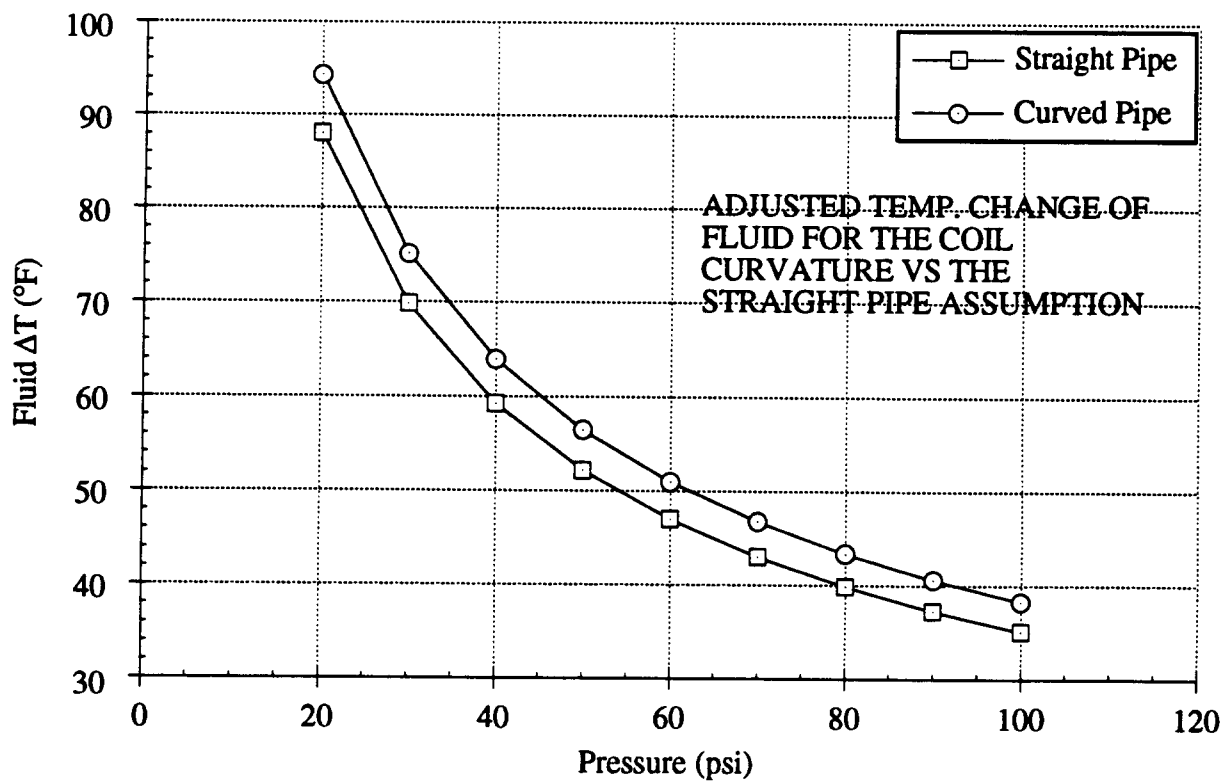


Fig. C-2. Effect of Tubing Curvature on Fluid ΔT

APPENDIX D

APPENDIX D

DETAILS OF STRUCTURAL ANALYSIS.

A section view of the motor is shown in Fig. D-1. The inner shaft is supported by two pairs of bearings 23.8 inches apart. These bearings transmit the weight of the inner shaft to the outer shaft. The outer shaft is also supported by two pairs of bearings just outboard of the inner shaft bearings. The outer shaft bearings support the total weight of both shafts in the housing. The housing is assumed to be held at the bolted flange connections of the service and drive end plates.

The inner shaft material is 1018 hot rolled steel. The outer shaft material is 304 stainless steel, with iron bars and copper coils adding weight but not structural stiffness. The housing is composed of 316 stainless steel, A36 steel and A53 steel pipe. Table D-1 contains the material properties for the components. The nomenclature of the variables referred to is also listed. The endurance strength for each material has been calculated.

TABLE D-1. Material Properties:

Material	S _y (psi)	S _t (psi)	μ	E (psi)	δ (lb/in ³)
1018 Steel, Rod	32,000	58,000	.3	29E6	.29
304 Stainless Steel, Pipe	30,000	75,000	.3	28E6	.29
316 Stainless Steel, Pipe	35,000	85,000	.3	28E6	.29
A53 Steel, Pipe	35,000	60,000	.3	29E6	.29
A36 Steel, Plate	36,000	58,000	.3	29E6	.29
Iron, Bar	for the iron and copper only the density was used in the model				.26
Copper, Plate					.32

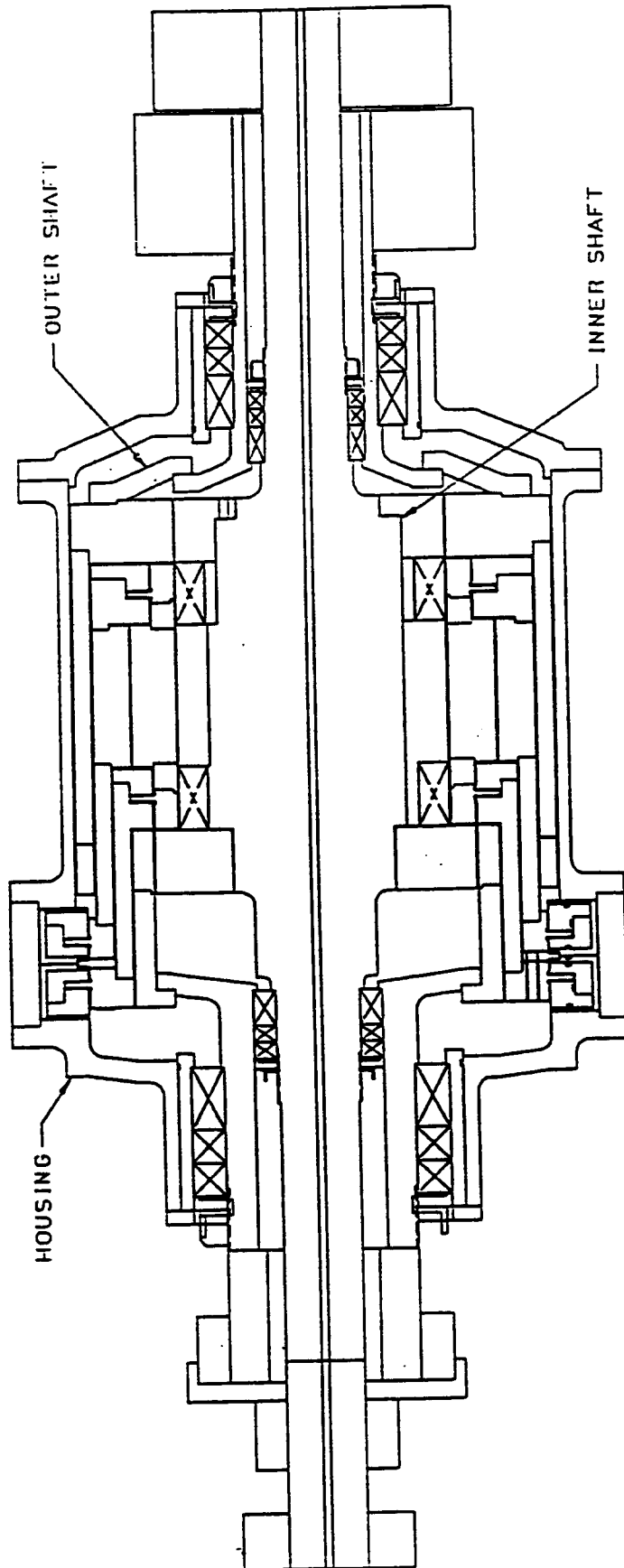


Fig. D-1. Section View

NOMENCLATURE:

A_s	= Shear Area, sq in.		
A_t	= Tensile Area, sq in.		
D	= Outer Diameter, in.		
p	= Inner Diameter, in.		
F	= Belt Tension, lb		
F_{bn}	= Axial Force of Bolt due to Moment, M_{bn} , lb		
K	= Endurance Modification Factors		
K_b	= Bending Stress Concentration Factor		
K_c	= Combined Stress Concentration Factor		
K_L	= Load Connection Factor		
K_t	= Torque Stress Concentration Factor		
L	= Distance from restraint to load, in.		
M	= Total Moment, in-lb		
M_{bn}	= Moment of Bolt, in-lb		
M'	= Corrected Moment, in-lb		
N	= Rotational Speed, rpm		
P	= Power, hp		
p	= axial force on bolt, lb		
r	= Radius, in.		
S_a	= Alternating Strength, psi		
S_e	= Fully Corrected Endurance Strength, psi		
S_e'	= Endurance Strength, psi		
S_m	= Mean Strength, psi		
S_{se}	= Shear Endurance Strength, Psi		
S_{sy}	= Shear Yield Strength, psi		
S_t	= Tensile Strength, psi		
S_y	= Yield Strength, psi		
s	= Shear force on bolt, lb		
T	= Torque, in-lb		
wt	= weight, lb		
z_n	= Height of Bolt to center, in.		
z_n'	= Corrected Height, in.		
α	= Angle, degrees	σ	= Principle Stress, psi
μ	= Poission's Ratio	σ'	= Von Mises Stress, psi
δ	= Density, lb/cu in.	σ_a	= Alternating Stress, psi

Σ = Summation

σ_m = Mean Stress, psi

τ = Shear Stress, psi

ENDURANCE STRENGTH CALCULATIONS

Endurance Strength

$$S_e = K_1 * K_2 * K_3 * S_e' \quad (\text{REF. 11})$$

K_1 = Surface Factor

K_2 = Size Factor, $.869 d^{-.097}$ (select largest diameter)

K_3 = Reliability Factor

Inner Shaft, 1018 Steel

K_1 = Surface Factor, hot rolled, = .7

K_2 = Size Factor, $.869 7.4^{-.097}$, = .72

K_3 = Reliability Factor, .999, = .75

$$S_e' = 1/2 S_t = 29,000 \text{ psi} \quad S_e = \underline{10.962 \text{ psi}}$$

Outer Shaft, 304 Stainless Steel

K_1 = Surface Factor, hot rolled, = .7

K_2 = Size Factor, $.869 17^{-.097}$, = .66

K_2 = Size Factor, $.869 5.1^{-.097}$, = .74 @ node 46

K_3 = Reliability Factor, .999, = .75

$$S_e' = 1/2 S_t = 42,5000 \text{ psi} \quad S_e = \underline{14.726 \text{ psi}}$$
$$S_e = \underline{16.511 \text{ psi}} \text{ @ node 46}$$

Housing, 316 Stainless Steel

K_1 = Surface Factor, hot rolled, = .7

K_2 = Size Factor, $.869 11^{-.097}$, = .69

K_3 = Reliability Factor, .999, = .75

$$S_e' = 1/2 S_t = 42,5000 \text{ psi} \quad S_e = \underline{15.396 \text{ psi}}$$

Housing, A53 Steel

K_1 = Surface Factor, hot rolled, = .7

K_2 = Size Factor, $.869 18^{-.097}$, = .66

K_3 = Reliability Factor, .999 = .75

S_e' = $1/2 S_t = 30,000$ psi $S_e = \underline{10,395}$ psi

Housing, A36 Steel

K_1 = Surface Factor, hot rolled, = .7

K_2 = Size Factor, .869 $21.6^{-.097}$, = .65

K_3 = Reliability Factor, .999 = .75

S_e' = $1/2 S_t = 29,000$ psi $S_e = \underline{9,896}$ psi

The two shafts and the housing were modeled using a PC based finite element package, MSC/PAL2. The finite element model comprised of circular beams represented the geometry of the three components were used. The flanged connections were modeled as rigid connections. The modeling of the inner shaft with circular beams is very accurate. However, the analogy is flawed when modeling the outer shaft and the housing for pieces such as the stub shaft or transition flange. Those pieces are disks, not cylinders. To properly model those shapes would require detailed modeling of them as 3-D brick elements.

The shafts were subject to two types of loads. The mean loads are due to the torque from the motor. The alternating loads are from the shaft bending under its weight or a side force. The stress results were separated into mean and alternating cases. Three load cases were used;

- a) The steady torque from the 300 hp at 1200 rpm, 15,756 in-lb.
- b) The weight of the components plus side forces (e.g. from belt force on outer shaft)
- c) Load case a and b combined.

The bearings were modeled as very stiff springs connecting the components in translations but not in rotation. The torque, 15,756 in-lb due to 300 hp at 1200 rpm, was placed at the middle of the iron bars between the bearings on each shaft. The rotations for the housing and the shafts were fixed along their centerline, x-axis. All water boxes, bearings, carriers and pulleys were modeled as cylinders with estimated weights and dimensions. See Figs. D-2, D-3, and D-4 for individual finite element (FE) models showing the inner shaft, outer shaft and housing, respectively.

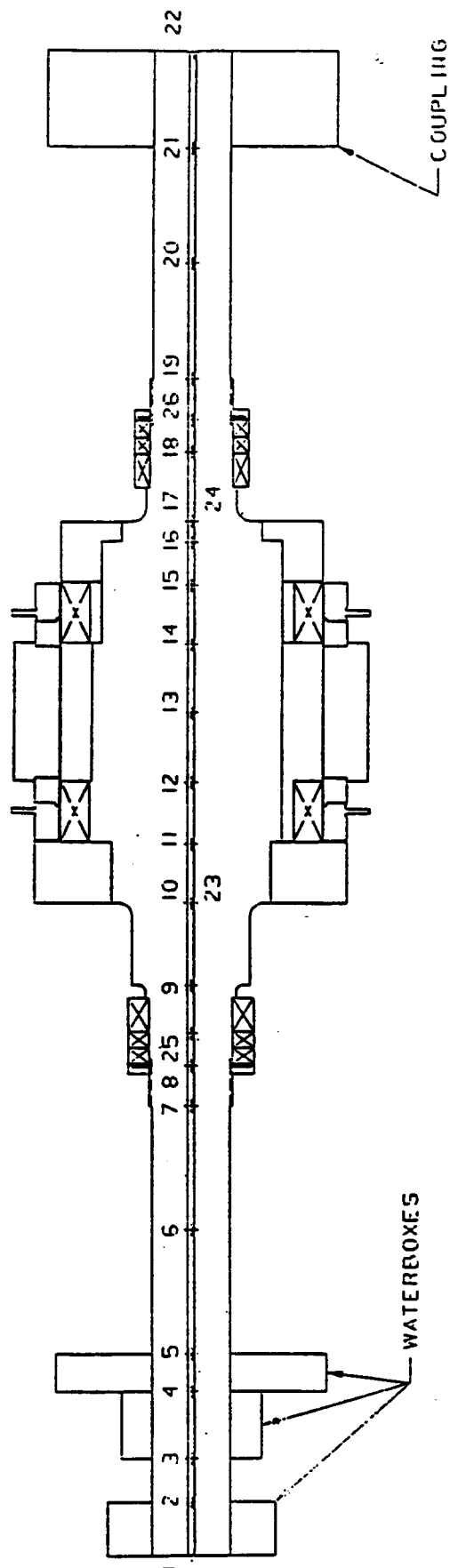


Fig. D-2. Inner Shaft

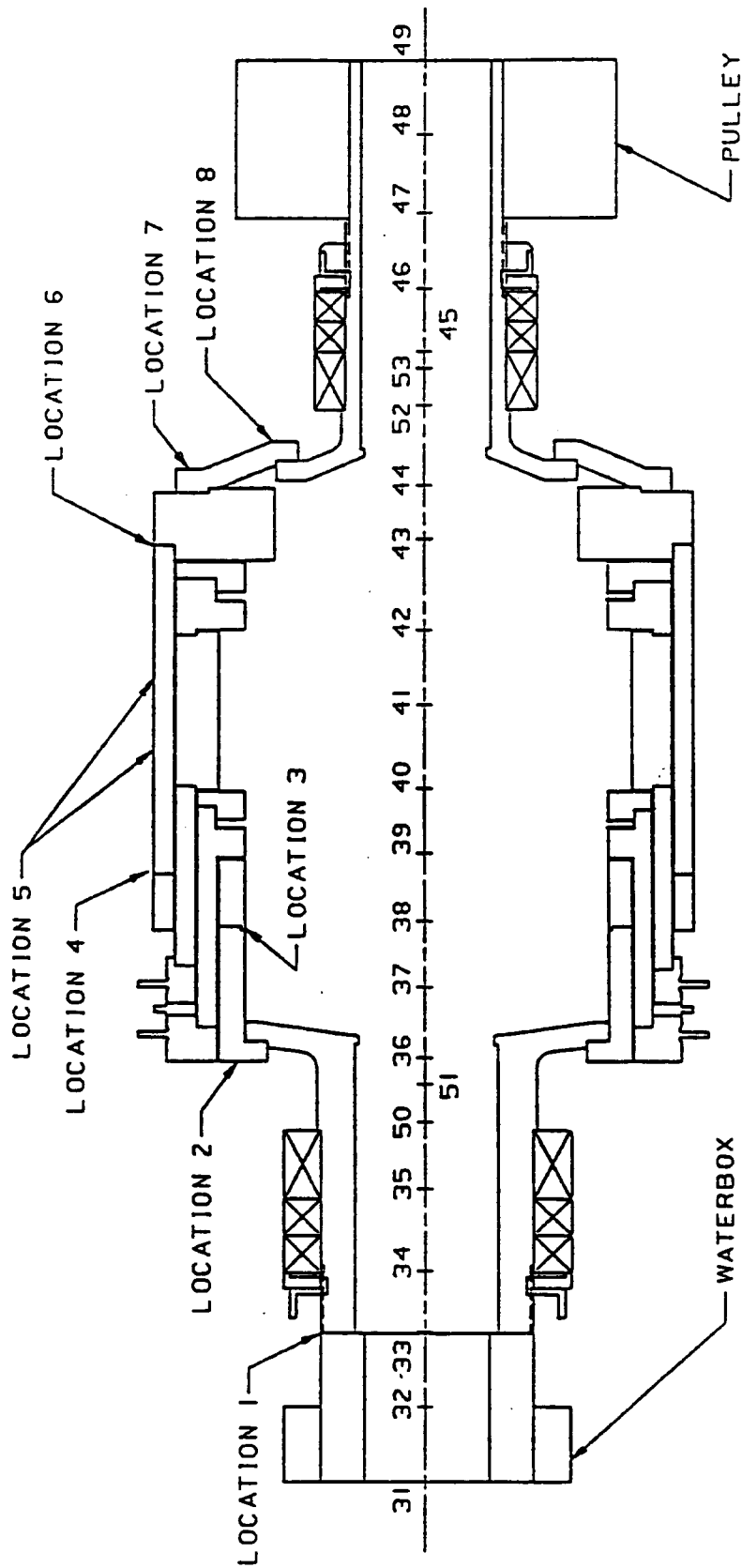


Fig. D-3. Outer Shaft

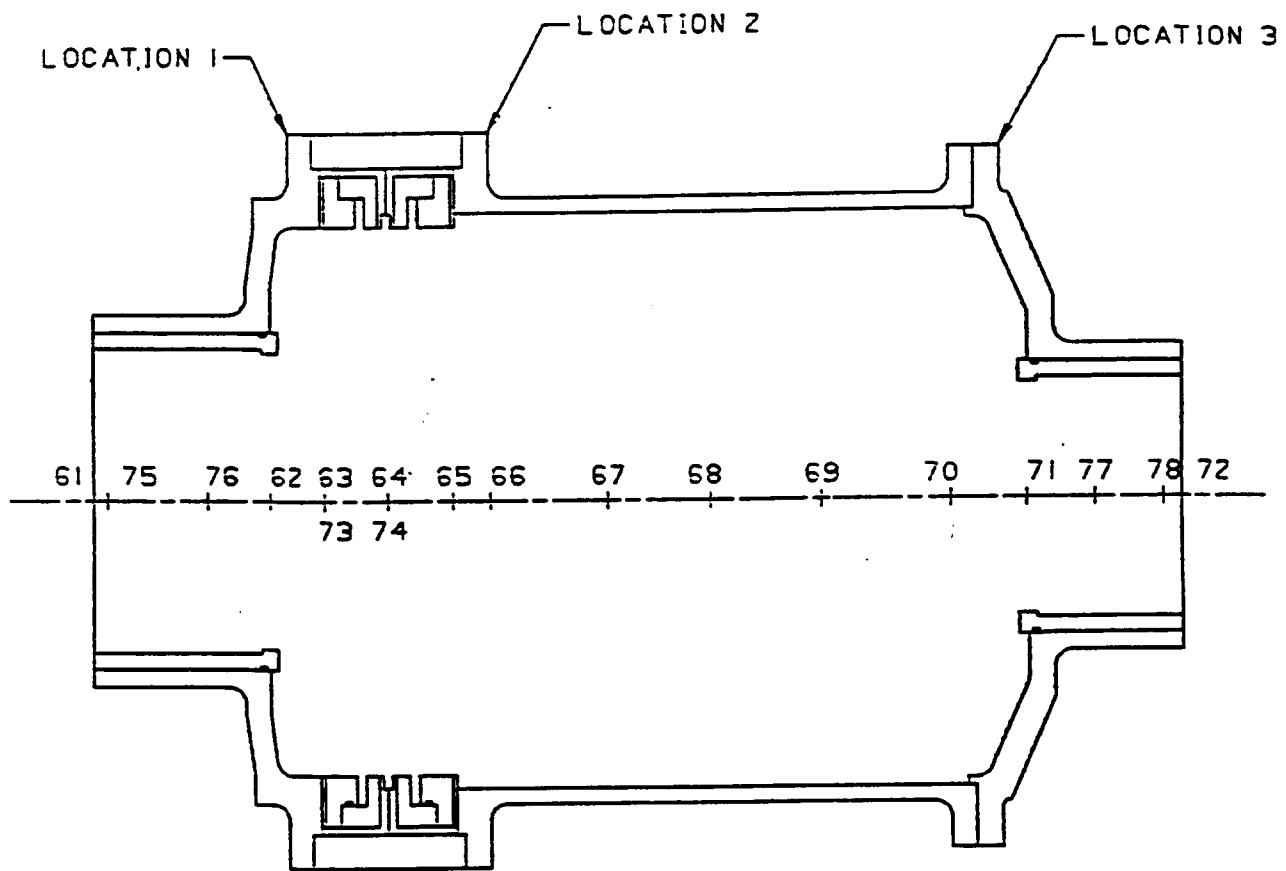


Fig. D-4. Housing

For the dynamic cases, the FE model was held from translations and was held from rotating in all directions as the drive end so as to have a stable model. A satisfactory result would have the lowest natural frequency well above the maximum operating speed.

The lowest natural frequency of the assembly was at 69 Hz or 4140 rpm, which is more than three times higher than the maximum operating speed. The shafts and housing supported as described should be acceptable.

At locations where changes in diameter occur, the stresses were multiplied by stress concentrations factors, torsion or bending, respectively for the first two cases. For the combined case, the larger of the two factors was used. To calculate the actual combined stress concentration factor, K_c , is very involved and assuming the larger of the two separate cases is to err conservatively. See tables D-2 through D-4 for the stress concentration factors applied to the three load cases.

TABLE D-2. Inner Shaft Stress Concentration Factors

NODE	D/d	r/d	K_t	K_b	K_c
8	1.07	.01*	1.8	2.58	2.58
9	1.10	.01*	1.8	2.7	2.7
10	1.35	.06	1.65	1.9	1.9
11	1.30	.01*	2.15	2.8	2.8
12	1.02	0*	1.8	2.3	2.3
14	1.11	0	1.9	2.7	2.7
16	1.29	.01	2.15	2.8	2.8
17	1.59	.08	1.55	1.7	1.7
18	1.10	.01*	1.8	2.7	2.7
26	1.07	.01*	1.8	2.58	2.58

TABLE D-3. Outer Shaft Stress Concentration Factors

NODE	D/d	r/d	K_t	K_b	K_c
50	1.04	.01	1.8	2.6	2.6
36	1.65	.14	1.3	1.5	1.5
44	1.77	.19*	1.25	1.4	1.4
52	1.05	.01*	1.8	2.6	2.6

TABLE D-4. Housing Stress Concentration Factors

NODE	D/d	r/d	K _t	K _b	K _c
62	1.6	.09	1.45	1.7	1.7
63	1.2	.06	1.55	1.9	1.9
66	1.1	.05	1.3	1.85	1.85
70	1.1	.05	1.3	1.85	1.85
71	1.5	.13	1.4	1.6	1.6

* - Radius is determined by bearing company specs.
assumed 1/32" radius

These values were calculated from diagrams from Ref. 11.

The results from the first two load cases generated mean Von Mises stresses and alternating Von Mises stresses, respectively. The alternating and mean stresses were multiplied by the appropriate stress concentration factors and then plotted on the stress axes of a Soderberg diagram. The fatigue safety factor was calculated by dividing the alternating strength by the alternating stress (of the mean strength by the mean stress). The alternating and mean strengths are derived from a line drawn from the origin through the plotted stress point and intersecting the Soderberg line. The results from the third load case generated maximum Von Mises stresses for the static load condition. These stresses, after being multiplied by K_c, were compared to the yield strength for the static factor of safety per reference 11.

It was assumed that direct drive coupling would be used to transmit power from the motors inner shaft to a dynamometer since calculations proved that the inner shaft could not support the side loads imposed by a belt type drive.

To transmit power from the motor to a dynamometer, the outer shaft was assumed to have a belt-pulley type connection. For this application a custom pulley will be required. A Browning type pulley (12" diameter, 104 lb) provided a weight estimate. A belt force of 3939 pounds was applied at the drive end of the shaft.

The stress and safety factors for the three components are displayed in Table D-5. The deflections are in Table D-6. The Soderberg graphs for the three components are

shown in Figs. D-5, D-6, and D-7. Hand calculations verifying stress levels for the inner and outer shafts are also presented.

TABLE D-5. Stress And Safety Factors

COMPONENT	CASE	NODE	VON MISES STRESS	K	MOD. STRESS	SAFETY FACTOR
INNER SHAFT	a	18	5399	1.8	9718	-
	b	18	580	2.7	1566	2.4
	c	18	5430	2.7	14661	2.2
OUTER SHAFT	a	52	1796	1.8	3233	-
	b	52	2810	2.6	7306	1.9
	c	52	3131	2.6	8141	3.7
HOUSING	a	-	-	-	-	-
	b	70	182	1.9	337	46
	c	70	182	1.9	337	104

TABLE D-6. Deflections

COMPONENT	NODE	MAX. DEFL	NODE	DEFLECT. BETWEEN BEARINGS
INNER SHAFT	1	1.1E-3	17	1.6E-4
OUTER SHAFT	49	3.6E-3	44	6.4E-5
HOUSING	72	2.0E-4	68	8.2E-6

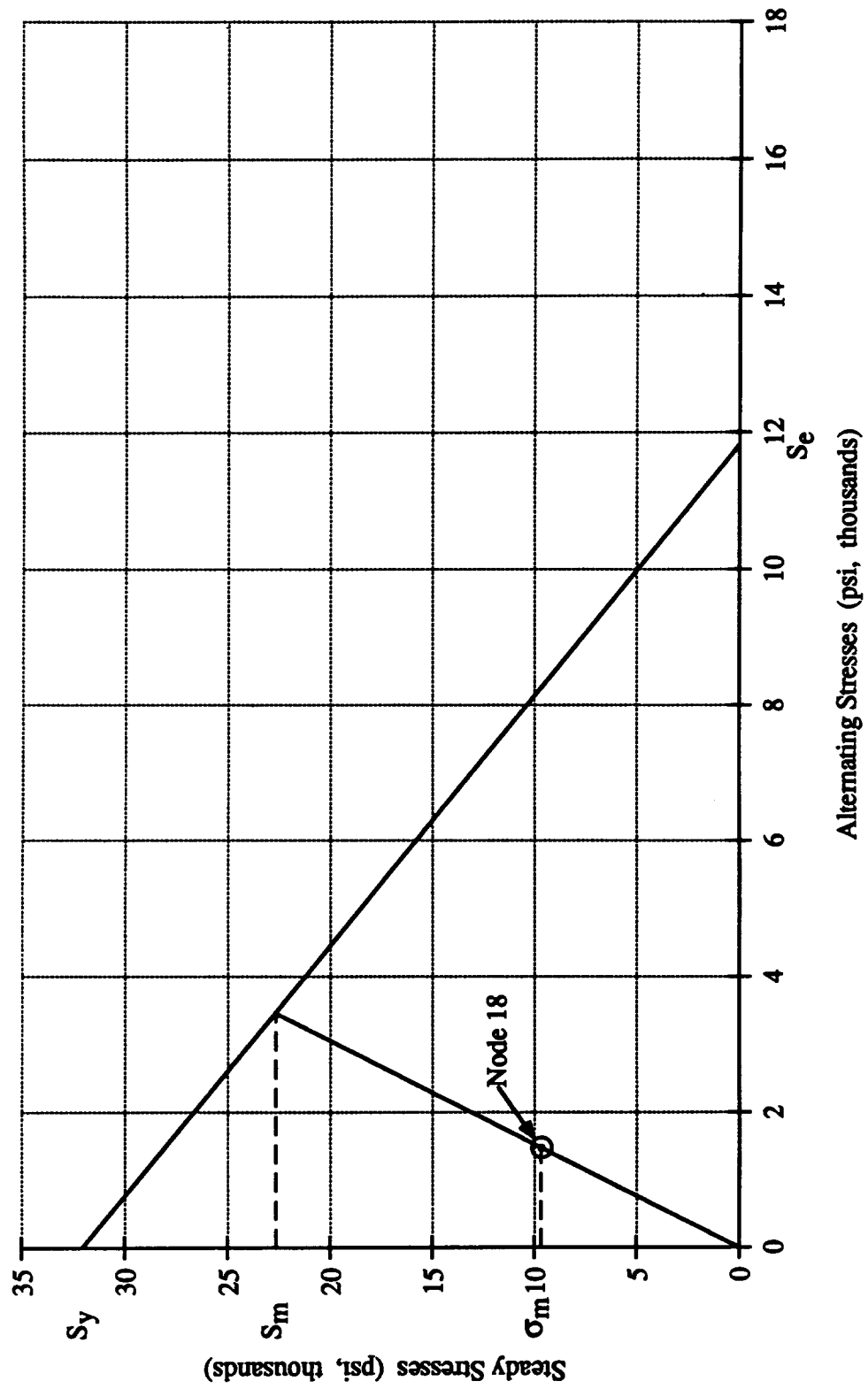


Fig. D-5. Inner Shaft Fatigue Stress

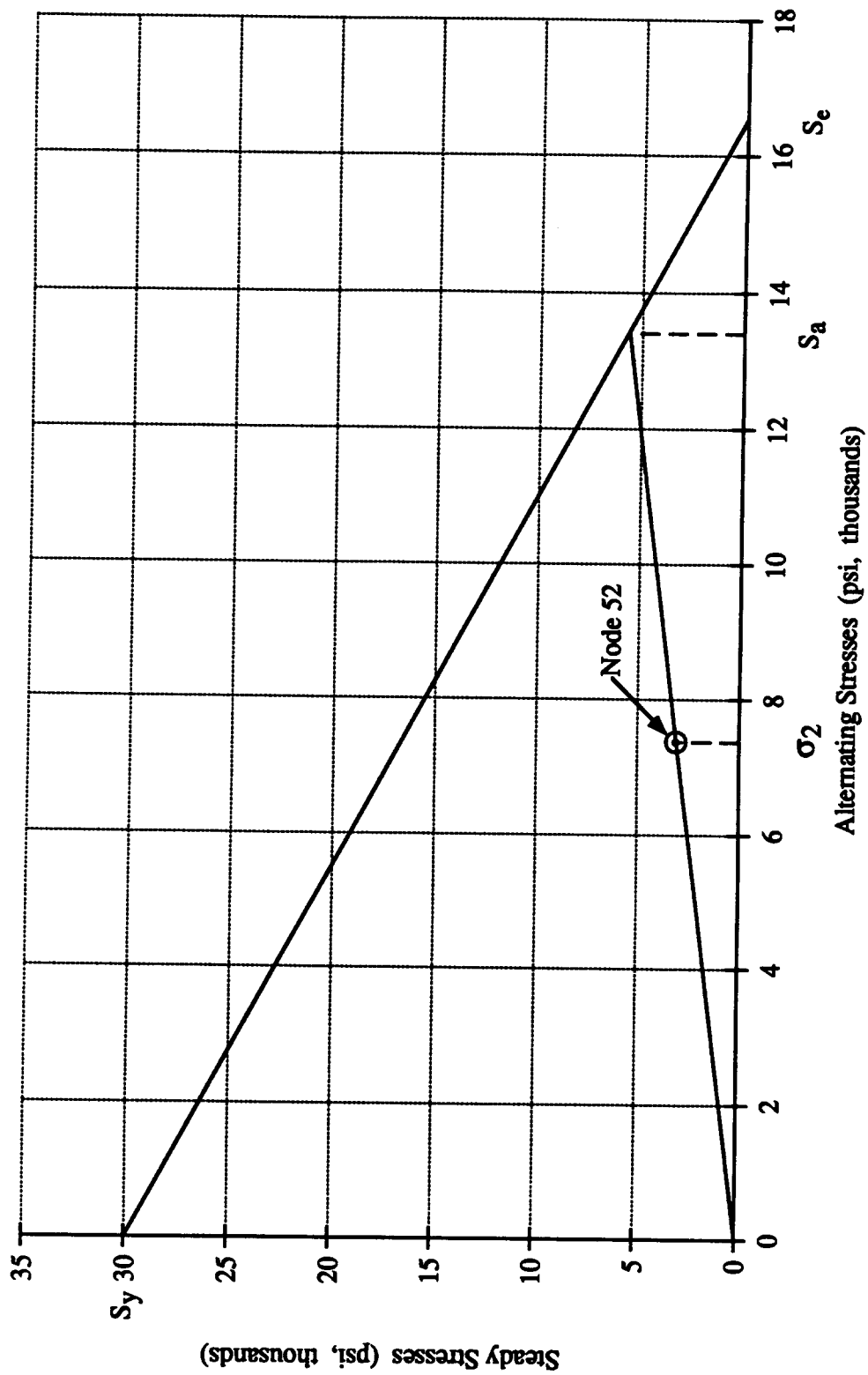


Fig. D-6. Outer Shaft Fatigue Stress

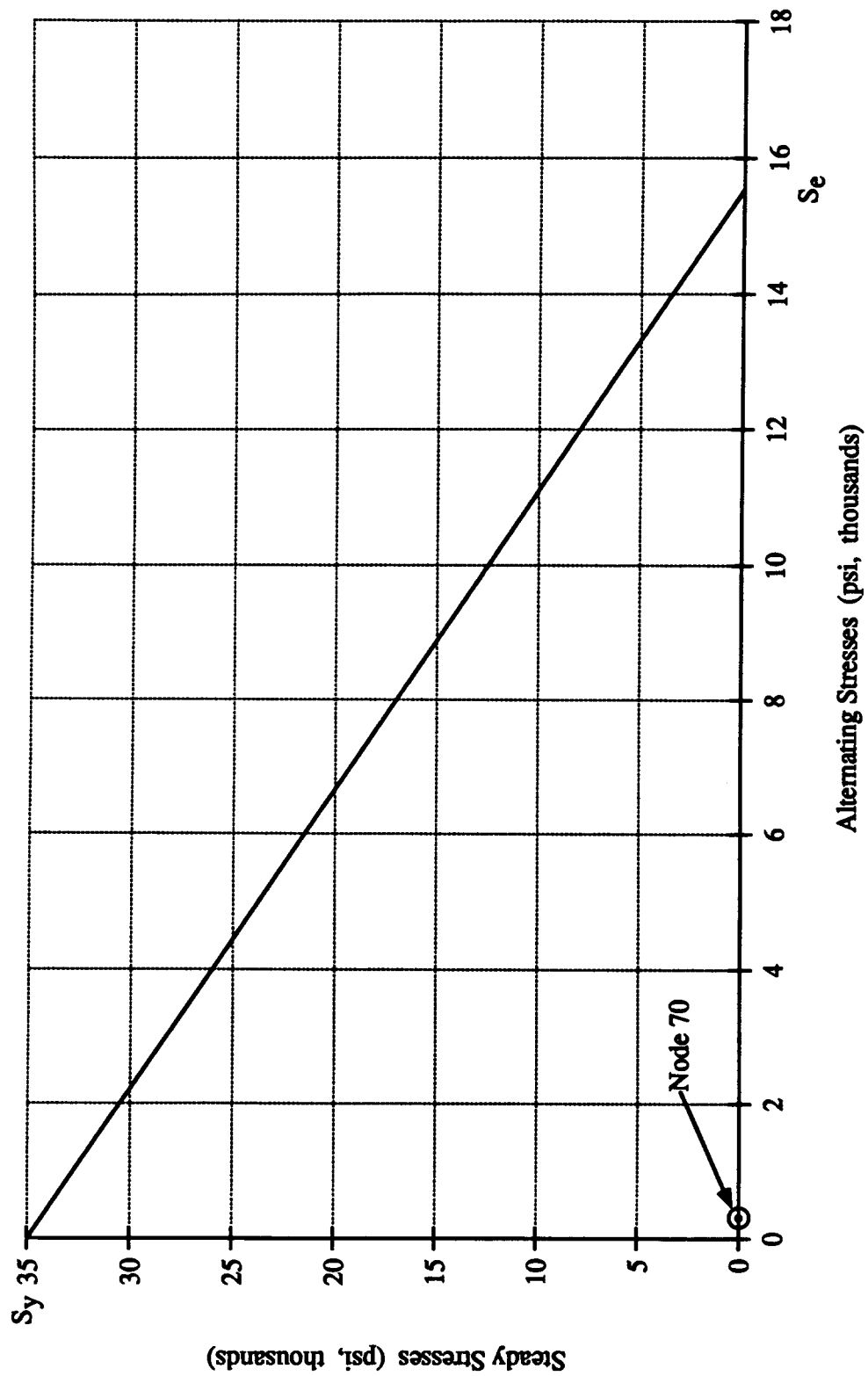


Fig. D-7. Housing Fatigue Stress

PRELIMINARY CALCULATION OF HOMOPOLAR MOTOR INNER SHAFT

Assumptions:

Power to be transmitted is 300 hp.

Shaft material is 1018, hot rolled steel.

A pulley was found from the Browning Catalog to transmit 300 hp on a 2 3/4" diameter shaft, a Poly V drive with 15" diameter. The weight of the pulley and half the belt is 113 lb.

Calculations:

$$T = 63026 P / N = 63025 * 300 / 1200 = 15,756 \text{ in-lb}$$

$$F = 2 T K_L = 1.5 \text{ for pulley connection}$$

$$= 2 * 15756 * 1.5 / 15 = 113 = 3264 \text{ lb}$$

Reverse Bending

this calculation is based on belt tension acting at the right end of shaft, the longest unsupported span. The calculation is simplified by assuming a constant diameter of 2 3/4" from right bearing to end of shaft.

$$M = F L = 3264 * 12 = 39,168 \text{ in-lb}$$

$$s_a = \frac{32 M D^4}{\pi (D^4 - d^4)} = 19,190 \text{ psi} \quad (\text{REF 11})$$

$$S_e = 10,962 \text{ psi}$$

$s_a > S_e$ therefore shaft is too small
for overhung load

STRESS CALCULATION VERIFICATION

Assumptions:

Power to be transmitted is 300 hp.

The weight of half the coupling is 15 lb.

The weight of the pulley and half the belt is 102 lb.

Shaft is cantilever beam, double bearings act as fixed end condition, with uniform load due to weight and a concentrated load due to weight of pulley or coupling.

INNER SHAFT

Calculations:

$$I = \pi (D^4 - d^4) / 64 = \pi (2.953^4 - .375^4) / 64 = 3.7 \text{ in}^4$$

$$J = \pi (D^4 - d^4) / 32 = \pi (2.953^4 - .375^4) / 32 = 7.5 \text{ in}^4$$

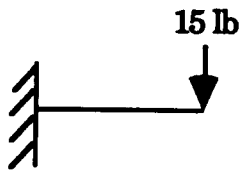
$$w = d \pi (D^2 - d^2) / 4 = .28 \pi (2.953^2 - .375^2) / 4 = 1.9 \text{ lb/in}$$

Steady Stress

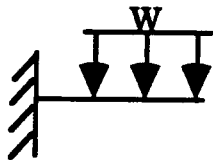
$$t_m = T r / J = 15756(1.48) / 7.5 = \underline{3120 \text{ psi}}$$

3117 psi from MSC/PAL2

Alternating Stress



$$\begin{aligned} M &= F l \\ &= 15 (13.4) \\ &= 201 \text{ in-lb} \end{aligned}$$



$$\begin{aligned} M &= w l^2 / 2 \\ &= 1.9 (13.4^2) / 2 \\ &= 171 \text{ in-lb} \end{aligned}$$

$$s = M c / I = (201 + 171) 1.48 / 3.7 = 147 \text{ psi}$$

Maximum Von Mises Stress

$$s' = (s^2 + 3 t_m^2)^{1/2} = (147^2 + 3(3120^2))^{1/2}$$

$$s' = \underline{5406 \text{ psi}}$$

5400 psi from MSC/PAL2

OUTER SHAFT

Calculations:

$$I = \pi (D^4 - d^4) / 64 = \pi (5.12^4 - 4.13^4) / 64 = 19.5 \text{ in}^4$$

$$J = \pi (D^4 - d^4) / 32 = \pi (5.12^4 - 4.13^4) / 32 = 38.9 \text{ in}^4$$

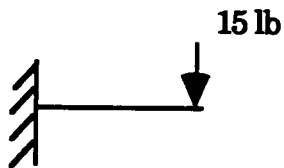
$$w = d \pi (D^2 - d^2) / 4 = .28 \pi (5.12^2 - 4.13^2) / 4 = 2.0 \text{ lb/in}$$

Steady Stress

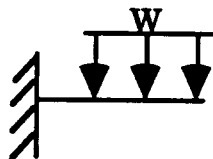
$$t_m = T r / J = 15756(2.56) / 38.9 = \underline{1037 \text{ psi}}$$

1037 psi from MSC/PAL2

Alternating Stress



$$\begin{aligned} M &= F l \\ &= 102(4.9) \\ &= 499.8 \text{ in-lb} \end{aligned}$$



$$\begin{aligned} M &= w l^2 / 2 \\ &= 2(7.4^2) / 2 \\ &= 54.8 \text{ in-lb} \end{aligned}$$

$$s = M c / I = (500 + 55)2.56 / 19.5 = 72.8 \text{ psi}$$

Maximum Von Mises Stress

$$s' = (s^2 + 3t_m^2)^{1/2} = (73^2 + 3(1037^2))^{1/2}$$

$$s' = \underline{1798 \text{ psi}}$$

1796 psi from MSC/PAL2

BOLT LOADING, STRESSES AND SAFETY FACTORS

The bolt loads for the major connections of the outer shaft and the housing were calculated for shear and axial stresses. All the bolts are assumed to be preloaded so that none will be subject to cyclic loading. A high preload improves the fatigue resistance of a bolted connection. The bolt connection locations are shown in Figs D-3 and D-4. Note, this model was developed to determine the stress and deflections of large components, which was accomplished by using coarse circular beam elements. It was not intended to be used to solve areas of local stress on a small scale. These results for the bolts are only useful as a rough guide for sizing and numbers required. See tables D-7 through D-12 for the results of the calculations of the bolt loading, stresses and safety factors.

$$\text{Shear Stress} \\ t = \frac{(s + T/d)}{A_s}$$

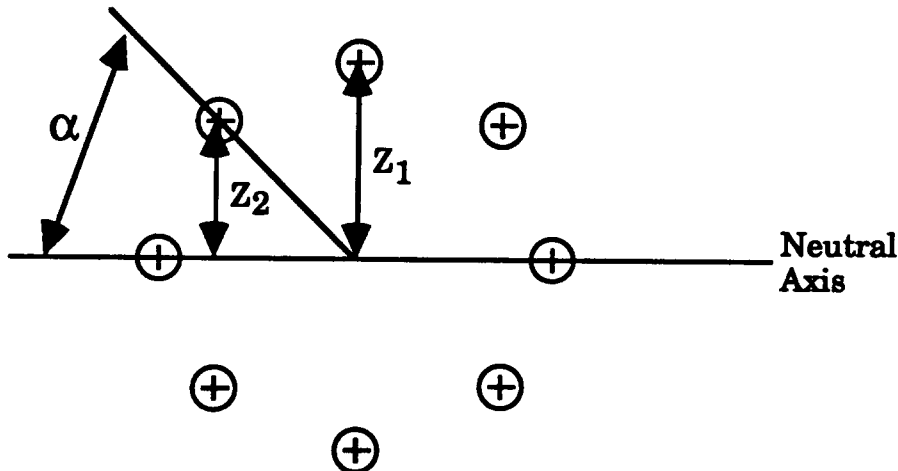
$$\text{Axial Stress} \\ s = \frac{(p + F_b)}{A_t}$$

$$S_{sy} = .577 * S_y \text{ (REF. 11)}$$

$$t_{\max} = ((s/2)^2 + t^2)^{1/2}$$

$$s_{\max} = t_{\max} + s/2$$

Assume all bolts are preloaded so that there will be no cyclic loading on any bolts.



Calculation of Axial Bolt Load from a Moment

The force on each bolt is proportional to the distance from the neutral axis. It is assumed that the ration of force on each bolt was a quadratic of the distance.

For an 8 bolt connection:

$$z_1 = r \quad z_2 = r \sin a \quad \sum z = 2*z_1' + 4*z_2'$$
$$z_n' = z_n^2 / z_1^2 \quad z_1' = 1 \quad z_2' = .5, \text{ for any radius}$$

$$\text{Therefore } \sum z = 2*1 + 4*.5 = 4$$

$$M' = M / \sum z \quad M_{bn} = M' * z_n' \quad F_{bn} = M_{bn} / z_n$$

In table D-7 axial bolt load was only calculated for the bolt farthest away from the center, F_{b1} , the worst case; $F_{b1} = M_{b1} / z_1$

For any insulated bolts, it is assumed that only the shank is turned down and insulated and that the shank diameter is not less than the minor diameter.

BOLT LOADING, STRESSES AND SAFETY FACTORS OUTER SHAFT

Group 1

Assume 1/4-20 UNC bolts, 8 per connection

$$S_y = 55,000 \text{ psi}$$

$$S_{sy} = 31,735 \text{ psi Grade 2 Steel}$$

$$A_s = .027 \text{ sq in}$$

$$A_t = .032 \text{ sq in}$$

TABLE D-7. Total Forces At Connection

Bolt	Axial	Shear	Torsion	Moment
	p	s	T	M
Location	LB	LB	IN-LB	IN-LB
1	0	65	0	177
2	0	904	0	2170
3	0	962	0	6181
4	0	1140	0	8491
5	0	0	15760	0

TABLE D-8. Stresses Per Bolt

	AXIAL Fb	t PSI	s PSI	tmax PSI	smax PSI	FS t	FS s
1	22	301	691	458	804	69	68
2	103	4185	3229	4486	6100	7	9
3	252	4454	3229	5948	9890	5	6
4	260	5278	8139	6665	10734	5	5
5	0	9728	0	9728	9728	3	6

Group 2

Sy = 170,000 psi Ssy = 98,090 psi Unbrako Series 1960

TABLE D-9. Total Forces At Connection

BOLT	AXIAL	SHEAR	TORSION	MOMENT
	p	s	T	M
LOCATION	LB	LB	IN-LB	IN-LB
6	0	1356	15760	21100
7	0	1451	15760	23580
8	0	1494	15760	23590

TABLE D-10. Stresses Per Bolt

BOLT	AXIAL Fb	t PSI	s PSI	tmax PSI	smax PSI	FS t	FS s
6	649	15258	20288	18322	28467	5	6
7	813	16781	25409	21048	33753	5	6
8	1311	23131	40955	30893	51370	3	3

BOLT LOADING, STRESSES AND SAFETY FACTORS HOUSING

Assume 1/4-20 UNC bolts, 8 per connection

Sy = 55,000 psi Ssy = 31,735 psi Grad 2 Steel

As = .027 sq in At - .032 sq in

TABLE D-11. Total Forces At Connection

BOLT LOCATION	AXIAL p LB	SHEAR s LB	TORSION T IN-LB	MOMENT M IN-LB
1	0	392	0	399
2	0	1132	0	4938
3	0	1232	0	21290

TABLE D-12. Stresses Per Bolt

	AXIAL Fb	t PSI	s PSI	tmax PSI	smax PSI	FS t	FS s
1	10	1815	300	18322	1971	17	28
2	119	5241	3718	21048	7420	6	7
3	374	5704	11672	30893	13996	4	4

APPENDIX E

DRAWING LIST

[illegible][illegible]

NOTES:

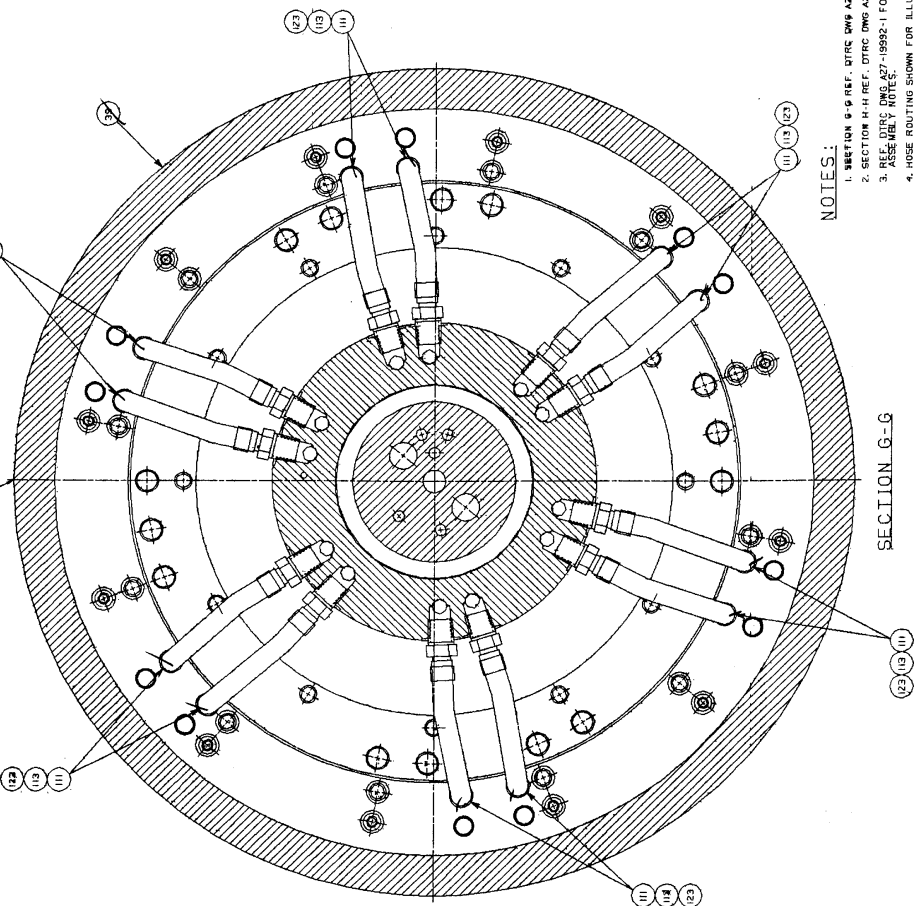
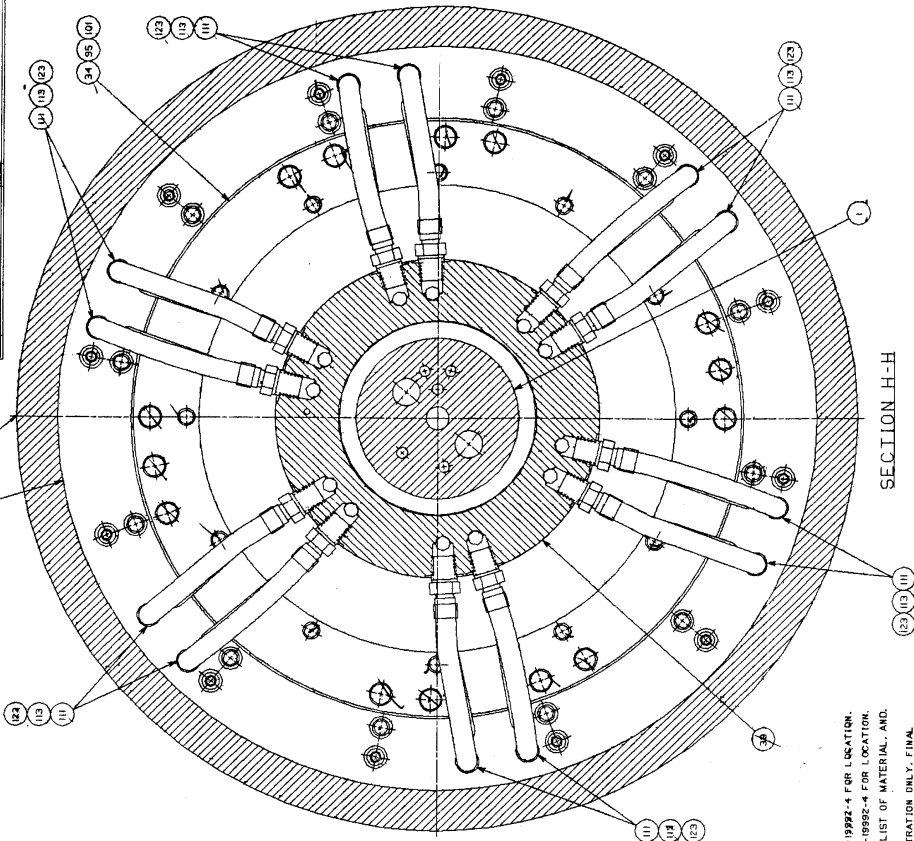
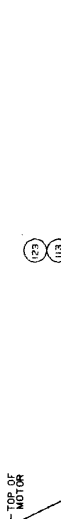
1. DETAILS OF INLET/OUTLET TUBES, PC NO 88 AND 89, TO BE SPECIFIED BY CDR 27H.
2. USE ACRYLIC ADHESIVE TO BOND INSULATIONS TO METAL RINGS. THE ADHESIVE SHOULD BE APPLIED TO BOTH SURFACES OF THE ADHESIVE, ON EQUAL, IS RECOMMENDED.
3. USE THREAD LOCKING AGENT ON THREADS OF FASTENERS. LOCITITE IS RECOMMENDED.
4. USES MOLDED RUBBER HOSE ELBOWS TO BE TRIMMED TO SUIT INSTALLATION.
5. ARRANGEMENT TO BE USED AS A PART OF MAX INJECTION ARRANGEMENT MODIFICATIONS TO ID OF FITTING TO BE SPECIFIED BY CDR 27H.
6. ARRANGEMENT MODIFICATIONS TO ID OF FITTINGS TO BE SPECIFIED BY CDR 27H. THIS ALTERNATE TO BE USED FOR REMAINING REMOVAL OF ID OF FITTINGS TO BE MODIFIED. ID MUST BE 255.005-500.
7. NYLON FRONT AND BACK FERRULES TO BE USED TO MOUNT THERMOCOUPLES IN THESE FITTINGS MODIFIED WITH 255 ID.
8. 10 AIR LINES LOCKING THE AIR LINE FROM PROVIDING MONITORING FOR DETAIL OF INSULATED LOCK PIN TO BE SPECIFIED BY CDR 27H.
9. DETAIL LENGTH OF ADAPTER FITTING TO BE SHORTENED TO .389 LONG.
10. DETAILS OF BARBED HOSE FITTING TO BE SPECIFIED BY CDR 27H.
11. TUBE FITTING TO BE USED FOR AM INJECTION. DETAILS OF TUBE TO BE SPECIFIED BY CDR 27H.
12. REF MANORANDUM TITLED "CONTRACTING HEMPOLD MOTOR SHAFT REMOVAL LOCATION" BY THOMAS HANE CODE 1473 FOR INFORMATION

[illegible]

REV.	ZONE	DESCRIPTION	BY	APP'D
<p align="center">REVISIONS</p> <p>DATE 4/2/2011 NORMAL CONVECTION, HORIZONTAL, CONTRAST AT 147, 175 IP MOTOR</p> <p align="center">PARTS LIST</p> <p>DATE 4/2/2011 CHANGED DIMAN DATE 4/2/2011 REDESIGNED DIMAN DATE 4/2/2011 REDESIGNED DIMAN</p>				
DEPARTMENT OF ARMY RAND TAYLOR RESEARCH CENTER			DRAWING NO. - 1000000-0000 TITLE - 1000000-0000 DATE 4/2/2011	
SCALE: NONE			427-19392-1 -	

[illegible]

TOP OF
MOTOR



NOTES:

1. SECTION G-G REF. DTRC DWG A27-19992-4 FOR LOCATION.
2. SECTION H-H REF. DTRC DWG A27-19992-4 FOR LOCATION.
3. REF. DTRC DWG A27-19992-1 FOR LIST OF MATERIAL. AND, ASSEMBLY NOTES.
4. HOSE ROUTING SHOWN FOR ILLUSTRATION ONLY. FINAL CONFIGURATION TO BE DETERMINED BY CODE 2711.

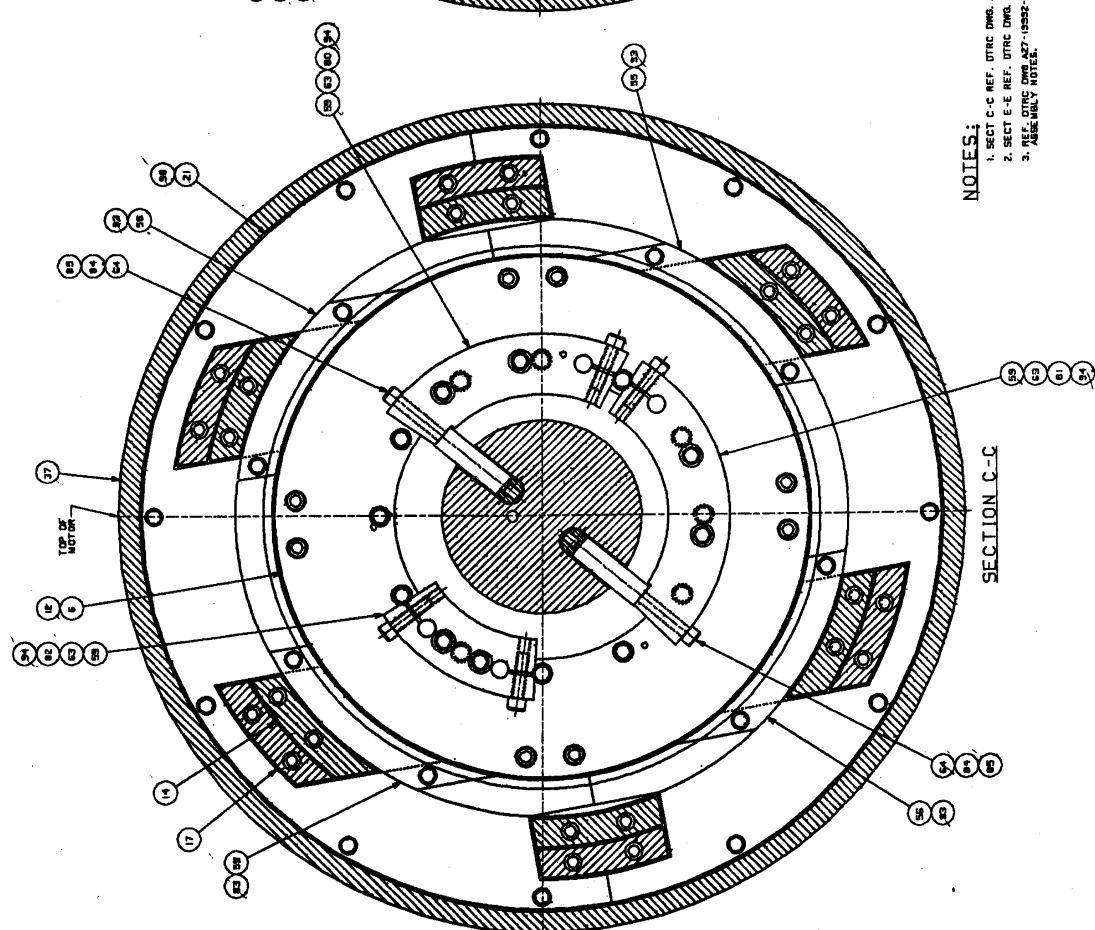
SECTION H-H

SECTION G-G

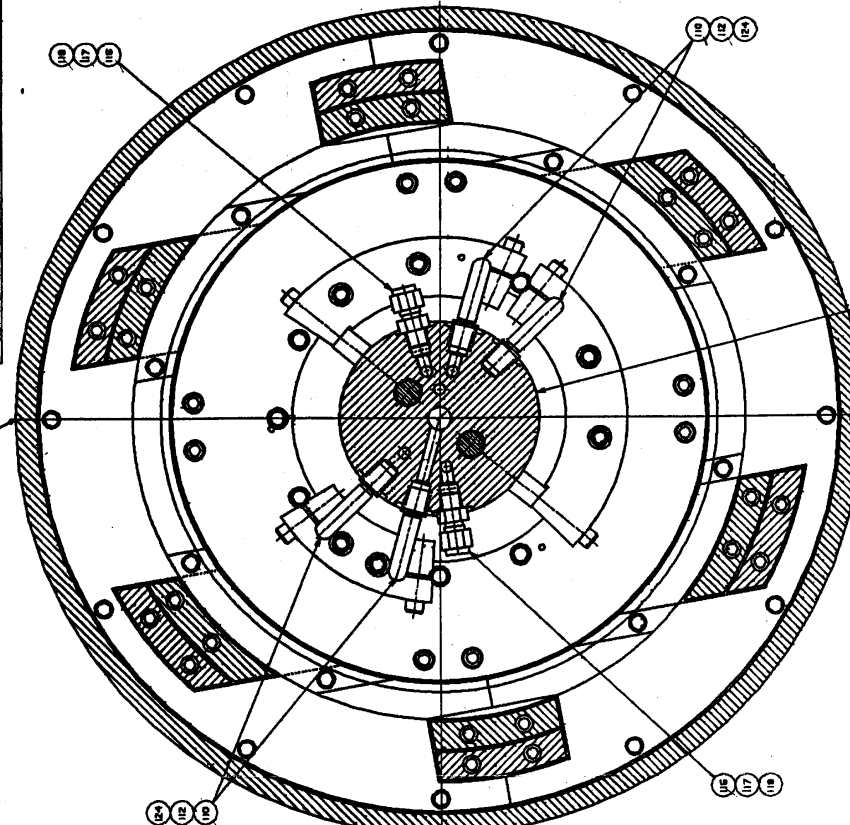
REC'D		ZONE		RECEIVED FROM		DATE		BY		DATE	
CASSER PART NAME		DATE		ZONE		DATE		BY		DATE	
AIR FILTER, 100MM X 2557		10/20/78		2000		10/20/78		JW		10/20/78	
APPROVED		DATE		ZONE		DATE		BY		DATE	
A2713957-1 - A		10/27/78		2000		10/27/78		JW		10/27/78	
APPROVED		DATE		ZONE		DATE		BY		DATE	
A2713957-1 - A		10/27/78		2000		10/27/78		JW		10/27/78	
APPROVED		DATE		ZONE		DATE		BY		DATE	
A2713957-1 - A		10/27/78		2000		10/27/78		JW		10/27/78	
APPROVED		DATE		ZONE		DATE		BY		DATE	
A2713957-1 - A		10/27/78		2000		10/27/78		JW		10/27/78	
APPROVED		DATE		ZONE		DATE		BY		DATE	
A2713957-1 - A		10/27/78		2000		10/27/78		JW		10/27/78	
APPROVED		DATE		ZONE		DATE		BY		DATE	
A2713957-1 - A		10/27/78		2000		10/27/78		JW		10/27/78	
APPROVED		DATE		ZONE		DATE		BY		DATE	
A2713957-1 - A		10/27/78		2000		10/27/78		JW		10/27/78	
APPROVED		DATE		ZONE		DATE		BY		DATE	
A2713957-1 - A		10/27/78		2000		10/27/78		JW		10/27/78	
APPROVED		DATE		ZONE		DATE		BY		DATE	
A2713957-1 - A		10/27/78		2000		10/27/78		JW		10/27/78	
APPROVED		DATE		ZONE		DATE		BY		DATE	
A2713957-1 - A		10/27/78		2000		10/27/78		JW		10/27/78	
APPROVED		DATE		ZONE		DATE		BY		DATE	
A2713957-1 - A		10/27/78		2000		10/27/78		JW		10/27/78	
APPROVED		DATE		ZONE		DATE		BY		DATE	
A2713957-1 - A		10/27/78		2000		10/27/78		JW		10/27/78	
APPROVED		DATE		ZONE		DATE		BY		DATE	
A2713957-1 - A		10/27/78		2000		10/27/78		JW		10/27/78	
APPROVED		DATE		ZONE		DATE		BY		DATE	
A2713957-1 - A		10/27/78		2000		10/27/78		JW		10/27/78	
APPROVED		DATE		ZONE		DATE		BY		DATE	
A2713957-1 - A		10/27/78		2000		10/27/78		JW		10/27/78	
APPROVED		DATE		ZONE		DATE		BY		DATE	
A2713957-1 - A		10/27/78		2000		10/27/78		JW		10/27/78	
APPROVED		DATE		ZONE		DATE		BY		DATE	
A2713957-1 - A		10/27/78		2000		10/27/78		JW		10/27/78	
APPROVED		DATE		ZONE		DATE		BY		DATE	
A2713957-1 - A		10/27/78		2000		10/27/78		JW		10/27/78	
APPROVED		DATE		ZONE		DATE		BY		DATE	
A2713957-1 - A		10/27/78		2000		10/27/78		JW		10/27/78	
APPROVED		DATE		ZONE		DATE		BY		DATE	
A2713957-1 - A		10/27/78		2000		10/27/78		JW		10/27/78	
APPROVED		DATE		ZONE		DATE		BY		DATE	
A2713957-1 - A		10/27/78		2000		10/27/78		JW		10/27/78	
APPROVED		DATE		ZONE		DATE		BY		DATE	
A2713957-1 - A		10/27/78		2000		10/27/78		JW		10/27/78	
APPROVED		DATE		ZONE		DATE		BY			

REVISIONS		DATE	BY	REASON
1				
2				
3				
4				
5				
6				
7				
8				
9				
10				
11				
12				
13				
14				
15				
16				
17				
18				
19				
20				
21				
22				
23				
24				
25				
26				
27				
28				
29				
30				
31				
32				
33				
34				
35				
36				
37				
38				
39				
40				
41				
42				
43				
44				
45				
46				
47				
48				
49				
50				
51				
52				
53				
54				
55				
56				
57				
58				
59				
60				
61				
62				
63				
64				
65				
66				
67				
68				
69				
70				
71				
72				
73				
74				
75				
76				
77				
78				
79				
80				
81				
82				
83				
84				
85				
86				
87				
88				
89				
90				
91				
92				
93				
94				
95				
96				
97				
98				
99				
100				

TOP OF MOTOR



SECTION C-C



SECTION E-E

- NOTES:
1. SECT C-C REF. DTRC DWS. A27-19992-4 FOR LOCATION.
 2. SECT E-E REF. DTRC DWS. A27-19992-4 FOR LOCATION.
 3. SEE DWS. A27-19992-1 FOR LIST OF MATERIAL, AND SEE DWS. A27-19992-2 FOR LIST OF MATERIAL, AND SEE DWS. A27-19992-3 FOR LIST OF MATERIAL.

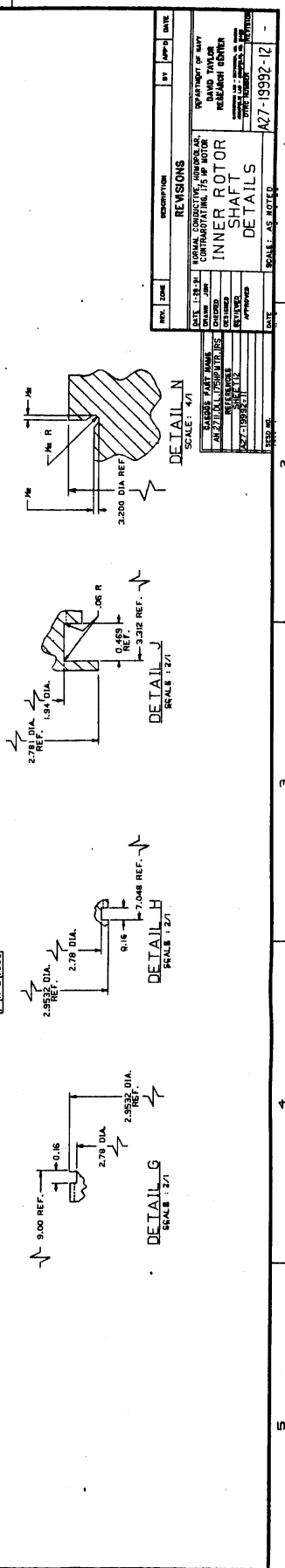
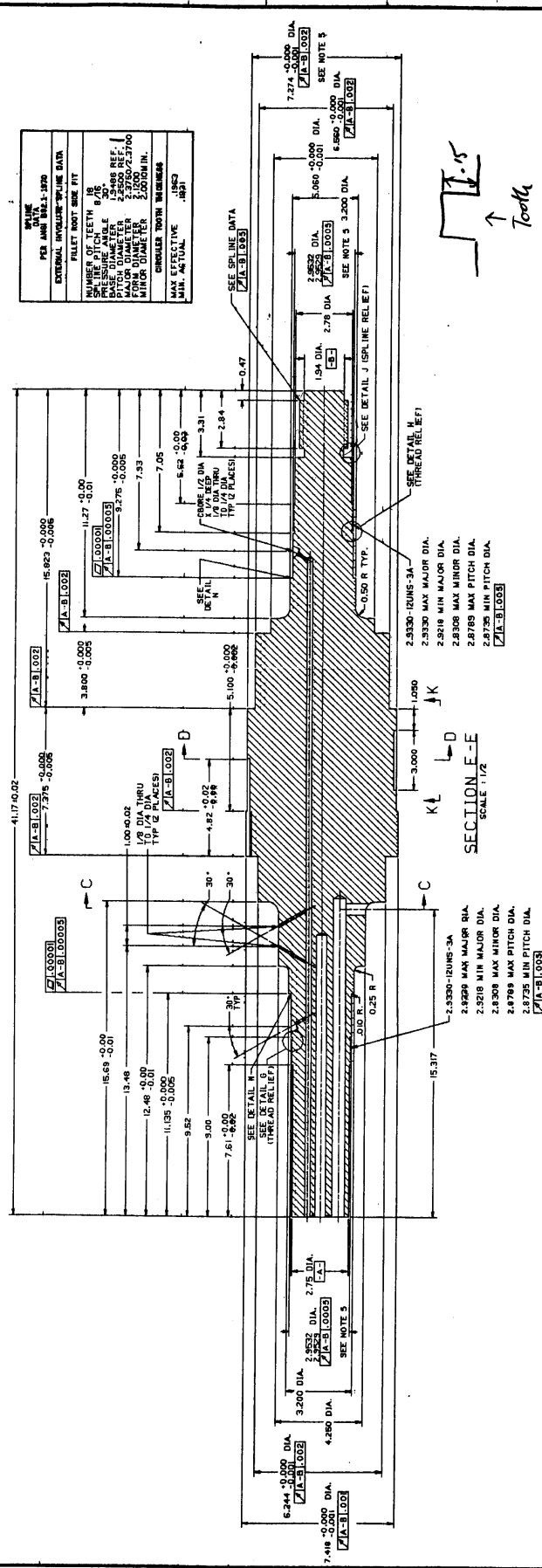
REVISIONS		DATE	BY	REASON
1				
2				
3				
4				
5				
6				
7				
8				
9				
10				
11				
12				
13				
14				
15				
16				
17				
18				
19				
20				
21				
22				
23				
24				
25				
26				
27				
28				
29				
30				
31				
32				
33				
34				
35				
36				
37				
38				
39				
40				
41				
42				
43				
44				
45				
46				
47				
48				
49				
50				
51				
52				
53				
54				
55				
56				
57				
58				
59				
60				
61				
62				
63				
64				
65				
66				
67				
68				
69				
70				
71				
72				
73				
74				
75				
76				
77				
78				
79				
80				
81				
82				
83				
84				
85				
86				
87				
88				
89				
90				
91				
92				
93				
94				
95				
96				
97				
98				
99				
100				

PROJECT NO.	REV.	DATE	BY	APP'D	DATE
1-2700-205-12	1	12/11/71	DAVID TAYLOR		
1-2700-205-12	2	12/11/71	DAVID TAYLOR		
1-2700-205-12	3	12/11/71	DAVID TAYLOR		
1-2700-205-12	4	12/11/71	DAVID TAYLOR		
1-2700-205-12	5	12/11/71	DAVID TAYLOR		
1-2700-205-12	6	12/11/71	DAVID TAYLOR		
1-2700-205-12	7	12/11/71	DAVID TAYLOR		
1-2700-205-12	8	12/11/71	DAVID TAYLOR		
1-2700-205-12	9	12/11/71	DAVID TAYLOR		
1-2700-205-12	10	12/11/71	DAVID TAYLOR		
1-2700-205-12	11	12/11/71	DAVID TAYLOR		
1-2700-205-12	12	12/11/71	DAVID TAYLOR		
1-2700-205-12	13	12/11/71	DAVID TAYLOR		
1-2700-205-12	14	12/11/71	DAVID TAYLOR		
1-2700-205-12	15	12/11/71	DAVID TAYLOR		
1-2700-205-12	16	12/11/71	DAVID TAYLOR		
1-2700-205-12	17	12/11/71	DAVID TAYLOR		
1-2700-205-12	18	12/11/71	DAVID TAYLOR		
1-2700-205-12	19	12/11/71	DAVID TAYLOR		
1-2700-205-12	20	12/11/71	DAVID TAYLOR		

ITEM	QTY	UNIT	PRICE	TOTAL
1	1	EA	1.00	1.00
2	1	EA	1.00	1.00
3	1	EA	1.00	1.00
4	1	EA	1.00	1.00
5	1	EA	1.00	1.00
6	1	EA	1.00	1.00
7	1	EA	1.00	1.00
8	1	EA	1.00	1.00
9	1	EA	1.00	1.00
10	1	EA	1.00	1.00
11	1	EA	1.00	1.00
12	1	EA	1.00	1.00
13	1	EA	1.00	1.00
14	1	EA	1.00	1.00
15	1	EA	1.00	1.00
16	1	EA	1.00	1.00
17	1	EA	1.00	1.00
18	1	EA	1.00	1.00
19	1	EA	1.00	1.00
20	1	EA	1.00	1.00

NAME OF PIECE	MATERIAL OR SOURCE
1	1-2700-205-12
2	1-2700-205-12
3	1-2700-205-12
4	1-2700-205-12
5	1-2700-205-12
6	1-2700-205-12
7	1-2700-205-12
8	1-2700-205-12
9	1-2700-205-12
10	1-2700-205-12
11	1-2700-205-12
12	1-2700-205-12
13	1-2700-205-12
14	1-2700-205-12
15	1-2700-205-12
16	1-2700-205-12
17	1-2700-205-12
18	1-2700-205-12
19	1-2700-205-12
20	1-2700-205-12

NOTE:
1. REF DETAILS. AND NOTES ON DTRC DWG A27-19992-11.



REV.	DATE	BY	APP'D	DATE
1	12/11/71	DAVID TAYLOR		
2	12/11/71	DAVID TAYLOR		
3	12/11/71	DAVID TAYLOR		
4	12/11/71	DAVID TAYLOR		
5	12/11/71	DAVID TAYLOR		
6	12/11/71	DAVID TAYLOR		
7	12/11/71	DAVID TAYLOR		
8	12/11/71	DAVID TAYLOR		
9	12/11/71	DAVID TAYLOR		
10	12/11/71	DAVID TAYLOR		
11	12/11/71	DAVID TAYLOR		
12	12/11/71	DAVID TAYLOR		
13	12/11/71	DAVID TAYLOR		
14	12/11/71	DAVID TAYLOR		
15	12/11/71	DAVID TAYLOR		
16	12/11/71	DAVID TAYLOR		
17	12/11/71	DAVID TAYLOR		
18	12/11/71	DAVID TAYLOR		
19	12/11/71	DAVID TAYLOR		
20	12/11/71	DAVID TAYLOR		

NOTES:

1. TUBE MATERIAL: COPPER OFC 102-218 1/2 IN. TUBE WITH CONDUCTOR SHALL BE CONTINUOUSLY WELDED TO TUBE AND WELDING SHALL BE TESTED BEFORE AND AFTER WINDING AS FOLLOWS:
PRESSURIZE HELIUM CIRCUIT TO 100 PSI WITH CLEAN DRY SHOP AIR.
CLEAN DRY SHOP AIR SOURCE AND MONITOR PRESSURE FOR 24 HOURS.
OBSERVED PRESSURE DECREASE AFTER 24 HOURS SHALL NOT EXCEED 1 PSI.
2. CONDUCTOR INSULATION: 200 MICA PAPER GLASS TAPE (A-STANDARD) INSULATION THICKNESS: LAY WRAPPING ON TUBE FOR 24 HOURS.
3. COIL INSULATION: 100 MICA PAPER GLASS TAPE (A-STANDARD) INSULATION THICKNESS: LAY WRAPPING ON TUBE FOR 24 HOURS. INSULATION SHALL BE CONTINUOUSLY WELDED TO TUBE AND WELDING SHALL BE TESTED BEFORE AND AFTER WINDING AS FOLLOWS:
PRESSURIZE HELIUM CIRCUIT TO 100 PSI WITH CLEAN DRY SHOP AIR.
CLEAN DRY SHOP AIR SOURCE AND MONITOR PRESSURE FOR 24 HOURS.
OBSERVED PRESSURE DECREASE AFTER 24 HOURS SHALL NOT EXCEED 1 PSI.
4. FOLLOWING WINDING AND INSULATING, ALL RESINS TO BE USED SHALL BE TESTED AS FOLLOWS:
INSULATION TEST FATTY ACID TEST, 100% PASS F OR BETTER.
5. CONDUCTOR TUBE BEND RADIUS: 3/4 IN. TO INSIDE OF BEND.
6. CONDUCTOR TUBE BEND RADIUS: 3/4 IN. TO INSIDE OF BEND.
7. COIL TOLERANCES: 100% ±0.001
8. PRIOR TO FINISH DIMENSIONS
FINISH DIMENSIONS SHALL BE MEASURED FOR THE COILS 20" MAXIMUM FOR THE 50" OF THE COILS 20" MAXIMUM.

COILS ARE 20" TOTAL
COILS ARE 20" TOTAL
COILS ARE 20" TOTAL

20" SEE NOTE 8

ISOMETRIC VIEW

SECTION A-A

SECTION B-B

FRONT

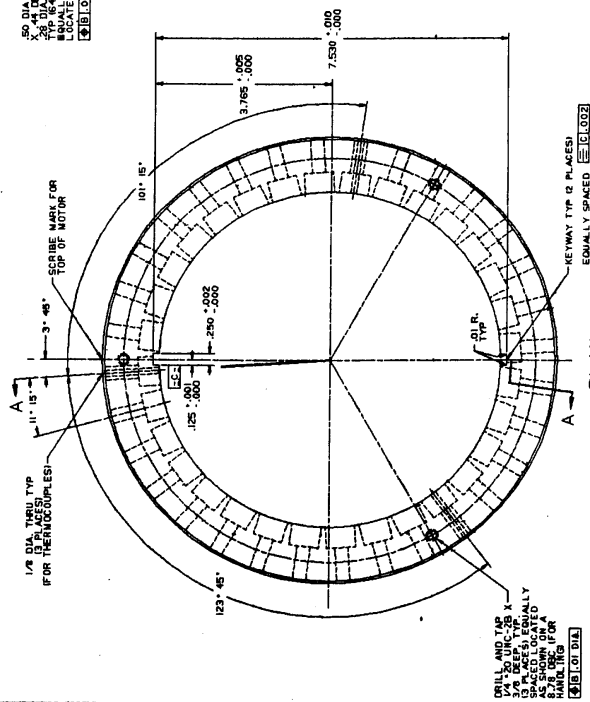
TOP

REVISIONS		DATE	BY	CHKD	DATE
1	ISSUED FOR CONSTRUCTION	10/1/77	J. H. HARRIS		
2	ISSUED FOR CONSTRUCTION	10/1/77	J. H. HARRIS		
3	ISSUED FOR CONSTRUCTION	10/1/77	J. H. HARRIS		
4	ISSUED FOR CONSTRUCTION	10/1/77	J. H. HARRIS		
5	ISSUED FOR CONSTRUCTION	10/1/77	J. H. HARRIS		
6	ISSUED FOR CONSTRUCTION	10/1/77	J. H. HARRIS		
7	ISSUED FOR CONSTRUCTION	10/1/77	J. H. HARRIS		
8	ISSUED FOR CONSTRUCTION	10/1/77	J. H. HARRIS		
9	ISSUED FOR CONSTRUCTION	10/1/77	J. H. HARRIS		
10	ISSUED FOR CONSTRUCTION	10/1/77	J. H. HARRIS		
11	ISSUED FOR CONSTRUCTION	10/1/77	J. H. HARRIS		
12	ISSUED FOR CONSTRUCTION	10/1/77	J. H. HARRIS		
13	ISSUED FOR CONSTRUCTION	10/1/77	J. H. HARRIS		
14	ISSUED FOR CONSTRUCTION	10/1/77	J. H. HARRIS		
15	ISSUED FOR CONSTRUCTION	10/1/77	J. H. HARRIS		
16	ISSUED FOR CONSTRUCTION	10/1/77	J. H. HARRIS		
17	ISSUED FOR CONSTRUCTION	10/1/77	J. H. HARRIS		
18	ISSUED FOR CONSTRUCTION	10/1/77	J. H. HARRIS		
19	ISSUED FOR CONSTRUCTION	10/1/77	J. H. HARRIS		
20	ISSUED FOR CONSTRUCTION	10/1/77	J. H. HARRIS		
21	ISSUED FOR CONSTRUCTION	10/1/77	J. H. HARRIS		
22	ISSUED FOR CONSTRUCTION	10/1/77	J. H. HARRIS		
23	ISSUED FOR CONSTRUCTION	10/1/77	J. H. HARRIS		
24	ISSUED FOR CONSTRUCTION	10/1/77	J. H. HARRIS		
25	ISSUED FOR CONSTRUCTION	10/1/77	J. H. HARRIS		
26	ISSUED FOR CONSTRUCTION	10/1/77	J. H. HARRIS		
27	ISSUED FOR CONSTRUCTION	10/1/77	J. H. HARRIS		
28	ISSUED FOR CONSTRUCTION	10/1/77	J. H. HARRIS		
29	ISSUED FOR CONSTRUCTION	10/1/77	J. H. HARRIS		
30	ISSUED FOR CONSTRUCTION	10/1/77	J. H. HARRIS		
31	ISSUED FOR CONSTRUCTION	10/1/77	J. H. HARRIS		
32	ISSUED FOR CONSTRUCTION	10/1/77	J. H. HARRIS		
33	ISSUED FOR CONSTRUCTION	10/1/77	J. H. HARRIS		
34	ISSUED FOR CONSTRUCTION	10/1/77	J. H. HARRIS		
35	ISSUED FOR CONSTRUCTION	10/1/77	J. H. HARRIS		
36	ISSUED FOR CONSTRUCTION	10/1/77	J. H. HARRIS		
37	ISSUED FOR CONSTRUCTION	10/1/77	J. H. HARRIS		
38	ISSUED FOR CONSTRUCTION	10/1/77	J. H. HARRIS		
39	ISSUED FOR CONSTRUCTION	10/1/77	J. H. HARRIS		
40	ISSUED FOR CONSTRUCTION	10/1/77	J. H. HARRIS		
41	ISSUED FOR CONSTRUCTION	10/1/77	J. H. HARRIS		
42	ISSUED FOR CONSTRUCTION	10/1/77	J. H. HARRIS		
43	ISSUED FOR CONSTRUCTION	10/1/77	J. H. HARRIS		
44	ISSUED FOR CONSTRUCTION	10/1/77	J. H. HARRIS		
45	ISSUED FOR CONSTRUCTION	10/1/77	J. H. HARRIS		
46	ISSUED FOR CONSTRUCTION	10/1/77	J. H. HARRIS		
47	ISSUED FOR CONSTRUCTION	10/1/77	J. H. HARRIS		
48	ISSUED FOR CONSTRUCTION	10/1/77	J. H. HARRIS		
49	ISSUED FOR CONSTRUCTION	10/1/77	J. H. HARRIS		
50	ISSUED FOR CONSTRUCTION	10/1/77	J. H. HARRIS		
51	ISSUED FOR CONSTRUCTION	10/1/77	J. H. HARRIS		
52	ISSUED FOR CONSTRUCTION	10/1/77	J. H. HARRIS		
53	ISSUED FOR CONSTRUCTION	10/1/77	J. H. HARRIS		
54	ISSUED FOR CONSTRUCTION	10/1/77	J. H. HARRIS		
55	ISSUED FOR CONSTRUCTION	10/1/77	J. H. HARRIS		
56	ISSUED FOR CONSTRUCTION	10/1/77	J. H. HARRIS		
57	ISSUED FOR CONSTRUCTION	10/1/77	J. H. HARRIS		
58	ISSUED FOR CONSTRUCTION	10/1/77	J. H. HARRIS		
59	ISSUED FOR CONSTRUCTION	10/1/77	J. H. HARRIS		
60	ISSUED FOR CONSTRUCTION	10/1/77	J. H. HARRIS		
61	ISSUED FOR CONSTRUCTION	10/1/77	J. H. HARRIS		
62	ISSUED FOR CONSTRUCTION	10/1/77	J. H. HARRIS		
63	ISSUED FOR CONSTRUCTION	10/1/77	J. H. HARRIS		
64	ISSUED FOR CONSTRUCTION	10/1/77	J. H. HARRIS		
65	ISSUED FOR CONSTRUCTION	10/1/77	J. H. HARRIS		
66	ISSUED FOR CONSTRUCTION	10/1/77	J. H. HARRIS		
67	ISSUED FOR CONSTRUCTION	10/1/77	J. H. HARRIS		
68	ISSUED FOR CONSTRUCTION	10/1/77	J. H. HARRIS		
69	ISSUED FOR CONSTRUCTION	10/1/77	J. H. HARRIS		
70	ISSUED FOR CONSTRUCTION	10/1/77	J. H. HARRIS		
71	ISSUED FOR CONSTRUCTION	10/1/77	J. H. HARRIS		
72	ISSUED FOR CONSTRUCTION	10/1/77	J. H. HARRIS		
73	ISSUED FOR CONSTRUCTION	10/1/77	J. H. HARRIS		
74	ISSUED FOR CONSTRUCTION	10/1/77	J. H. HARRIS		
75	ISSUED FOR CONSTRUCTION	10/1/77	J. H. HARRIS		
76	ISSUED FOR CONSTRUCTION	10/1/77	J. H. HARRIS		
77	ISSUED FOR CONSTRUCTION	10/1/77	J. H. HARRIS		
78	ISSUED FOR CONSTRUCTION	10/1/77	J. H. HARRIS		
79	ISSUED FOR CONSTRUCTION	10/1/77	J. H. HARRIS		
80	ISSUED FOR CONSTRUCTION	10/1/77	J. H. HARRIS		
81	ISSUED FOR CONSTRUCTION	10/1/77	J. H. HARRIS		
82	ISSUED FOR CONSTRUCTION	10/1/77	J. H. HARRIS		
83	ISSUED FOR CONSTRUCTION	10/1/77	J. H. HARRIS		
84	ISSUED FOR CONSTRUCTION	10/1/77	J. H. HARRIS		
85	ISSUED FOR CONSTRUCTION	10/1/77	J. H. HARRIS		
86	ISSUED FOR CONSTRUCTION	10/1/77	J. H. HARRIS		
87	ISSUED FOR CONSTRUCTION	10/1/77	J. H. HARRIS		
88	ISSUED FOR CONSTRUCTION	10/1/77	J. H. HARRIS		
89	ISSUED FOR CONSTRUCTION	10/1/77	J. H. HARRIS		
90	ISSUED FOR CONSTRUCTION	10/1/77	J. H. HARRIS		
91	ISSUED FOR CONSTRUCTION	10/1/77	J. H. HARRIS		
92	ISSUED FOR CONSTRUCTION	10/1/77	J. H. HARRIS		
93	ISSUED FOR CONSTRUCTION	10/1/77	J. H. HARRIS		
94	ISSUED FOR CONSTRUCTION	10/1/77	J. H. HARRIS		
95	ISSUED FOR CONSTRUCTION	10/1/77	J. H. HARRIS		
96	ISSUED FOR CONSTRUCTION	10/1/77	J. H. HARRIS		
97	ISSUED FOR CONSTRUCTION	10/1/77	J. H. HARRIS		
98	ISSUED FOR CONSTRUCTION	10/1/77	J. H. HARRIS		
99	ISSUED FOR CONSTRUCTION	10/1/77	J. H. HARRIS		
100	ISSUED FOR CONSTRUCTION	10/1/77	J. H. HARRIS		

FIELD COIL ASSEMBLY

SCALE: 1/2"

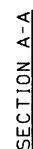
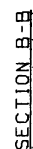
427-19992-13 A



NOTES:

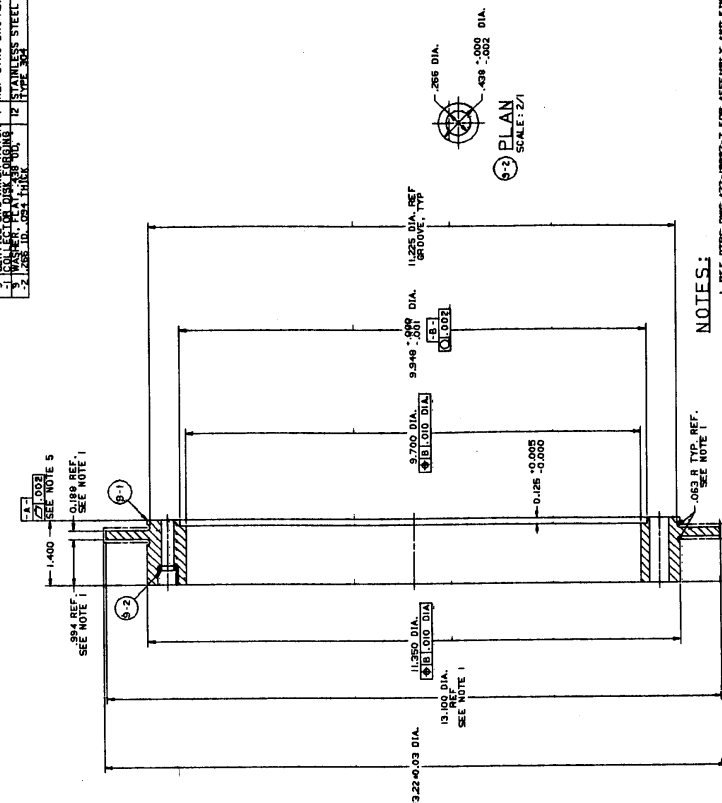
1. UNLESS OTHERWISE SPECIFIED, BREAK SHARP CORNERS WITH A CHAMFER, .03 X 45°.
2. UNLESS OTHERWISE SPECIFIED, MACHINED FILLETS TO BE .03 R.
3. ESTIMATED WEIGHT OF PC. NO. 6 IS 46.4 LB.

1. UNLESS OTHERWISE SPECIFIED, BREAK SHARP CORNERS WITH A CHAMFER, .03 X 45°.
2. UNLESS OTHERWISE SPECIFIED, MACHINED FILLETS TO BE .03 R.
3. ESTIMATED WEIGHT OF PC. NO. 6 IS 46.4 LB.



REC.	2266	DESCRIPTION	REASONS	BY	DATE
		RECEIVED 7/28/83 FEDERAL BUREAU OF INVESTIGATION CONTRIBUTION DIVISION OF MOTOR VEHICLE SAFETY	DEPARTMENT OF ARMY DAVID TAYLOR RESEARCH CENTER ATTENTION: MR. JAMES L. HARRIS 3715 BELT ROAD WASHINGTON, D.C. 20315		
		DISCORDER	SERVICE END, INNER		
		RECEIVED 7/28/83	ROTOR, RETURN RING		
		RECEIVED 7/28/83	DETAILS		
		APPROVED	SCALE: 1/4		
		DATE			427-19932-16

REC.	2266	DESCRIPTION	REASONS	BY	DATE
		RECEIVED 7/28/83 FEDERAL BUREAU OF INVESTIGATION CONTRIBUTION DIVISION OF MOTOR VEHICLE SAFETY	DEPARTMENT OF ARMY DAVID TAYLOR RESEARCH CENTER ATTENTION: MR. JAMES L. HARRIS 3715 BELT ROAD WASHINGTON, D.C. 20315		
		DISCORDER	SERVICE END, INNER		
		RECEIVED 7/28/83	ROTOR, RETURN RING		
		RECEIVED 7/28/83	DETAILS		
		APPROVED	SCALE: 1/4		
		DATE			427-19932-16



NOTES:

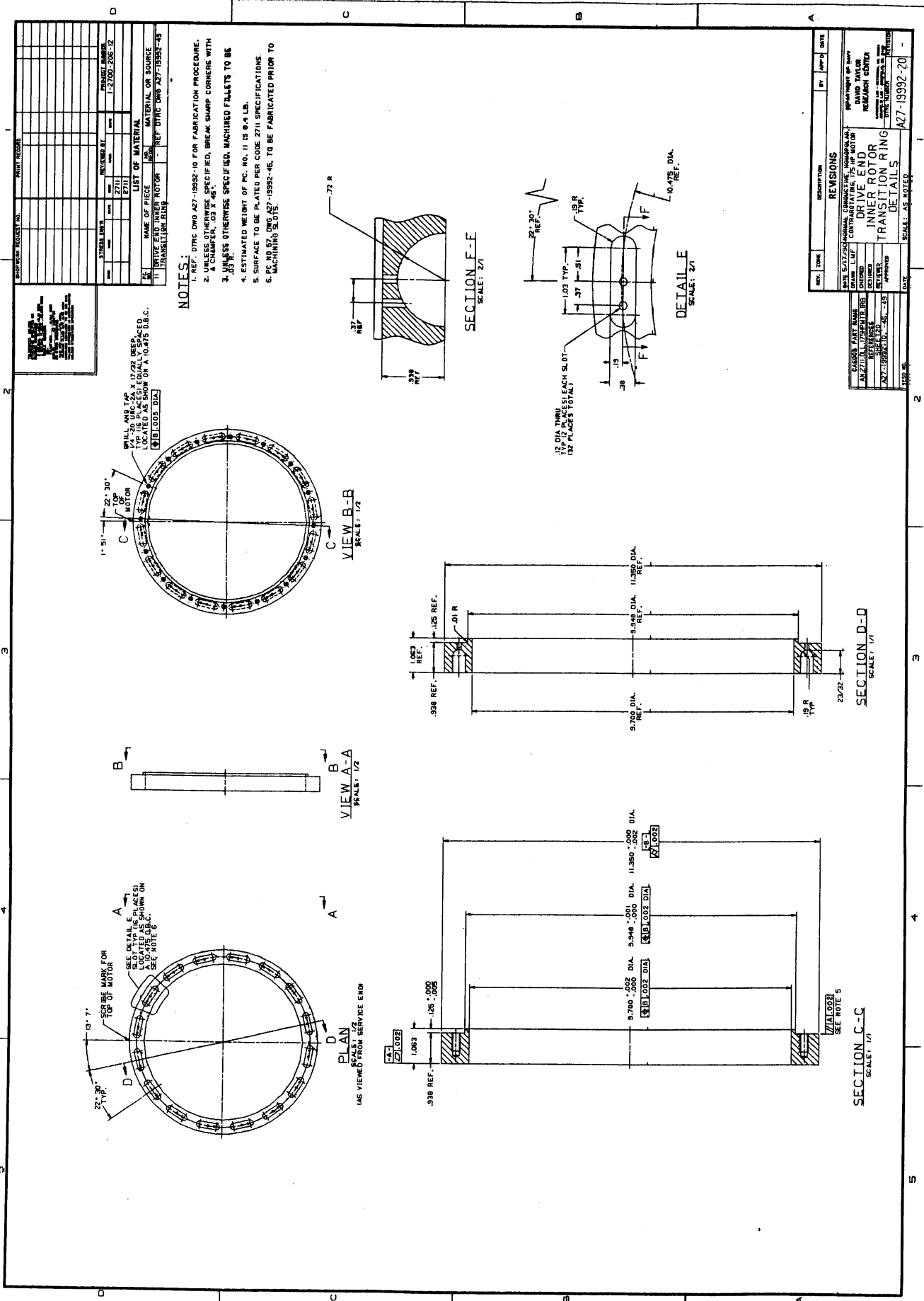
1. REF. DTC DWG A27-19992-7 FOR ASSEMBLY AND FINAL MACHINING PROCEDURE.
2. UNLESS OTHERWISE SPECIFIED, BREAK SHARP CORNERS WITH A CHAMFER, .03 X 45°.
3. UNLESS OTHERWISE SPECIFIED, MACHINED FILLETS TO BE .03 R.
4. ESTIMATED WEIGHT OF PC. NO. 9 IS 14.1 LB.
5. SURFACE TO BE PLATED PER CODE 2711 SPECIFICATIONS.

SECTION A-A
SCALE: FULL

9 PLAN
SCALE: FULL
AS VIEWED FROM SERVICE END

[illegible]

REV.	ZONE	DESCRIPTION	BY	APP'D	DATE
REVISIONS					
	DATE: 4-24-90	NORMAL CONDUCTIVE, HUMPOULAR CONTRADICTION, 175 HP MOTOR			
	DRAWN: LWF	DAVID TAYLOR			
	CHECKED:	RECEIVED: 4/24/90			
	DESIGNED:	BY: 4/24/90			
	REVISED:	DATE: 4/24/90			
	APPROVED:	DATE: 4/24/90			
	DETAILS		A77-19992-18		
	REMARKS: AS NOTED		-		
	DATE:				



NOTES:

1. REF. DTC DWG 427-1992-10 FOR FABRICATION PROCEDURE.
2. UNLESS OTHERWISE SPECIFIED, BREAK SHARP CORNERS WITH A CHAMFER, .03 X 45°.
3. UNLESS OTHERWISE SPECIFIED, MACHINED FILLETS TO BE .015 R.
4. ESTIMATED WEIGHT OF PC. NO. 11 IS 8.4 LB.
5. SURFACE TO BE PLATED PER CODE 2711 SPECIFICATIONS.
6. PC. NO. 11 IS DWG 427-1992-46, TO BE FABRICATED PRIOR TO MACHINING SLOT.

LIST OF MATERIAL

ITEM NO.	QTY	DESCRIPTION	UNIT	REMARKS
1	1	DRIVE END INNER ROTOR	PC. NO. 11	REF. DTC DWG 427-1992-46

REVISIONS

REV.	DATE	DESCRIPTION
1	10/1/92	ISSUED FOR FABRICATION

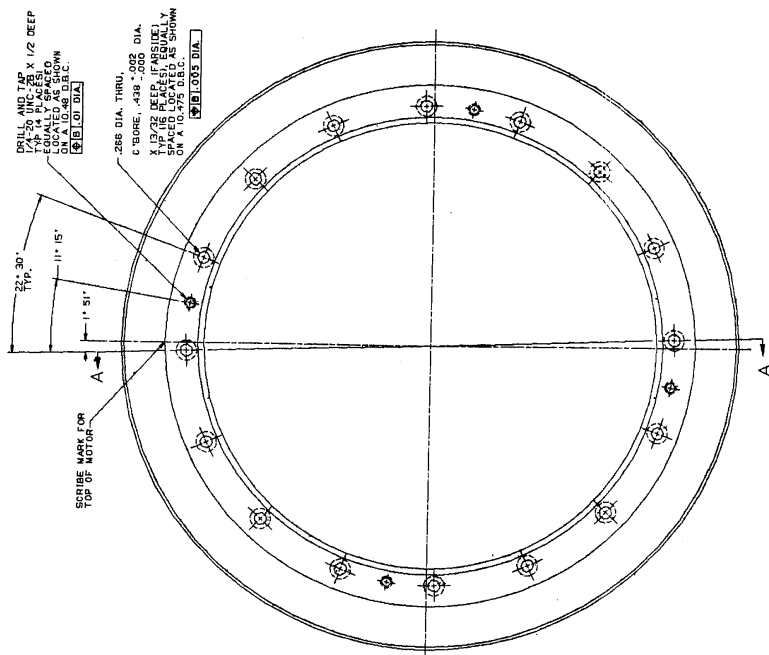
APPROVED
DAVID TAYLOR
DESIGN CENTER
10/1/92

DATE
10/1/92

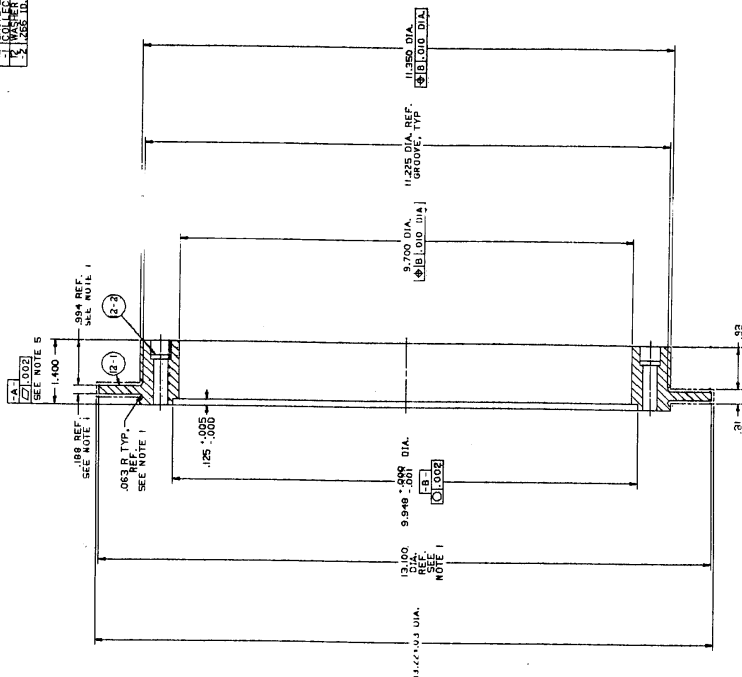
SCALE
AS NOTED

427-1992-20

1. REF. DTRC DWG 427-9992-7 FOR ASSEMBLY AND FINAL MACHINING PROCEDURE.
2. UNLESS OTHERWISE SPECIFIED, BREAK SHARP CORNERS WITH A CHAMFAN, .02 X 45°.
3. UNLESS OTHERWISE SPECIFIED, MACHINED FILLETS TO R1.03 R.
4. ESTIMATED WEIGHT OF PC, NO. 12 IS 14.1 LB.
5. SURFACE TO BE PLATED PER CODE 2711 SPECIFICATION.

[illegible]

12 PLAN SCALE: 1/1
AS VIEWED FROM SERVICE END



SECTION A-A
SCALE: 1/1

2-2 PLAN
SCALE : 2/1
Ø .438 ±.000 DIA.
Ø .266 DIA.

REV.	ZONE	DESCRIPTION	BY	APP'D	DATE
		REVISIONS			
		NORMAL, COUNTERMOUNTED CONTRACTOR (177), 75 HP MOTOR DRIVE END INNER ROTOR COLLECTOR DISK DETAILS			
		SCALE, AS NOTED			
DATE	2/2/92	APPROVED	DATE	2/2/92	APPROVED
CHUCK LAY		DAVID TAYLOR			
DESIGNED		RESEARCH CENTER			
DATE	2/2/92	DATE	2/2/92	DATE	2/2/92
APPROVED		APPROVED			
		DEPARTMENT OF MARY DAVID TAYLOR RESEARCH CENTER 10000 W. 100th Ave. Golden, CO 80401-1000 PHONE 303-440-1000 FAX 303-440-1001			

CASE'S PART NAME
AN.2711.DLL.175HPTN DE IRCD
REFERENCES
SHEET 21
A27-1992-1, -49

1



SCALE: FULL
(AS VIEWED FROM SERVICE END)

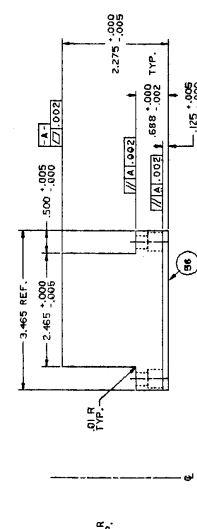
1. REF. DTC DWG A27-1992-8 FOR FABRICATION PROCEDURE.
 2. 1/4" CHAMFER, .0315" X 45°.
 3. UNLESS OTHERWISE SPECIFIED, BREAK SHARP CORNERS WITH .03 R.
 4. ESTIMATED WEIGHT OF PC. NO 55 IS 1.7 LB.
 5. ESTIMATED WEIGHT OF PC. NO 56 IS 1.7 LB.
 6. MATCH MARK WITH LETTERS AT ASSEMBLY FOR PC. NO. 55, AND 56 WITH PC. NO. 21.

ITEM	DATE	REVISION	BY	APP'D	DATE
1	2/7/11	2711			

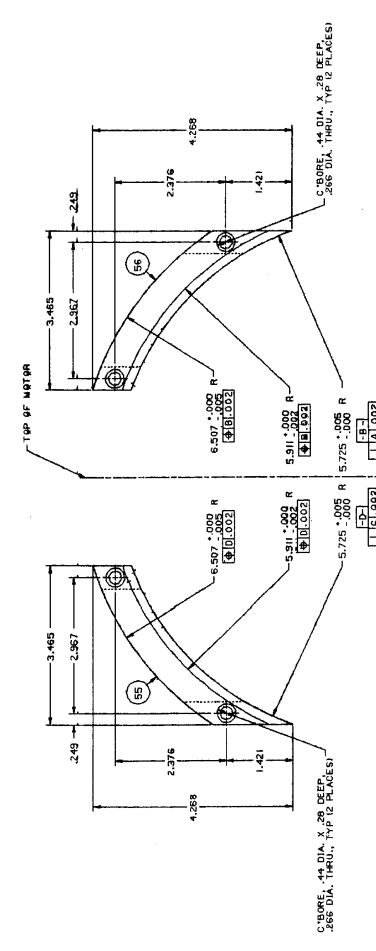
NAME OF PIECE	MATERIAL OR SOURCE
55 SERVICE END OUTER ROTOR	CARBON STEEL, PER ASTM A36
56 SERVICE END OUTER ROTOR	CARBON STEEL, PER ASTM A36
57 SERVICE END OUTER ROTOR	CARBON STEEL, PER ASTM A36

LIST OF MATERIAL
 55 SERVICE END OUTER ROTOR - CARBON STEEL, PER ASTM A36
 56 SERVICE END OUTER ROTOR - CARBON STEEL, PER ASTM A36
 57 SERVICE END OUTER ROTOR - CARBON STEEL, PER ASTM A36

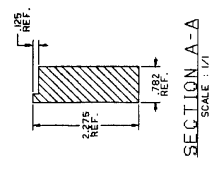
NOTES:
 1. REF. DTC DWG A27-1992-8 FOR FABRICATION PROCEDURE.
 2. 1/4" CHAMFER, .0315" X 45°.
 3. UNLESS OTHERWISE SPECIFIED, BREAK SHARP CORNERS WITH .03 R.
 4. ESTIMATED WEIGHT OF PC. NO 55 IS 1.7 LB.
 5. ESTIMATED WEIGHT OF PC. NO 56 IS 1.7 LB.
 6. MATCH MARK WITH LETTERS AT ASSEMBLY FOR PC. NO. 55, AND 56 WITH PC. NO. 21.



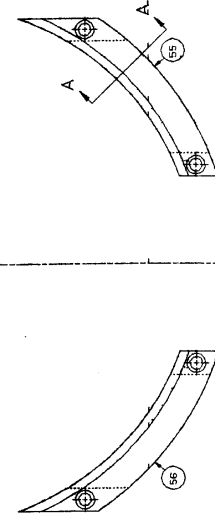
PLAN VIEW
SCALE: 1/1



ELEVATION
SCALE: 1/1



SECTION A-A
SCALE: 1/1



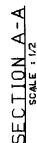
ELEVATION
SCALE: 1/1

REV.	DATE	DESCRIPTION	BY	APP'D	DATE
1	2/7/11	2711			

DATE	BY	APP'D	DATE
2/7/11	2711		

DATE	BY	APP'D	DATE
2/7/11	2711		

DATE	BY	APP'D	DATE
2/7/11	2711		



SCALE : 1/2
(AS VIEWED FROM SERVICE END)

ES:

1. REF DTRC DWG 427-13932-7 FOR ASSEMBLY AND FINAL MACHINING.
2. UNLESS OTHERWISE SPECIFIED, BREAK SHARP CORNERS WITH A CHAMFER, .25 X 45°.
3. UNLESS OTHERWISE SPECIFIED, MACHINED FILLETS TO BE .05 R.
4. ESTIMATED WEIGHT OF PC, NO. 29 IS 1.3 LB.

[illegible]

6.44 D

6.44 D

DETAIL

SCALE: 2/1

DATE 3-29-90	CON	SI	\$
PRWNN JOW			
HECRD			
SSIGNED			
VIEWED			
APPROVED			

CASD'S PART NAME
2711.0LL.175HPMTR
REFERENCES
SHEET 137
A27-19992-0

"K"
/A
(CES)

0.015 R
0.005

0.010
0.000
DIA.

15" REF. TAIL "G" SCALE: 2/1

4.497 ± 0.002 DIA
4.497 -0.000 DIA
SEE NOTE 8

5

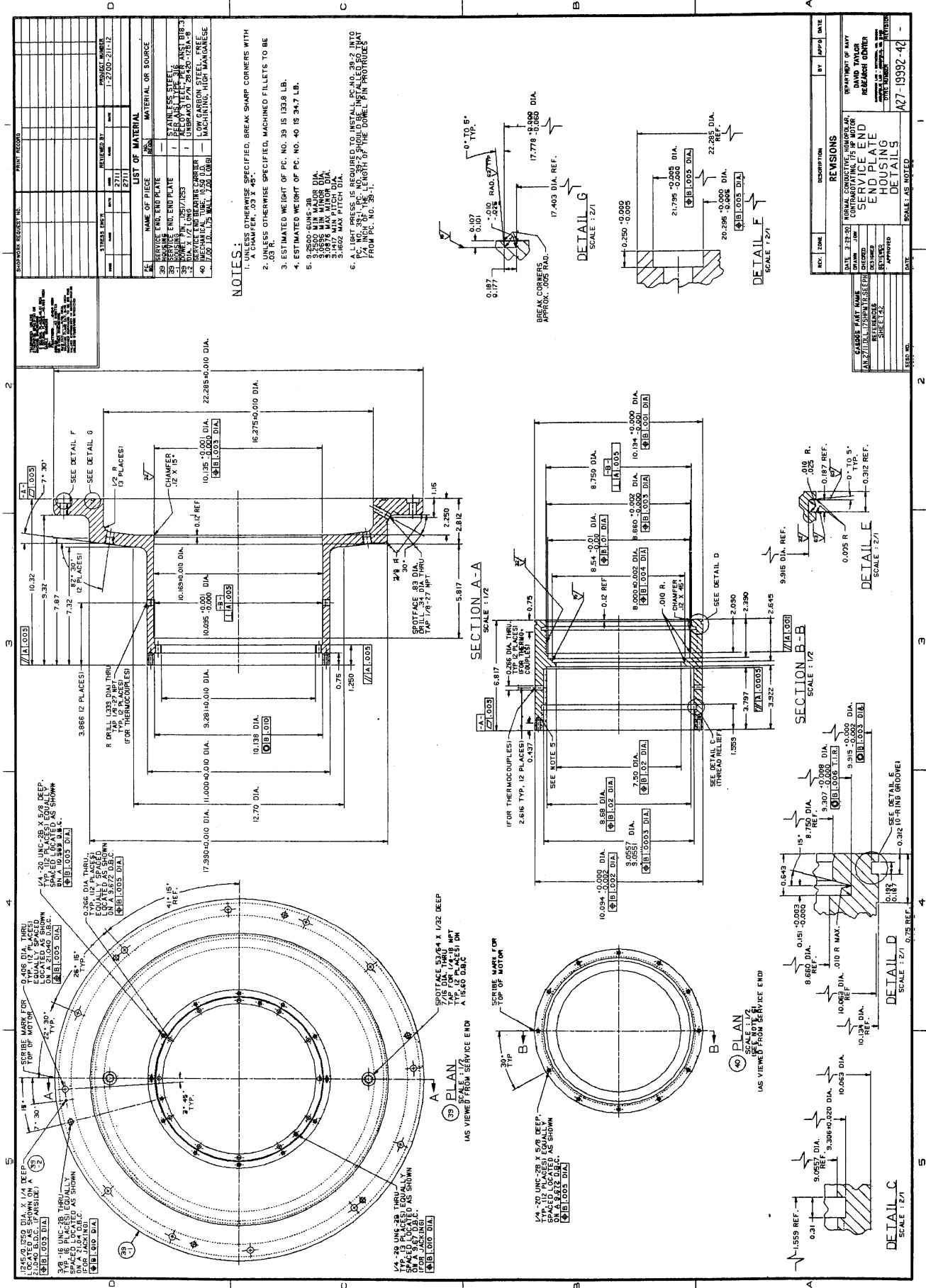
[illegible]

DE-

6.44 D 

DETAIL "E"

SCALE: 2/1



REVISIONS

REV.	DATE	DESCRIPTION	BY	APP'D.	DATE
1	12-10-60	REVISIONS			
2	12-10-60	REVISIONS			
3	12-10-60	REVISIONS			
4	12-10-60	REVISIONS			
5	12-10-60	REVISIONS			
6	12-10-60	REVISIONS			
7	12-10-60	REVISIONS			
8	12-10-60	REVISIONS			
9	12-10-60	REVISIONS			
10	12-10-60	REVISIONS			
11	12-10-60	REVISIONS			
12	12-10-60	REVISIONS			
13	12-10-60	REVISIONS			
14	12-10-60	REVISIONS			
15	12-10-60	REVISIONS			
16	12-10-60	REVISIONS			
17	12-10-60	REVISIONS			
18	12-10-60	REVISIONS			
19	12-10-60	REVISIONS			
20	12-10-60	REVISIONS			
21	12-10-60	REVISIONS			
22	12-10-60	REVISIONS			
23	12-10-60	REVISIONS			
24	12-10-60	REVISIONS			
25	12-10-60	REVISIONS			
26	12-10-60	REVISIONS			
27	12-10-60	REVISIONS			
28	12-10-60	REVISIONS			
29	12-10-60	REVISIONS			
30	12-10-60	REVISIONS			
31	12-10-60	REVISIONS			
32	12-10-60	REVISIONS			
33	12-10-60	REVISIONS			
34	12-10-60	REVISIONS			
35	12-10-60	REVISIONS			
36	12-10-60	REVISIONS			
37	12-10-60	REVISIONS			
38	12-10-60	REVISIONS			
39	12-10-60	REVISIONS			
40	12-10-60	REVISIONS			
41	12-10-60	REVISIONS			
42	12-10-60	REVISIONS			
43	12-10-60	REVISIONS			
44	12-10-60	REVISIONS			
45	12-10-60	REVISIONS			
46	12-10-60	REVISIONS			
47	12-10-60	REVISIONS			

427-19992-42

[illegible]

0.375 REF.

0.250 REF.

0.260 REF.

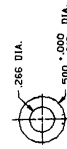
15.32 LENGTH (INSULATION)

1 REF.

1/4-20UNC-3A

59

1. CAP SCREW, 12 POINT HEAD, 1/4-20UNC-3A, 1960 SERIES, FERRY CAP AND SET SCREW CO., ALLOY STEEL, ELECTRICAL INSULATION, MEDIUM TEMPERATURE, INSUL-BOLT MANUFACTURING, INC.
2. ELECTRICAL INSULATING WASHER, INSUL-BOLT MANUFACTURING INC. MATERIAL COMPARABLE TO INSULATION APPLIED TO SCREW



THICKNESS: 1/16

3

CAGE CODE PART NAME
AN.2711.D.L.175HPT.R.1B
REFERENCES
SHEET 44

DRAWING REQUEST NO.		PRINT RECORD	
DATE	REVISED BY	DATE	PROJECT NUMBER
1/27/92	2711	1/27/92	12710-209-12
LIST OF MATERIAL			
NO.	NAME OF PIECE	QTY	MATERIAL OR SOURCE
57	180° TUBE BEND	1	CONCRETE
58	180° TUBE BEND	1	CONCRETE
127	180° TUBE BEND	1	CONCRETE
128	180° TUBE BEND	1	CONCRETE
129	180° TUBE BEND	1	CONCRETE
130	180° TUBE BEND	1	CONCRETE
131	180° TUBE BEND	1	CONCRETE
132	180° TUBE BEND	1	CONCRETE
133	180° TUBE BEND	1	CONCRETE
134	180° TUBE BEND	1	CONCRETE
135	180° TUBE BEND	1	CONCRETE
136	180° TUBE BEND	1	CONCRETE
137	180° TUBE BEND	1	CONCRETE
138	180° TUBE BEND	1	CONCRETE
139	180° TUBE BEND	1	CONCRETE
140	180° TUBE BEND	1	CONCRETE
141	180° TUBE BEND	1	CONCRETE
142	180° TUBE BEND	1	CONCRETE
143	180° TUBE BEND	1	CONCRETE
144	180° TUBE BEND	1	CONCRETE
145	180° TUBE BEND	1	CONCRETE
146	180° TUBE BEND	1	CONCRETE
147	180° TUBE BEND	1	CONCRETE
148	180° TUBE BEND	1	CONCRETE
149	180° TUBE BEND	1	CONCRETE
150	180° TUBE BEND	1	CONCRETE

DATE	REVISED BY	DATE	PROJECT NUMBER
1/27/92	2711	1/27/92	12710-209-12

DATE	REVISED BY	DATE	PROJECT NUMBER
1/27/92	2711	1/27/92	12710-209-12

DATE	REVISED BY	DATE	PROJECT NUMBER
1/27/92	2711	1/27/92	12710-209-12

DATE	REVISED BY	DATE	PROJECT NUMBER
1/27/92	2711	1/27/92	12710-209-12

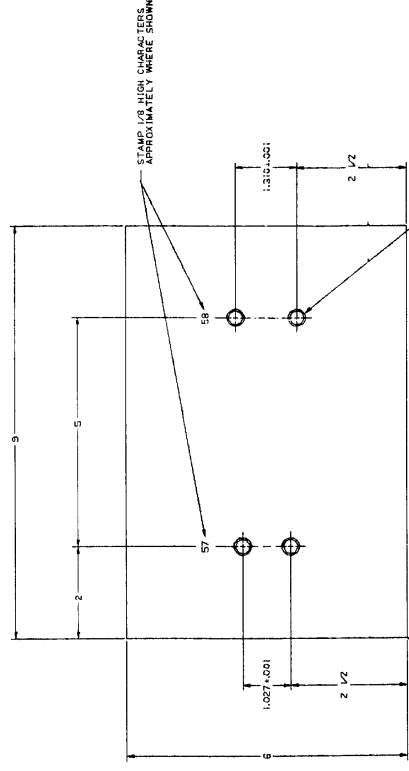
DATE	REVISED BY	DATE	PROJECT NUMBER
1/27/92	2711	1/27/92	12710-209-12

DATE	REVISED BY	DATE	PROJECT NUMBER
1/27/92	2711	1/27/92	12710-209-12

DATE	REVISED BY	DATE	PROJECT NUMBER
1/27/92	2711	1/27/92	12710-209-12

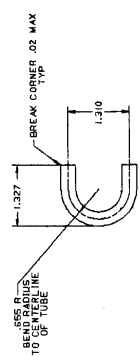
DATE	REVISED BY	DATE	PROJECT NUMBER
1/27/92	2711	1/27/92	12710-209-12

DATE	REVISED BY	DATE	PROJECT NUMBER
1/27/92	2711	1/27/92	12710-209-12



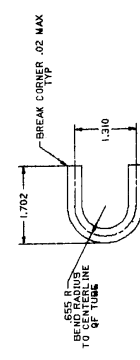
GAGE BLOCK
QUANTITY: 1

MATERIAL: STEEL LOW CARBON
1/2" THICK PLATE



57 SCALE: 1/1

- TUBE OD: .3125 (5/16)
- TUBE WALL THICKNESS: .028
- TUBE MATERIAL: COPPER ARMOR STEEL
- TUBE TO BE STRESS RELIEVED AFTER BENDING.
- QUANTITY: 12
- NOTE: DIMENSIONS ARE NOMINAL AND MUST BE MAINTAINED AFTER STRESS RELIEVING. PART TO PART REPEATABILITY WHICH SHOULD BE ADJUSTED TO FIT GAGE BLOCK.



58 SCALE: 1/1

- TUBE OD: .3125 (5/16)
- TUBE WALL THICKNESS: .028
- TUBE MATERIAL: COPPER ARMOR STEEL
- TUBE TO BE STRESS RELIEVED AFTER BENDING.
- QUANTITY: 18
- NOTE: DIMENSIONS ARE NOMINAL AND MUST BE MAINTAINED AFTER STRESS RELIEVING. PART TO PART REPEATABILITY WHICH SHOULD BE ADJUSTED TO FIT GAGE BLOCK.

DATE	REVISED BY	DATE	PROJECT NUMBER
1/27/92	2711	1/27/92	12710-209-12

DATE	REVISED BY	DATE	PROJECT NUMBER
1/27/92	2711	1/27/92	12710-209-12

DATE	REVISED BY	DATE	PROJECT NUMBER
1/27/92	2711	1/27/92	12710-209-12

DATE	REVISED BY	DATE	PROJECT NUMBER
1/27/92	2711	1/27/92	12710-209-12

DATE	REVISED BY	DATE	PROJECT NUMBER
1/27/92	2711	1/27/92	12710-209-12

DATE	REVISED BY	DATE	PROJECT NUMBER
1/27/92	2711	1/27/92	12710-209-12

DATE	REVISED BY	DATE	PROJECT NUMBER
1/27/92	2711	1/27/92	12710-209-12

DATE	REVISED BY	DATE	PROJECT NUMBER
1/27/92	2711	1/27/92	12710-209-12

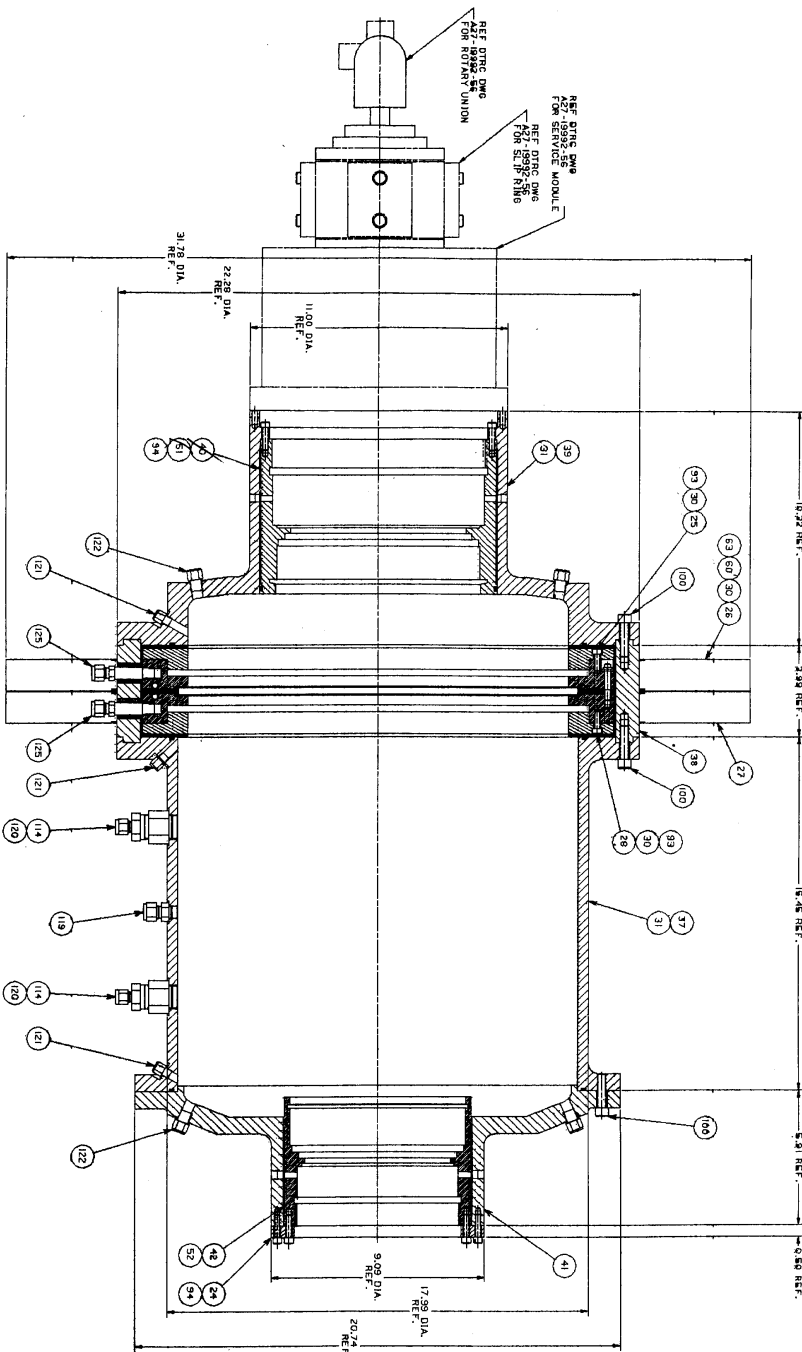
DATE	REVISED BY	DATE	PROJECT NUMBER
1/27/92	2711	1/27/92	12710-209-12

DATE	REVISED BY	DATE	PROJECT NUMBER
1/27/92	2711	1/27/92	12710-209-12

DATE	REVISED BY	DATE	PROJECT NUMBER
1/27/92	2711	1/27/92	12710-209-12

NOTES:

1. REF. DING DNG 427-1992-1 FOR LIST OF MATERIAL, AND
2. USE THERMOSEAL ADHESIVE ON THROATS OF FASTENERS. LOCATE IS RECOMMENDED.
3. IF OF TUBE FITTING TO BE ADJUSTED TO PROVIDE MOUNTING FOR
4. DETAILS OF INSULATED LOCK PIN TO BE SPECIFIED BY CODE 2711.
5. TUBE FITTING TO BE USED FOR MAX INJECTION. DETAILS OF TUBE



DATE: 10/10/92
BY: [Signature]
CHECKED BY: [Signature]
APPROVED BY: [Signature]

ITEM NO.	DESCRIPTION	QTY	UNIT	REVISION	DATE
1	1.00 DIA. REF.	1	REF.		
2	2.00 REF.	1	REF.		
3	16.46 REF.	1	REF.		
4	5.81 REF.	1	REF.		
5	0.50 REF.	1	REF.		
6	17.20 DIA.	1	DIA.		
7	20.74 DIA.	1	DIA.		
8	9.00 DIA.	1	DIA.		
9	11.00 DIA.	1	DIA.		
10	22.28 DIA.	1	DIA.		
11	31.78 DIA. REF.	1	DIA. REF.		
12	1.00 DIA. REF.	1	DIA. REF.		

ITEM NO.	DESCRIPTION	QTY	UNIT	REVISION	DATE
13	1.00 DIA. REF.	1	REF.		
14	2.00 REF.	1	REF.		
15	16.46 REF.	1	REF.		
16	5.81 REF.	1	REF.		
17	0.50 REF.	1	REF.		
18	17.20 DIA.	1	DIA.		
19	20.74 DIA.	1	DIA.		
20	9.00 DIA.	1	DIA.		
21	11.00 DIA.	1	DIA.		
22	22.28 DIA.	1	DIA.		
23	31.78 DIA. REF.	1	DIA. REF.		
24	1.00 DIA. REF.	1	DIA. REF.		
25	2.00 REF.	1	REF.		
26	16.46 REF.	1	REF.		
27	5.81 REF.	1	REF.		
28	0.50 REF.	1	REF.		
29	17.20 DIA.	1	DIA.		
30	20.74 DIA.	1	DIA.		
31	9.00 DIA.	1	DIA.		
32	11.00 DIA.	1	DIA.		
33	22.28 DIA.	1	DIA.		
34	31.78 DIA. REF.	1	DIA. REF.		
35	1.00 DIA. REF.	1	DIA. REF.		
36	2.00 REF.	1	REF.		
37	16.46 REF.	1	REF.		
38	5.81 REF.	1	REF.		
39	0.50 REF.	1	REF.		
40	17.20 DIA.	1	DIA.		
41	20.74 DIA.	1	DIA.		
42	9.00 DIA.	1	DIA.		
43	11.00 DIA.	1	DIA.		
44	22.28 DIA.	1	DIA.		
45	31.78 DIA. REF.	1	DIA. REF.		
46	1.00 DIA. REF.	1	DIA. REF.		
47	2.00 REF.	1	REF.		
48	16.46 REF.	1	REF.		
49	5.81 REF.	1	REF.		
50	0.50 REF.	1	REF.		
51	17.20 DIA.	1	DIA.		
52	20.74 DIA.	1	DIA.		
53	9.00 DIA.	1	DIA.		
54	11.00 DIA.	1	DIA.		
55	22.28 DIA.	1	DIA.		
56	31.78 DIA. REF.	1	DIA. REF.		
57	1.00 DIA. REF.	1	DIA. REF.		
58	2.00 REF.	1	REF.		
59	16.46 REF.	1	REF.		
60	5.81 REF.	1	REF.		
61	0.50 REF.	1	REF.		
62	17.20 DIA.	1	DIA.		
63	20.74 DIA.	1	DIA.		
64	9.00 DIA.	1	DIA.		
65	11.00 DIA.	1	DIA.		
66	22.28 DIA.	1	DIA.		
67	31.78 DIA. REF.	1	DIA. REF.		
68	1.00 DIA. REF.	1	DIA. REF.		
69	2.00 REF.	1	REF.		
70	16.46 REF.	1	REF.		
71	5.81 REF.	1	REF.		
72	0.50 REF.	1	REF.		
73	17.20 DIA.	1	DIA.		
74	20.74 DIA.	1	DIA.		
75	9.00 DIA.	1	DIA.		
76	11.00 DIA.	1	DIA.		
77	22.28 DIA.	1	DIA.		
78	31.78 DIA. REF.	1	DIA. REF.		
79	1.00 DIA. REF.	1	DIA. REF.		
80	2.00 REF.	1	REF.		
81	16.46 REF.	1	REF.		
82	5.81 REF.	1	REF.		
83	0.50 REF.	1	REF.		
84	17.20 DIA.	1	DIA.		
85	20.74 DIA.	1	DIA.		
86	9.00 DIA.	1	DIA.		
87	11.00 DIA.	1	DIA.		
88	22.28 DIA.	1	DIA.		
89	31.78 DIA. REF.	1	DIA. REF.		
90	1.00 DIA. REF.	1	DIA. REF.		
91	2.00 REF.	1	REF.		
92	16.46 REF.	1	REF.		
93	5.81 REF.	1	REF.		
94	0.50 REF.	1	REF.		
95	17.20 DIA.	1	DIA.		
96	20.74 DIA.	1	DIA.		
97	9.00 DIA.	1	DIA.		
98	11.00 DIA.	1	DIA.		
99	22.28 DIA.	1	DIA.		
100	31.78 DIA. REF.	1	DIA. REF.		

REVISIONS

REV.	DATE	DESCRIPTION	BY	APP'D	DATE
1	10/10/92	INITIAL CONSTRUCTION, REVISIONS BY			
2	10/10/92	CONTRIBUTING THE 1/2 MOTOR			
3	10/10/92	REVISIONS			
4	10/10/92	REVISIONS			
5	10/10/92	REVISIONS			
6	10/10/92	REVISIONS			
7	10/10/92	REVISIONS			
8	10/10/92	REVISIONS			
9	10/10/92	REVISIONS			
10	10/10/92	REVISIONS			

SCALE: 1/2

DATE: 10/10/92

BY: [Signature]

CHECKED BY: [Signature]

APPROVED BY: [Signature]

PROJECT NAME: MOTOR HOUSING ASSEMBLY SECTION

PROJECT NO: 427-1992-6-4

APPENDIX F

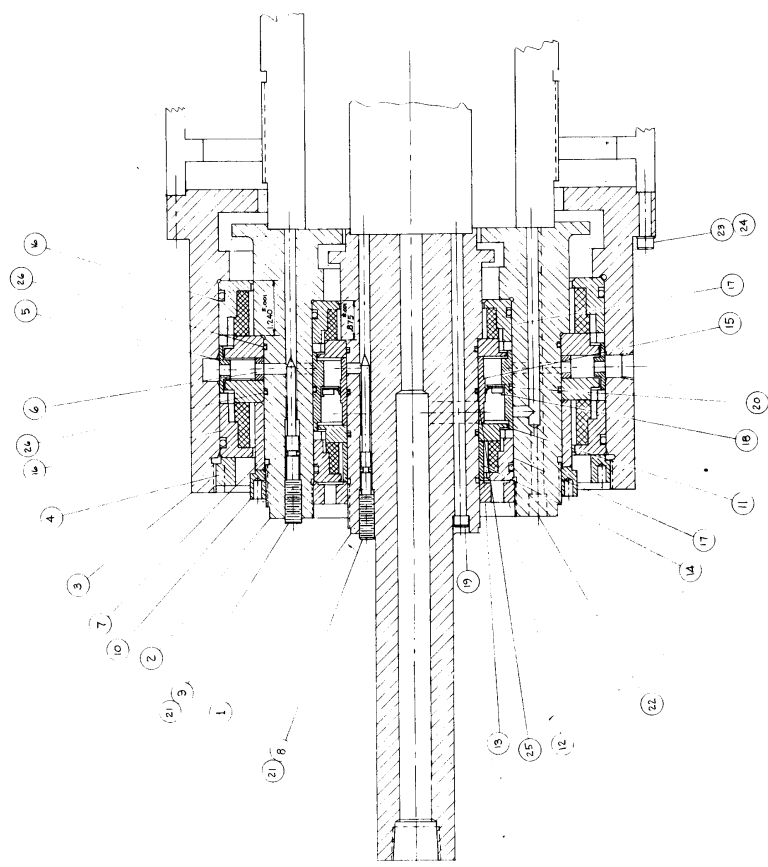
INITIAL DISTRIBUTION

CENTER DISTRIBUTION

Copies			Copies	Code	Name
4	ONR		1	0113	Winegrad
2	334	Volgelsong	1	0114	Martin
2	334	Gagorik	1	802	Levedahl
			1	804	Quandt
			1	808	Cox
5	NAVSEA		1	808	Robey
1	03Z	Krolick	1	81	Stevens
1	08K	Levin	1	811	Bagley
1	03E	Yee	5	811	Cannell
1	03R	Tobin	5	811	McConnell
1	PEOSUB-RD3	Sofia	5	811	Martino
			15	811	Smith
			1	812	Superczynski
			5	823	Drake
12	DTIC		1	3421	TIC (C)
			1	3422	TIC (A)
			1	3431	Office Services

PARTS LIST

QTY	DESCRIPTION	MATL.
1	INNER SHAFT EXTENSION	1 SST (SH 2, DET 3A)
2	OUTER SHAFT EXTENSION	1 SST (SH 3, DET 3A)
3	HOUSING EXTENSION	1 AL (SH 4, DET 3A)
4	LOCK RING, 200-BUNG-3A	1 SST (SH 4, DET 2D)
5	SPACER, 8.658 O.D.	1 SST (SH 2, DET 2D)
6	SPACER, 6.697 I.D. x .5 L4	1 SST (SH 3, DET 5D)
7	SPACER, 6.697 I.D. x 1.5 L4	1 SST (SH 4, DET 5D)
8	NEEDLE VALVE, 3.93 L4	4 SST (SH 2, DET 5C)
9	NEEDLE VALVE, 3.53 L4	4 SST (SH 4, DET 5C)
10	LOCK RING, 6.459-BUNG-3-B	1 SST (SH 4, DET 2D)
11	SPACER, 4.494 O.D.	1 SST (SH 3, DET 5D)
12	LOCK RING, 4.425-IUN-3A	1 SST (SH 3, DET 3D)
13	LOCK RING, 2.935-IUN-3B	1 SST (SH 2, DET 4C)
14	SPACER, 2.954 I.D. x 1.5 L4	1 SST (SH 2, DET 5C)
15	SPACER, 2.953 I.D. x 1.5 L4	1 SST (SH 2, DET 5C)
16	OUTER FACE SEAL, 8.658 O.D.	2 CONAL. KODON T1810A
17	INNER FACE SEAL, 4.495 O.D.	2 CONAL. KODON T1810A
18	LIP SEAL, 3.83 I.D.	1 CONAL. ANTER. VARI SEAL
19	SCREW, SOC. HD, 1/20 x 4.89 L4	5 STL
20	ORING, 4.237 I.D., 3/16 CROSS SECT.	2 BUNAN. PACKER # 215
21	ORING, 1.716 I.D., 1/16 CROSS SECT.	10 BUNAN. PACKER # 215
22	SCREW, SOC. HD, 1/20 x 6.5 L4	12 STL
23	SCREW, SOC. HD, 1/20 x 1.5 L4	12 STL
24	WASHER, 1/4, REG.	12 STL
25	ORING, 2.864 I.D., 1/16 CROSS SECT.	1 BUNAN. PACKER # 215
26	ORING, 6.487 I.D., 3/16 CROSS SECT.	2 BUNAN. PACKER # 215



REV.	DATE	DESCRIPTION
1	10/15/54	DESIGNED BY: DAVID M. TAYLOR CHECKED BY: DAVID M. TAYLOR APPROVED BY: DAVID M. TAYLOR
<p>DAVID M. TAYLOR, NAVAL SUPPLY CENTER ANNAPOLIS, MARYLAND</p>		
<p>SERVICE MODULE ASSEMBLY VIEW</p>		
<p>DATE: 10/15/54 DRAWN BY: DAVID M. TAYLOR CHECKED BY: DAVID M. TAYLOR APPROVED BY: DAVID M. TAYLOR</p>		

